MICROCOPY RESOLUTION TEST CHART

NATIONAL BUREAU OF STANDARDS-1963-A

Report No. 8

An Investigation of Bonding Mechanisms at the Interface of a Prosthetic Material

L.L. Hench, Department of Materials Science
and Engineering, University of Florida

and

R.W. Petty, College of Medicine,
Department of Orthopedics,
J. Hillis Miller Health Center

and

G. Piotrowski, Department of Mechanical
Engineering, University of Florida.

December, 1977

AD

Report No. 8

An Investigation of Bonding Mechanisms at the
Interface of a Prosthetic Material

L.L. Hench, Department of Materials Science
and Engineering, University of Florida

and

R.W. Petty, College of Medicine,
Department of Orthopedics,
J. Hillis Miller Health Center

and

G. Piotrowski, Department of Mechanical
Engineering, University of Florida

December, 1977

Supported by

D D C
RECEIVED
MAY 11 1978
D

REPORT DOCUMENTATION PAGE	READ INSTRUCTIONS BEFORE COMPLETING FORM

1. REPORT NUMBER TR-8	2. GOVT ACCESSION NO.	3. RECIPIENT'S CATALOG NUMBER

4. TITLE (and Subtitle) AN INVESTIGATION OF BONDING MECHANISMS AT THE INTERFACE OF A PROSTHETIC MATERIAL.	5. TYPE OF REPORT & PERIOD COVERED Oct. 1, 1976–Sept. 30, 1977 Annual Report
	6. PERFORMING ORG. REPORT NUMBER

7. AUTHOR(s) L. L. Hench, R. W. Petty and George Piotrowski	8. CONTRACT OR GRANT NUMBER(s) DAMD 17-76-C-6033

9. PERFORMING ORGANIZATION NAME AND ADDRESS University of Florida Department of Materials Science and Engineering Gainesville, Florida 32611	10. PROGRAM ELEMENT, PROJECT, TASK AREA & WORK UNIT NUMBERS 62772A 3S762772A814 00.050

11. CONTROLLING OFFICE NAME AND ADDRESS U.S. Army Medical Research and Development Command Washington, D. C. 20314	12. REPORT DATE December 1977
	13. NUMBER OF PAGES 144

14. MONITORING AGENCY NAME & ADDRESS(If different from Controlling Office)	15. SECURITY CLASS. (of this report) Unclassified
	15a. DECLASSIFICATION/DOWNGRADING SCHEDULE

Rept. no. 8 (Annual), 1 Oct 76 - 30 Sep 77

16. DISTRIBUTION STATEMENT (of this Report)

Approved for public release; distribution unlimited *147p.*

17. DISTRIBUTION STATEMENT (of the abstract entered in Block 20, If different from Report)

18. SUPPLEMENTARY NOTES

19. KEY WORDS (Continue on reverse side if necessary and identify by block number)

Bioceramics	Transmission electron microscopy	Glass-ceramics
Glass	Scanning electron microscopy	Bioglass
Orthopaedics	Electron microprobe analysis	Interfacial bonding
Hydroxyapatite	Bone	Mechanical strength
Collagen	Bone growth	Proteins

20. ABSTRACT (Continue on reverse side if necessary and identify by block number)

This research program has had two primary objectives since its inception: (1) to achieve a direct chemical bond between orthopaedic devices and bone using surface active glass and glass-ceramic materials or coatings, and (2) to develop a scientific understanding of the chemical and mechanical interfacial reactions occurring between materials and bone. This report summarizes progress toward realizing these objectives by reviewing accomplishments of the past eight years and presenting a series of new findings.

Results from this past year include establishing the compositional

19. (continued)

Histology	Cancellous bone	Rats	Fibula
Stress analysis	flame spray	Monkeys	Bone graft
Implant	Femur	Stainless steel	Autologous graft
Surfaces	Segmental bone	Prostheses	Tissue culture
Bioceramics	replacement	Coblat-chrome alloy	Cell culture
			Mucopolysaccharides

20. (continued)

dependence for the bonding of bioglass to bone. When critical concentrations of SiO_2, Na_2O, CaO, or P_2O_5 are reached bonding no longer occurs. The absence of bonding may be due to 1) insufficient reactivity resulting in formation of a fibrous capsule, 2) excessive reactivity resulting in dissolution and resorption of the implant, and 3) inability to form a glass and control properties. Partial or complete substitution of potassium for sodium does not affect bonding. Substitution of Mg for Ca prevents bonding.

Use of the compositional bone bonding boundary has been made to establish optimal compositions for coating Co-Cr and 316L stainless steel surgical alloys using the new immersion coating process. A strong reliable glass-metal interface is achieved with these coatings. Femoral head prostheses for monkey have been coated with 45S5 bioglass by this process and implanted. After 8 weeks the stems withstood tensile loads of more than 137 lbs force without failure of the bioglass-bone interface.

However, canine fibula grafts using bioglass did not develop bonding at the bone-bioglass interface. The implant did serve as an exceolent scaffold for the bone to bridge a larger defect than would have been accomodated without the presence of the graft. Failure of bonding is attributed to either biomechanics factors, since the grafts were not immobilized, or lack of cancellous bone in the canine fibula.

A new experimental technique using the electron microprobe (EMP) was developed during this year for analyzing the compositional gradient across the bone-bioglass interface. The EMP procedure was used to show that the Ca-P bonding film that develops at the bone-bioglass interface matures at 3 months in rat and shows no evidence of deterioration of the interfacial layer even after 28 months.

Further understanding of the bone cell-bioglass interface was achieved by using analytical scanning transmission electron microscopy to investigate samples of bone cells grown on bioglass for 2 and 6 weeks. Stable cells were able to be maintained on bioglass at multiple levels, 40-50 cells deep. Extensive intercellular collagen generation was observed but no analytical evidence of mineralization. The cells appear to be adherant to portions of the thin Ca-P film formed on the SiO_2-rich bonding interface of the bioglass samples. An amorphous non-cellular phase is often present between the cells and the Ca-P rich film.

A calorimetric study of adsorption of physiological constituents on bioglass shows a high bond energy between collagen and bioglass and mucopolysaccharides and bioglass. These findings are consistent with both the in vitro and in vivo studies reported herein.

A general review of the current field of bioceramics is also included to put the results of this investigation of controlled surface reactive biomaterials in context with the field as a whole.

SUMMARY

This research program has had two primary objectives since its inception: (1) to achieve a direct chemical bond between orthopaedic devices and bone using surface active glass and glass-ceramic materials or coatings, and (2) to develop a scientific understanding of the chemical and mechanical interfacial reactions occurring between materials and bone. This report summarizes progress toward realizing these objectives by reviewing accomplishments of the past eight years and presenting a series of new findings.

Results from this past year include establishing the compositional dependence for the bonding of bioglass to bone. When critical concentations of SiO_2, Na_2O, CaO, or P_2O_5 are reached bonding no longer occurs. The absence of bonding may be due to 1) insufficient reactivity resulting in formation of a fibrous capsule, 2) excessive reactivity resulting in dissolution and resorbtion of the implant, and 3) inability to form a glass and control properties. Partial or complete substitution of potassium for sodium does not affect bonding. Substitution of Mg for Ca prevents bonding.

Use of the compositional bone bonding boundary has been made to establish optimal compositions for coating Co-Cr and 316L stainless steel surgical alloys using the new immersion coating process. A strong reliable glass-metal interface is achieved with these coatings. Femoral head prostheses for monkey have been coated with 45S5 bioglass by this process and implanted. After 8 weeks the stems withstood tensile loads of more than 137 lbs force without failure of the bioglass-bone interface.

However, canine fibula grafts using bioglass did not develop bonding at the bone-bioglass interface. The implant did serve as an excellent scaffold for the bone to bridge a larger defect than would have been accomodated without the presence of the graft. Failure of bonding is attributed to either biomechanics factors, since the grafts were not immobilized, or lack of cancellous bone in the canine fibula.

A new experimental technique using the electron microprobe (EMP) was developed during this year for analyzing the compositional gradient across the bone-bioglass interface. The EMP procedure was used to show that the Ca-P bonding film that develops at the bone-bioglass interface matures at 3 months in rat and shows no evidence of deterioration of the interfacial layer even after 28 months.

Further understanding of the bone cell-bioglass interface was achieved by using analytical scanning transmission electron microscopy to investigate samples of bone cells grown on bioglass for 2 and 6 weeks. Stable cells were able to be maintained on bioglass at multiple levels,

40-50 cells deep. Extensive intercellular collagen generation was
observed but no analytical evidence of mineralization. The cells
appear to be adherant to portions of the thin Ca-P film formed on the
SiO_2-rich bonding interface of the bioglass samples. An amorphous
non-cellular phase is often present between the cells and the Ca-P
rich film.

A calorimetric study of adsorption of physiological constituents
on bioglass shows a high bond energy between collagen and bioglass and
mucopolysaccharides and bioglass. These findings are consistent with
both the in vitro and in vivo studies reported herein.

A general review of the current field of bioceramics is also
included to put the results of this investigation of controlled surface
reactive biomaterials in context with the field as a whole.

2

FOREWORD

The program undertaken in the contract is an interdisciplinary effort of the Departments of Materials Science and Engineering and Mechanical Engineering, College of Engineering, University of Florida and the Department of Orthopaedics, College of Medicine, University of Florida.

In conducting the research described in this report, the investigators adhered to the "Guide for Laboratory Animal Facilities and Care," as promulgated by the Committee on the Guide for Laboratory Animal Resources, National Academy of Sciences-National Research Council.

3

TABLE OF CONTENTS

4

LIST OF FIGURES

LIST OF FIGURES (Continued)

LIST OF FIGURES (Continued)

LIST OF FIGURES (Continued)

Figure   Page

Part I (continued)

LIST OF TABLES

I. INTRODUCTION AND OBJECTIVES

There are two primary objectives in this program. 1) To achieve a direct chemical bond between a ceramic material and bone. Accomplishment of this objective will enable the development of a wide range of orthopaedic prosthetic devices which will not loosen with time and require removal from the patient; and 2) to develop a scientific understanding of the chemical, biological and mechanical interfacial reactions occurring between materials and bone. Accomplishment of this objective will enable the engineer and physician to design collaboratively a materials system to satisfy a specific combination of mechanical and physiological requirements in medical applications.

Previous progress in achieving these objectives has been discussed in Reports No. 1, 2, 3, 4, 5, 6 and 7 prepared for this contract in August 1970, August 1971, August 1972, September 1973, September 1974, September 1975, and September 1976, respectively.

II. PROJECT OVERVIEW

In order to meet the above objectives, glass and glass-ceramic materials have been developed which promote the formation of a direct chemical bond at the interface of the material and bone. The direct bond is obtained without the use of a porous structure in the glass and glass-ceramics, thereby retaining the intrinsic strength of these materials and also enabling the glass or glass-ceramics to be used as coatings on high strength metal or other high strength ceramic substrates. As discussed in Reports No. 1, 2, 3, 4, 5, 6 and 7, promotion of the chemical bonding is accomplished by incorporating into the glass and glass-ceramic structures soluble sodium, calcium and phosphate ions in ratios which can influence the precipitation of hydroxyapatite in bone. Variable rates of ion release have been achieved by varying (1) Ca/P ratio, (2) the percentage of network formers in the glass, (3) the type of network former (SiO_2 or B_2O_3), and (4) F^- additions.

Previous in vitro studies have been conducted to establish parameters controlling the bonding of the glass and glass-ceramic materials with bone. These studies have demonstrated that the phosphate containing bioglass surface enhances surface crystallization of hydroxyapatite. Studies presented in Report No. 4 showed what appeared to be a hydroxyapatite-like layer forming on top of a silica-rich layer, due to the reaction of bioglass with an aqueous medium in vitro. The role of a soluble SiO_2 gel layer at the implant interface appears to be critical for bonding in light of recent studies showing SiO_2 present as an osteogenic precursor. Certain protein macromolecules also bond to the bioglass surface in a dense, randomly distributed conformation in contrast to a highly oriented distribution on quartz surfaces and a complete lack of bonding on other mineral and non-reactive ceramic surfaces.

The degree of selective attack of the silicate network and the resulting reaction layers are influenced by the quantity of phosphate in the glass, with the addition of phosphate producing a double layered reaction film which is more effective in protecting the bulk glass from aqueous attack. Detailed concentration profiles of reacted bioglass surfaces have been obtained with Auger Electron Spectroscopy and ion beam milling which confirm the existence of the silica-rich gel and a very thin calcium phosphate film at the surface. The crystalline product which grows from the initially amorphous calcium phosphate film has been identified as hydroxyapatite which contains a considerable quantity of CO_2 within its structure.

Implantation of duplicate bioglass-ceramic samples in rat femurs has been used to evaluate the formation of the chemical bond at a living interface. Tetracycline tracers, microradiography, scanning electron microscopy, light microscopy and transmission electron microscopy all show evidence of new bone growth contiguous with the bioglass and bioglass-ceramic implant surface. A viable bond forms as early as 10 days postoperatively. A histological sequence shows that mature bone appears at points on the active glass-ceramic surface at four weeks. After twelve weeks a complete mature laminar interface has been established. Transmission electron micrographs show an amorphous gel-like layer immediately adjacent to the implant surface, with highly elongated hydroxyapatite crystals bridging the gap between the implant and the mature bone which has formed around the implant. These hydroxyapatite crystals apparently form after osteoblasts have laid down collagen fibers on this silica gel layer.

In vivo studies presented in Report No 5 support the contention that a silica-rich gel on the glass surface serves as the induction site for ossification. Four bioglasses, including a soda-lime-silica glass and three compositions produced by adding 3, 6 and 12 wt. % P_2O_5 to the ternary glass, exhibited direct attachment to bone at three weeks. As the ternary glass only forms a silica-rich surface, even when phosphates are present in solution, and the glass-bone interface appears very similar for all four compositions, it seems likely that the silica-rich layer is serving as the site for osteoblasts to lay down the organic intercellular substance of bone. The calcium phosphate layer which develops when phosphorus is added to the bioglass composition may serve as a source of ions to be incorporated into the mineralization process. However, an excess of calcium and phosphate ions lead to cell death and ectopic calcification.

The compositional dependence of the bone-bioglass bond, described in this report, shows that definite percentages of SiO_2, CaO, and Na_2O are necessary for the bond to develop within 30 days in the rat tibia. Compositions outside the bone bonding boundary are either: 1) too reactive and totally resorb in the bone; 2) nonreactive and develop a fibrous capsule; or 3) are nonglass forming compositions with the bone bonding boundary are certain compositions which can be used for coating surgical stainless steel prostheses. A second compositional range has

has been found which is particularly suited for coating Co-Cr alloy (Vitallium) prostheses. Compositions throughout the bone bonding region can be used for coating high density, high strength alumina ceramic devices.

Bioglass specimens implanted in rat femurs for one hour were examined using Auger electron microscopy and ion milling techniques in order to study compositional variations at the implant surface. As with the samples corroded in vitro, the silica-rich gel was found covered by a calcium phosphate layer. However, a very important difference was that the in vivo reactive surface contained organic constituents to a depth of 180 nm. The calcium phosphate film in the in vivo sample was also thinner, placing the silica-rich layer closer to the surface. Transmission electron microscopy of the bioglass-bone junction shows ultrastructure evidence of the same sequence of chemical constituents. In work supported by another grant it was discovered that collagen fibers exposed to bioglass in vitro became incorporated in hydroxylapatite agglomerates that formed on the bioglass surface. Addition of mucopolysaccharides to the suspension greatly enhanced the adsorbtion and attachment. It is the "graded interface" between organic and inorganic phases that apparently is responsible for the high mechanical strength of the bioglass-bone bond.

During this report period a new electron microprobe (EMP) analysis procedure was developed to measure the compositional gradients at the bioglass-bone bonding interface. This analysis procedure can be conducted on samples previously photographed by reflected light microscopy for histological features. Thus, correlations of the chemical properties of the interfacial bond can be made with cellular phenomena. Transmitted light micrograph sections of the bonding interface have also been prepared, completing the necessary range of light microscopy tools required for understanding bonding mechanisms.

Stability of the bioglass-bone bond has been a subject of interest for some time. The EMP procedure has been used to measure the thickness of the calcium phosphate and silica gel bonding layers in rat over a period of time from 1 to 28 months. Only minor changes in thickness of the calcium phosphate layer were determined. The silica-rich layer continued to increase in thickness throughout this period. Mechanical strength of the bond, measured by a minipushout test (see below), was maintained throughout the 28 month period.

The mechanical strength of the interfacial bond developed between a glass-ceramic bone implant with a reactive surface and a rat femur was measured. After 28 weeks sufficient strength was established that the bone failed under a torsional stress of 50 MPa (513 kg/cm^2) with the glass-ceramic interface remaining intact. Computer programs to evaluate stresses actually applied at the implant interface are used in the interpretation of the mechanical test data.

Statistical evaluation of segmental femur replacements in monkeys showed development of a strong interfacial bond. Torsional strength of the bone implant system was measured to be about 75% of the strength of the intact femur. Fractures were observed in either the bioglass-ceramic or in the bone, but did not preferentially propagate along the bone-implant interface. Since the interfaces were not fractured during the torsional tests, the strength of the interface could not be determined, but lower limits could be assigned. Analysis of the fracture and inter-facial shear stresses showed that the interface sustained stresses of over 78 MPa (800 kg/cm^2), which is about 75% of the strength of the healing bone. This strength level also represents about half the strength of normal cortical bone.

Partial hip prostheses for stumptail monkeys were designed using biomechanics factors. The 316L surgical stainless steel prostheses flame spray coated with bioglass showed stable fixation in the medullary canal without the use of screws or other mechanical means of fixation. Functional use of the hip was retained. Histological evaluation after one year showed complete protection of neighboring tissues from metal corrosion products.

The new immersion process for coating metal devices with bioglass described in Report No. 7 has been successfully applied to stainless steel hip prostheses for monkeys. Periodic corrosion failure of the glass-metal interface characteristic of the flame spray coated prostheses has been eliminated with the immersion coating process. Tensile loads as high as 609N have been withstood by the bioglass coated femoral stems bonded into the medullary cavity of the monkey. Although no PMMA was used the animals appeared to be full weight bearing from 1 to 2 days post-op and throughout the evaluation period.

An effort to utilize sintered alumina-bioglass composite materials as resorbable bone plates for the fixation of fractured bones led to a program to optimize the strength of the material. A bone plate was de-signed for the fixation of transverse fractures of canine femurs and six implantations were performed. While most plates failed within 10 days, one plate survived until the bone healed and was removed at 64 weeks. The plate showed no evidence of resorption or bonding to the bone. In fact the underlying bone showed radiological evidence of resorption away from the plate. Some tissue necrosis in the vicinity of sintered materials implanted in rat tibias was also noted, suggesting that for bioglasses to be effective they must be presented as an as-cast glass or as a glassy coating with minimal microporosity.

A rapid and inexpensive technique has been developed for assessing the bonding ability of bioglass formulations in vivo, and has been used to demonstrate that bonding is attained consistently with the 45S5 bio-glass. The same test is now being used as a quality control test for all other implantation studies, thereby assuring that materials used for biomechanical studies have the ability to form bonds with bone. The effect of variations in the composition of bioglass on the bonding

ability is also being scrutinized, and it has been found that substitution of potassium for sodium does not affect the bonding ability of bioglass. However, substitution of magnesium for calcium does inhibit formation of a stable bioglass-bone bond.

A new process for coating metallic implants with bioglass using an immersion technique has been developed. The metal-glass interface formed is quite resistant to attack by body fluids, and the metal-glass transition is only about two microns thick. Thus, a bioglass surface is presented to the in vivo environment. During this report period the immersion coating process has been optimized for coating of Co-Cr surgical alloys (Vitallium). Successful coating of human Moore-type hip prostheses of Vitallium have been made with the new process.

A series of canine fibular replacements have demonstrated a uniform lack of bond formation, despite the fact that the materials used had previously passed the in vivo test for bonding ability. Lack of fixation appears to be the prime interference to bond formation. The implants were encapsulated in callus within only a few weeks, and motion of the implant was thereby eliminated, but the bond did not form at this later time. Thus the mechanism of bond formation appears to involve a time sequence which, if interrupted, will not be completed.

III. SUMMARY OF MAJOR ACCOMPLISHMENTS, 1969-77

1. A systems analysis of the various activities in the research program has been completed and has been used to establish budget and personnel allocations as well as the time sequencing required for the interacting functions of the research.

Development of Materials Systems

2. The basic bioglass composition, 45S5, is an invert soda-lime glass, containing 45% SiO_2 as network former, equal amounts (24.5%) of Na_2O and CaO, and 6% P_2O_5, by weight. This material can be used in its as-cast (glassy) form, or partially crystallized, or completely crystallized to become a bioglass-ceramic.

3. Low viscosity, biocompatible glasses with a variable rate of release of surface ions and changes of surface pH have been developed. This series of glasses, $45B_{15}S5$ and $45B_5S5$, involved the partial replacement of the SiO_2 network forming oxide with B_2O_3 network formers. The $Na_2O-B_2O_3$ ions in the glass complex to form a tetrahedral structural unit akin to that of the SiO_2 units. However, the viscosity of the glass is greatly reduced, thus making it possible to flame spray or enamel the bioglass. Both in vitro and in vivo evaluations establish the equivalent behavior of this new line of bioglasses to that of the 45S5 composition originally developed in this program.

4. A third composition of bioglass, 45S5F, was developed by substituting CaF_2 for about half of the CaO. These glasses show similar

behavior to the other bioglasses, both in vivo and in vitro, and lower
viscosity than the original 45S5 composition. The 45S5F glasses evolved
for use in a flame-spraying process developed in collaboration with the
ceramics group at IITRI. The flame-spraying process was used to success-
fully coat such complex devices as femoral head replacement prostheses
for monkeys completely with 45S5 bioglass, thereby combining the strength
of the metal with the desirable surface characteristics of the bioglass.
Both in vitro and in vivo testing of flame spray coated devices however
show an alarming incidence of fatigue failure at the glass-metal inter-
face. Such failure has been diagnosed as due to lack of control over
variables in the flame spray process. Thus, large scale use of this
coating process is not recommended at this time.

5. An immersion process for coating metal with bioglass has been
developed and shown to produce surfaces equivalent to bulk bioglass in
terms of tissue response. With this process the strength of the metal
substrate can now be combined with the surface properties of bioglass
without interfacial failure between glass and metal. Crystallization
(ceraming) of the bioglass coatings prepared by the immersion process
can be performed. Bond strength between the glass and metal can be
optimized by control of variables of the immersion process and by ceram-
ing of the coating.

6. Compositional boundaries for the bonding of bioglasses to bone
have been established. Compositions outside the bone bonding boundary
are either: 1) too reactive and totally resorb in bone; 2) nonreactive
and develop a fibrous capsule with no interfacial bonding; or 3) are non-
glass-forming compositions. The ratio of SiO_2 to alkali in the glass is
an especially critical variable.

7. Substitution of K_2O for Na_2O as the alkali in the glass does not
affect bone bonding. However, substitution of MgO for CaO in the compo-
sition does detract from bonding to bone.

8. Within the bone bonding compositional boundary certain compo-
sitions have been found to be more favorable for bonding to surgical
stainless steel devices. Other compositions have been bound to produce
favorable interfacial bonding to Co-Cr alloys such as Vitallium. Large
Vitallium devices such as human Moore hip prostheses have been success-
fully coated with bioglass using the immersion coating process and
compositional control. Monkey hip prostheses of 316L stainless steel
are being coated routinely in this manner.

9. Other material systems, such as enameled stainless steel using
bioglass powders, sintered bioglasses and bioglass-ceramics, and bioglass-
alumina composites, have been tested and found to be unsuitable for
in vivo implantation. Additional work in these areas has been dropped
in favor of using bioglass coatings.

In Vitro Studies of Bioglass Surfaces

10. Methods for evaluating the specific ions released at the surface of the bioglasses and bioglass-ceramics and the structural changes in the implant surfaces have been developed. These include atomic absorption analysis, atomic emission analysis, colorimetry, infrared reflection spectroscopy, scanning electron microscopy, and electron microprobe analyses. Auger spectroscopy has neen recently used to understand the exact chemical nature of the interfacial surface of the implant materials. Ion-milling of the surface followed by segmental Auger electron spectroscopy reveals the detailed sequence of Na, Si, Ca and P ions released from the implant surface and build-up of surface gel layers.

11. In vitro evaluation of the surface chemical response of bioglasses to a simulated physiologic environment has been accomplished. A solution-glass interfacial reaction layer or layers are formed as a result of aqueous interaction with the glass structure. If phosphorus is absent from the bioglass composition, sodium and calcium are selectively leached, producing a silica-rich gel layer. The addition of phosphorus to the glass composition does not interfere with the development of a silica-rich gel layer initially. However, a second film composed of an amorphous calcium phosphate develops at the silica gel-water interface and with time crystallizes to form an apatite structure. Increasing the phosphorus content of the glass composition accelerates the formation of the calcium phosphate film. Partial substitution of B_2O_3 for SiO_2 accelerates the initial dissolution process. The addition of fluorine to the glass composition significantly enhances the resistance of the glass to aqueous attack, probably by substituting for hydroxyl ions in the apatite structure. The presence of phosphate ions in solution results in the formation of the amorphous calcium phosphate film even if phosphate is not present in the glass.

12. Composition profiles of the reaction layers formed on a series of bioglasses with increasing phosphorus content have been measured employing Auger electron spectroscopy and ion beam milling. The profiles provide detailed compositional maps which confirm the existence of the calcium phosphate gel-silica gel-bulk glass structure at the bioglass surface after reaction. When the phosphate concentration on the glass is too large the interfacial layers become too thick and are no longer stable.

13. Conditioning of bioglass with tissue culture medium prior to implantation fosters the formation of an intimate and ultrathin calcium phosphate film on the implant. This prevents spalling of the film which can occur with untreated implants of high phosphate concentration because the calcium phosphate film forms very rapidly and becomes quite thick. As a result, conditioned implants of certain compositions appear to form a stronger bond to bone.

14. Long-term studies (>10,000 hours) of the surface reactivity and pH-time dependence of the various bioglass and bioglass-ceramic compositions show a controlled release rate of Ca, Na, Si and P ions from the implant surfaces. The ion losses in buffered solutions provide the physical-chemical correlation required to interpret the soft tissue and hard tissue in vitro responses. Fluorine additions decrease the

19

ion release rate and thereby evoke a slower mineralization. Boron oxide additions accelerate the interfacial reactions. Thus, the bioglass and bioglass-ceramics can be designed to match specific metabolic activities.

15. In vitro reactivity studies of flame sprayed $45B_5S5$ and 45S5F bioglass-coatings, 45S5 double coatings on dense alumina ceramics, 45S5 immersion coatings on 316L stainless steel, and 52S4.6 coatings on Vitallium have shown that the relative solubilities of these materials are similar to bulk bioglass materials of the same composition.

16. Precipitation of polyaminoacids, polypeptides, polysacharrides, and proteins, on the surfaces of bioglasses and various other minerals have shown that the compatibility of metabolic constituents is a function of crystal structure of a crystalline bioceramics surface and is also a function of composition of bioglasses.

17. The bioglasses and bioglass-ceramics developed in this program bond with certain charged polypeptide groups. Strength of bonding depends upon composition of this biomaterial and the number and type of charged groups on the polypeptide.

18. Application of the protein-mineral epitaxial results obtained in this program has been made to the problem of urolithiasis. The interfacial interactions between the inorganic substances and organic matrix in the formation of urinary stones is akin to the type of interfacial interactions being examined in detail in this contract. Consequently, application of these results to other medical problems appears to be possible and our research has provided guidance on these matters wherever it seems justified.

In Vivo Studies of Bioglass-Tissue Interactions

19. Techniques to evaluate the nature of interfacial bonding between bioceramics and bone have been successfully developed. These techniques include transmission electron microscopy (TEM), scanning electron microscopy (SEM), microradiography, tetracycline tracers, optical microscopy, and electron microprobe analysis (EMP).

20. Nonporous 45S5 bioglass and crystallized bioglass-ceramics have been found to attach directly to bone by what appears to be a chemical bond. The strength of the bond is sufficient that implants in rat tibias or femurs and canine or monkey femurs cannot be forcibly extracted. The bonding strength is sufficient that the interfacial attachment of the bioglass implant to the bone will withstand the implant force of a milling machine cutting bar and diamond microtome.

21. Confirmation and extension of our earlier bone-bioglass interface reaction mechanism studies have been achieved by comparing 45S5, $45B_5S5$, 45S5F, and 52S4.6 bioglass-ceramics implanted in the cancellous bone of the proximal tibia of young rats. All of the implants grew with the newly forming bone away from the epiphyseal plate.

22. Ultrastructural studies of the bone-bioglass interface using TEM have led to a theory of the formation of the bond through the production of an amorphous surface gel on the bioglass extending over a distance of 800 to 1,000 Å. This layer may be equivalent to the substance comprising the "cement line" in mature bone. Osteoblasts lay down collagen fibers onto this amorphous bonding layer and mineralization then occurs within the collagen network. The resulting, highly elongated, crystals bridge the space between the implant surface and the mature bone.

23. Implantation of a series of bioglasses with variable phosphorus content has given support to the concept of the soluble silica-rich gel serving as an induction site for osteogenesis. In addition, there is an optimum phosphorus level in the bulk composition which leads to a situation where a sufficient but not excessive supply of calcium and phosphate ions is available for incorporation into the mineralization process.

24. Partial or complete substitution of potassium for sodium does not impair the formation of the bone-bioglass bond. This suggest that the role of these two elements in the formation of the bond is very similar. Substitution of magnesium for calcium does impair bond formation which is consistent with osteogenesis being sensitive to Ca/Mg ratios.

25. Bioglass surfaces implanted in rat femur and tibial cortical bone have been studied with Auger electron spectroscopy and ion milling. The existence of the calcium phosphate layer over the silica-rich gel, similar to what was found in vitro, has been confirmed. Organic constituents, C and N, were found in the calcium phosphate layer to a depth of 180 nm, resulting in a smooth transition between an organic composition at the outer surface to a composite organic-calcium phosphate layer that overlaps the silica-rich gel on the bioglass surface.

26. A technique has been developed for measuring the compositional gradient across the bone-bioglass bonding interface using electron microprobe analysis. Reflected light microscopy can be performed on the same sample which enables correlation between histological detail and compositional analysis.

27. Electron microprobe analysis of bioglass bonding layers in rat tibiae show that the Ca-P rich layer develops to a thickness of 30-40 μm during a period of 3 months after which it does not change.

28. Both compositional stability of the Ca-P rich layer and a strong mechanical bond at 28 months in rat tibiae indicate that no long term deterioration of the bonding interface occurs.

29. In vitro solubility studies show that crystallization does not significantly affect the rate of surface ion release from the bioglass-ceramics. Implants of identical specimens in rat cortices also show interfacial bonding of bone to the implant irrespective of degree of

crystallinity. This correlation shows for the first time that it is interfacial chemical variables that control ultrastructural compatibility of implants with bone rather than crystallographic or microstructural features of the implants.

30. Histological analyses of the tissue reactions at the interface of both 45S5F flame sprayed monkey hip prostheses and the new 52S4.6 immersion coated stainless steel prostheses show the absence of migration of metal particles into the tissue surrounding the implant with the bioglass coating. In contrast, the tissues around a surgical stainless steel screw of the same metal composition, without the bioglass coating, have been examined after an equivalent implantation time and show massive migration of metallic deposits into the tissues.

31. Sintered glasses and sintered composites behave quite differently than the bulk bioglasses. Necrosis and mineralization of the surrounding tissues was seen, and by 12 months the implants had become soft and friable. This reaction probably resulted from the microporosity of the glasses with an increased surface area for reaction with the surrounding tissues and fluids.

32. Physiological dosages of parathyroid extraction given to rats for 72 hours prior to sacrifice have not evoked an osteoclastic resorption at the interface of the bioglass-ceramic materials.

33. Human and chick fibroblastic tissues cultures exposed to glass-ceramic compositions (45S5F, $45B_5S5$ and 45S5) were fed and maintained under physiological conditions for periods of two and three weeks on bioglass substrates. During that time the cells were observed to attach to all of these bioglass-ceramic compositions and in some instances to multiply normally. A desensitization of the bioglass surface involving equilibration to solutions of tissue culture media is required to achieve maximum tissue culture compatibility.

34. Recent bone cell culture studies conducted in collaboration with Pfizer, Inc. show stable bone cells proliferating on bioglass samples to depths of 40-50 cells after 8 weeks. Active collagen generation has been demonstrated as early as three weeks.

35. Implants of the glass-ceramics of the 45S5F composition in the vastus lateralis muscle of the right hind leg of rats showed a fibrous tissue response with the tissues firmly adhering to the implant surface. The reactions to the implants can be interpreted to show early synovial cell type formation about the implant. It can be demonstrated that this cell layer is involved in phagocytosis of the implant.

36. Comparison of other glass-ceramic compositions, 45S5 and $45B_5S5$, in rat muscle showed that the more surface-reactive implant materials induced a more marked foreign body type reaction with multinucleated phagocytic cells attempting to destroy the implant. This general behavior is in marked contrast to that observed for the implant responses on bone. In bone, the more reactive glass surfaces induced osteoblastic formation and development of a chemical bond.

22

37. Implantation of metal and alumina canine fibular implants coated with bioglass with no internal immobilization led to non-unions of the artificial bone grafts, despite the encapsulation of the ends of the implants in generous callus. The implication is that the mechanism of bond formation depends on a sequence of events, and interruption of the sequence related to motion of the implant inhibits bond formation.

Mechanical Testing of the Bone-Bioglass Interface

38. Methods used for the mechanical testing of implants and implant-bone systems include a rapid loading torsional tester, a bi-axial flexure tests for disks of materials and a four-point loading bend test. A simple method for attaching strain gages to bone for the measurement of mechanical properties during mechanical loading has been accomplished.

39. A set of computer programs has been developed which allows the computation of torsional and bending stresses in arbitrary multiply-connected cross sections. The programs are user oriented, and allow a quite flexible input data structure. The program has been tested using certain configurations for which analytical stress distributions are available and has demonstrated accuracy to within five percent of the calculated value.

40. It has been shown that sufficient strength is developed at the interface of a bioglass-ceramic segmental bone replacement that a rat femur will fracture in the bone in torsion rather than at the materials-bone interface.

41. Biomechanical evaluation of femoral segemental replacement in primates has shown that the bond developed between the 45S5 bioglass-ceramic implants and bone was strong enough to cause the fracture developed in a torsional test to pass through the implant as well as the surrounding bone and the interface. This demonstrates that the bond strength is quite substantial. This type of strength has not been found in stainless steel implants flame sprayed with the 45S5F composition due to failure of the bioglass-metal interface.

42. An in vivo proof test for the ability of biomaterials to bond to bone has been developed. Small rectangular samples of the test material are implanted in rat tibiae and, after sacrifice at 10 or 30 days, subjected to a push-out force of 30 N. Implants which exhibit no gross motion due to this load are deemed bonded to bone.

43. The push-out test described above has been applied routinely to all materials undergoing implantation studies. This assures that any bonding failures are due to factors such as design of the implant or lack of fixation, rather than the chemical formulation of the material.

23

44. A partial hip prosthesis combining high strength mechanical behavior and controlled biocompatibility has been achieved on an exploratory scale by flame spray coating the 45S5F bioglass on 316L surgical stainless steel monkey hip prostheses. The hip prostheses have been evaluated in primate after a one-year implantation and show stable fixation in the intramedullary canal without the use of screws, cement, or any other means of mechanical fixation.

45. Fatigue studies of flame sprayed specimens show that stress and life are inversely related in a manner quite similar to that shown by ferrous materials. Specimens tested while submerged in distilled water exhibit a lower fatigue life than specimens tested dry. The wet specimens, however, exhibited much smaller cracks once failure began than the dry specimens.

46. The 316L stainless steel monkey femoral head prosthess has also been tested using bioglass coatings applied by the rapid immersion process. Post sacrifice tensile loads of 60 lbs could be applied to the prostheses after 8 weeks implantation. A second prostheses withstood a maximum of 137 lb force in tension without loosening after eight weeks. The ranges of motion of both legs in the animals appeared normal as did the capsule, cartilage and articulating surface of the prostheses.

47. In studies of the torsional strength of paired bones from three groups of animals it has been shown that there is no significant left-right bias in the measured strength, and that the standard deviation of the percent difference side-to-side strength is typically about 0.10.

48. Evaluation of implants, particularly after failure of the device, requires that biomechanical factors be studied as intensively as the composition and behavior of the material.

IV. CUMULATIVE LIST OF PUBLICATIONS
RESULTING FROM THE CONTRACT

1. L. L. Hench, R. J. Splinter, W. C. Allen and T. K. Greenlee, Jr., "Bonding Mechanisms at the Interface of Ceramic Prosthetic Materials," J. Biomed. Mater. Res. Symp., No. 2, Interscience, New York, 1972, pp. 117-141.

2. C. A. Beckham, T. K. Greenlee, Jr., and A. R. Crebo, J. Calcified Tissue Res., 8 [2] (1971).

3. G. Piotrowski and G. A. Wilcox, "The STRESS Program: A Computer Program for the Analysis of Stresses in Long Bones," J. Biomech., 4, 497-506 (1971).

4. T. K. Greenlee, Jr., C. A. Beckham, A. R. Crebo and J. C. Malmborg, J. Biomed. Mat. Res., 6, 244 (1972).

5. L. L. Hench and H. A. Paschall, "Direct Chemical Bonding Between Bio-Active Glass-Ceramic Materials and Bone," J. Biomed. Mater. Res. Symp., No. 4 (1973) 25-42.

6. B. A. Hartwig and L. L. Hench, "The Epitaxy of Poly-L-Alanine on L-Quartz and a Glass-Ceramic," J. Biomed. Mat. Res., 6 [5], 413-424 (1972).

7. L. L. Hench, "Factors in Protein-Mineral Epitaxy," in Urolithiasis: Physical Aspects, B. Finlayson, L. L. Hench and L. H. Smith, eds., National Academy of Sciences, Washington, D. C. (1972), pp. 203-215.

8. L. L. Hench, T. K. Greenlee, J., W. C. Allen and G. Piotrowski, "An Investigation of Bonding Mechanisms at the Interface of a Prosthetic Material," Reports #1, #2, #3, #4, #5, #6, and #7, U.S. Army Research and Development Command, Contract No. DADA17-70-C-0001 (1970, 1971, 1972, 1973, 1974, 1975, and 1976).

9. L. L. Hench, "Ceramics, Glass and Composites in Medicine," Medical Instrumentation, 7 [2] (March-April 1973) 136-144.

10. L. L. Hench and H. A. Paschall, "Histo-Chemical Responses at a Bio-materials Interface," J. Biomed. Mats. Res., No. 5 (Part 1) (1974) 49-64.

11. L. L. Hench, "Factors Affecting the Physiological Interface and Ceramics," Proceedings of Surfaces and Interfaces of Glass and Ceramics, Frechette, LaCourse, Burdick, eds., Plenum Press (1974) 265-283.

12. A. E. Clark, L. L. Hench and H. A. Paschall, "The Influence of Surface Chemistry on Implant Interface Histology: A Theoretical Basis for Implant Materials Selection," J. Biomed. Mats. Res. Symp., "Materials for Reconstructive Surgery," Clemson Univ. (1974).

13. L. L. Hench, "Biomedical Applications and Glass Corrosion," *Proceedings of Xth International Congress on Glass*, Kyoto, Japan (1974).

14. C. G. Pantano, Jr., A. E. Clark, Jr. and L. L. Hench, "Multilayer Corrosion Films on Glass Surfaces," *J. Amer. Ceram. Soc.*, 57 [9] (1974) 412-413.

15. G. Piotrowski, L. L. Hench, W. C. Allen and G. J. Miller, "Mechanical Studies of the Bone-Bioglass Interfacial Bond," *J. Biomed. Mats. Res. Symp.*, 9 [6] (1975) 47-61.

16. L. L. Hench, "Prosthetic Implant Materials," *Annual Review of Materials Science*, R. A. Huggins, R. H. Rube, R. W. Roberts, eds., Annual Reviews, Inc., Palo Alto, California (1975) 279-300.

17. L. L. Hench, H. A. Paschall, W. C. Allen and G. Piotrowski, "Interfacial Behavior of Ceramic Implants," National Bureau of Standards Special Publication 415, May 1975, 19-35.

18. L. L. Hench and E. C. Ethridge, "Biomaterials--The Interfacial Problem," *Advances in Biomedical Engineering*, J.H.U. Brown and J. F. Dickson, eds., Academic Press, N.Y. (1975) 36-139.

19. A. E. Clark, Jr., H. A. Paschall, L. L. Hench and M. S. Harrell, "Compositional Analysis of the Formation of Bone-Implant Bond," *J. Biomed. Mats. Res. Symp.*, "Materials for Reconstructive Surgery," Clemson Univ. (1975).

20. A. E. Clark, Jr., H. A. Paschall, L. L. Hench and M. S. Harrell, "Surface Chemical Analysis of Bioglass Orthopaedic Implants," *J. Biomed. Mats. Res. Symp.*, "Materials for Reconstructive Surgery," Clemson Univ. (1975).

21. L. L. Hench, "Ceramic Implants," Proceedings of the 15th Annual ASME Symp. on Resources Recovery, Albuquerque, New Mexico, March 6-7, 1975, pp. 197-207.

22. A. E. Clark, Jr., C. G. Pantano, Jr. and L. L. Hench, "Auger Spectroscopic Analysis of Bioglass Corrosion Films," *J. Amer. Ceram. Soc.*, 59, [1-2] (1976) 37-39.

23. A. E. Clark, Jr. and L. L. Hench, "The Influence of P^{+3}, B^{+3}, and F^{-} on the Corrosion Behavior of an Invert Soda-Lime-Silica Glass," accepted by *J. Amer. Ceram. Soc.* (1976).

24. L. L. Hench, "Development of a New Biomaterial-Prosthetic Device," *Orthopedic Mechanics*, D. Ghista, ed., Academic Press, in press.

25. G. J. Miller and G. Piotrowski, A Brief Note on the Variability of the Torsional Strength of Paired Bones, J. Biomech., 7 (1974) 247-248.

26. G. Piotrowski, Clinical Biomechanics," presented to the Symposium on Retrieval and Analysis of Orthopaedic Implants, March 5, 1976 (Proceedings to be published as N.B.S. Special Publication).

27. G. J. Miller, D. C. Greenspan, G. Piotrowski and L. L. Hench, "Mechanical Evaluation of Bone-Bioglass Bonding," 8th Annual International Biomaterials Symp., April 9-13, 1976, Philadelphia, Pa.

28. L. L. Hench, "The Processing of Bioceramics," in International Ceramurgica, Proceedings of Conf. in Rimini, Italy, July 1976.

29. L. L. Hench, G. Piotrowski, H. A. Paschall, G. Miller, P. Buscemi, D. Greenspan, and T. Carr, "Prosthetic Joint Fixation of Bioglass-Bone Bonding," Clinical Orthopedics (in press).

30. L. L. Hench, C. G. Pantano, P. J. Buscemi, and D. C. Greenspan, "Analysis of Bioglass Fixation of Hip Prostheses," J. Biomed. Maters. Res. 11, No. 2, (1977) 267-281.

31. D. E. Clark, C. G. Pantano, Jr., and L. L. Hench, Glass Durability, Glass Industry, publisher (in press).

32. L. L. Hench, Physical Chemistry of Glass Surfaces Proceedings of XIth International Congress on Glass, Prague, Czechlosovakia (1977).

33. L. L. Hench, "Bioceramics," 12th State of the Art Symposium on Ceramics in Service to Man, National Academy of Sciences, Washington, D. C., June 1976.

V. REVIEW OF PROGRESS

A detailed description of the progress made in this program during the 1976-1977 contract year is presented in the form of six papers, and three progress reports.

A. Compositional Dependence of the Bone-Bioglass Bond,
M. M. Walker and L. L. Hench

I. Introduction

The ability of bioglass to promote secure boney attachment has been
well established (1-2). The most successful glass tested so far has
been that of the 45S5 composition (Table I). The bonding ability of
45S5 bioglass has been compared over the years to controls of dense
alumina, stainless steel and fused silica. All three of these other
materials have been shown to produce no significant bonding. The dif-
ference in behavior shown by fused silica (pure glassy SiO_2) vs bioglass
which is also a silicate based glass, is quite significant. It shows
that bonding of a material such as bioglass to bone is determined by
compositional factors. It is this dependence of bond on composition
that is studied in this project.

Through systematic and progressive compositional variation of our
standard 45S5 bioglass, limits are determined beyond which bonding no
longer occurs. This process defines a compositional range of SiO_2,
P_2O_5, CaO and Na_2O in which bonding will occur. It also establishes
whether all four of these components are necessary for bonding and if
not, which are superfluous. The shape and limits of the composition
region of bonding when plotted on a triaxial chart provides valuable
insight into the compositional factors involved in the basic mechanisms
of bonding. It is possible that the determination of this acceptable
compositional range will provide glasses of more suitable mechanical
or fabricative properties to be employed in clinical prostheses. Glasses
of greater soft tissue stability that will also bond to bone may be an
added benefit from the study. Comparison of in vitro surface reactions
and in vivo response of pairs of compositions on either side of a bone
bonding boundary should establish the critical compositional factors
producing a stable bond or no bond.

II. Results

Bioglass implants of varying compositions have been mechanically
tested using the rat tibial mini-push-out technique developed by Miller,
Greenspan, Piotrowski and Hench (3). This technique is full described
in Annual Report #7. In brief, however, the mechanical integrity of the
bioglass-bone bond is tested in the following manner: 4 x 4 x 1 mm
bioglass chips are implanted into a surgical defect wholly through the
anterior border of the tibia in a mid sagittal plane. After a given
healing period the animal is sacrificed and the tibia excised. The
exposed ends of the implant on either side of the tibia are cleaned of
overlying boney tissues. Modified sponge forceps are used to apply
push-out loads up to 30 newtons to the implant. Those implants that
resist being forced out under the full 30 N proof load have passed this
test for bonding. Those that are freed at 30 N or less have failed.

To date this technique has been used to evaluate a number of glass compositions for bonding.

Bioglass 45S5 (see tables for composition) was evaluated in the original development of this test. Of 30 samples tested at 10 days, 22 or 73% passed the 30 newton proof load. At 30 days, 30 out of 30 passed for a 100% pass rate. Control implants of stainless steel and Al_2O_3 show no bonding and were pushed out at substantially less than 10 N.

Bioglasses in which none, part, or all of the Na_2O was replaced with K_2O have also been tested using this procedure. The compositions tested are as follows:

Table I

Mole % Composition

#	Glass Code	SiO_2	P_2O_5	CaO	Na_2O	K_2O
1*	45S5 N	46.1	2.6	26.9	24.4	0
2	45S5 N_3K	46.1	2.6	26.9	18.3	6.1
3	45S5 NK	46.1	2.6	26.9	12.2	12.2
4	45S5 NK_3	46.1	2.6	26.9	6.1	18.3
5	45S5 K	46.1	2.6	26.9	0	24.4

or expressed in wt %:

Table II

wt % Composition

#	Glass Code	SiO_2	P_2O_5	CaO	Na_2O	K_2O
1*	45S5 N	45.0	6.0	24.5	24.5	0
2	45S5 N_3K	43.6	5.8	23.8	17.8	9.0
3	45S5 NK	42.3	5.6	23.1	11.5	17.5
4	45S5 NK_3	41.1	5.5	22.3	5.6	25.5
5	45S5 K	39.9	5.3	21.8	0	33.0

Each composition was tested in triplicate after both 10 and 30 days implantation. The results are as follows:

In Table III a pass rating was given when the implant withstood the proof load of 30N. Further indication of the stability of the bond was seen when almost all of those passing the mini-push out test remained firmly attached to bone even when the implant was sectioned with a saw.

---

*These glasses are identical to 45S5

Table III

Mini Push Out Results

#	Glass Code		10 Days	30 Days
1	45S5 N	A	Failed	Passed
		B	No Test; Broken Leg	Passed
		C	Passed	Passed
2	45S5 N_3K	A	Pased	Passed
		B	Failed	Broken Leg No Test
		C	Failed	Passed
3	45S5 NK	A	Failed	Broken Leg No Test
		B	Failed	Passed
		C	No Test; Broken Leg	Passed
4	45S5 NK_3	A	Passed	Passed
		B	Passed	Passed
		C	No Test; Broken Leg	Passed
5	45S5 K	A	Failed	Passed
		B	Failed	Passed
		C	Failed	Passed

These results indicate that there is no major differences between the bonding abilities of glasses in which some or all of the Na_2O is replaced with K_2O. The role in bonding played by Na_2O is probably the same as K_2O.

This is an especially important finding because it is contrary to a claim of German Patent #DT 23 26 100. Although no data is presented, the German patent claims that a compositional modification of the 45S5 formula developed in our program and commonly in use in our studies by substituting K_2O for Na_2O results in an improvement of biological properties. The data of this study shows no difference within the 30 day test period. Data from 10 days implantation suggest that the K_2O substitution may in fact have decreased the rate of formation of a good bond. A statistical study would have to be conducted to prove this indication, however. We propose to examine this variable further.

One reason for our concern for understanding the importance of substitution of K_2O for Na_2O is the extensive tissue culture investigations of Rappaport (4), where she showed far superior compatibility of various cultures with glass discs containing K_2O. Her theory that this positive response was due to the K^+ ions interacting beneficially with cell membranes might suggest such an improvement in behavior with K_2O containing bioglasses. In another study involving tendon implants of

K_2O containing bioglasses we saw no beneficial effect. Also a previous dental implant study has shown a lack of bonding of KCP1 bioglass while the 45S5 composition bonds quite well. The composition of glasses used as the dental implants are shown below in mole percent.

	SiO_2	P_2O_5	CaO	Na_2O	K_2O
KCP1	50.3	2.8	24.4	0	17.5
45S5 K	46.1	2.6	26.9	0	24.4
45S5	46.1	2.6	26.9	24.4	0

Note that the KCP1 glass contains a significantly lower mole percentage of alkali (Na_2O or K_2O) than does 45S5 or 45S5 K. Since it has been shown that replacing Na_2O with an equal molar amount of K_2O produces no noticeable decrease in bonding to bone, it is probable that the lack of bonding of dental implants of KCP1 is due to the low alkali content. As discussed below, we now know that variations in SiO_2/alkali ratio strongly influence formation of the biological bond.

Bioglass compositions in which the molar SiO_2 content has been altered at the expense of (CaO + Na_2O) with P_2O_5 held constant have been tested. These compositions in which testing has been completed or is in progress are listed in Table IV and plotted triaxially on Figure 1.

Table IV

Mole % Composition

#	Glass Code	SiO_2	P_2O_5	CaO	Na_2O
6	42S 5.6	42.1	2.6	29.0	26.3
7*	46S 5.2	46.1	2.6	26.9	24.4
8	49S 4.9	49.1	2.6	25.3	23.0
9	52S 4.6	52.1	2.6	23.8	21.5
10	55S 4.3	55.1	2.6	22.2	20.1
11	60S 3.8	60.1	2.6	19.6	17.7
12	100S	100.0	0	0	0

*Same as the 45S5 composition
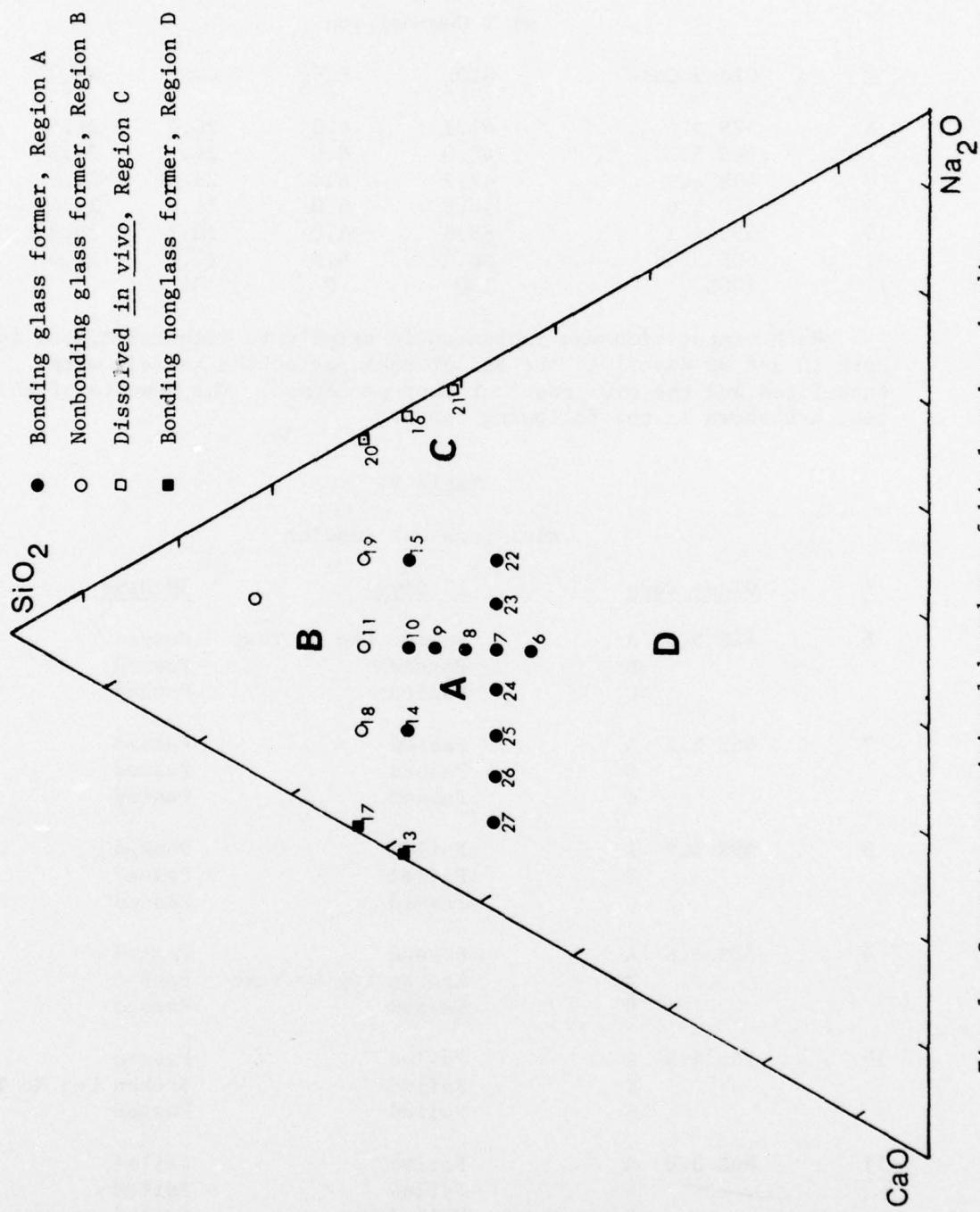
Fig. 1. Current compositional boundary of bioglass bone bonding.

Expressed at wt %:

Table V

wt % Composition

#	Glass Code	SiO_2	P_2O_5	CaO	Na_2O
6	42S 5.6	41.1	6.0	26.4	26.5
7*	46S 5.2	45.0	6.0	24.5	24.5
8	49S 4.9	47.9	6.0	23.0	23.1
9	52S 4.6	50.8	6.0	21.6	21.6
10	55S 4.3	53.6	6.0	20.2	20.2
11	60S 3.8	58.4	6.0	17.2	17.8
12	100S	100	0	0	0

Each composition was implanted in triplicate (labeled A,B,C) for both 10 and 30 days. At the end of each period the animals were sacrificed and the mini push out test performed. The results of this test are shown in the following table.

Table VI

Mini Push Out Results

#	Glass Code		10 Days	30 Days
6	42S 5.6	A	Broken Leg No Test	Passed
		B	Passed	Passed
		C	Failed	Passed
7	46S 5.2	A	Passed	Passed
		B	Passed	Passed
		C	Passed	Passed
8	49S 4.9	A	Failed	Passed
		B	Failed	Passed
		C	Passed	Passed
9	52S 4.6	A	Passed	Passed
		B	Broken Leg No Test	Passed
		C	Passed	Passed
10	55S 4.3	A	Failed	Passed
		B	Failed	Broken Leg No Test
		C	Failed	Passed
11	60S 3.8	A	Failed	Failed
		B	Failed	Failed
		C	Failed	Failed
12	100S	A	Failed	Failed
		B	Failed	Failed
		C	Failed	Failed

*Same as the 45S5 composition.

The samples tested at 10 days were loaded to 22-30 Newtons. The samples tested after 30 days were all loaded to approximately 30 N.

As shown above none of the composition 55S 4.3 were securely bonded after 10 days implantation, while those of lower SiO_2 content close to our standard 45S5 formula were firmly bonded.

The working theory of bioglass bonding (discussed in detail in other papers) indicates that the formation of a bond is at least in part due to the production of an active surface gel layer on the implant. The rate of production of this gel layer is thought to be determined by the ratio of network formers (SiO_2 and P_2O_5) to network modifiers (Na_2O and CaO). Glasses of higher SiO_2 content are generally less reactive and produce this gel layer less rapidly. The lack of bonding of the higher SiO_2 glasses tested seems to indicate that at least after ten days the glass has not formed a gel layer sufficient for secure bonding. It would seem that this is due to a low reactivity of the glass. Thus, if this were true, bonding at longer periods of implantation might occur after the implant had sufficient time to establish an acceptable gel layer.

The results of the thirty day implant series support this hypothesis. The 55% SiO_2 implants which would not bond at ten days were shown to bond at thirty days using the mini push out test.

The thirty day implant of 55% SiO_2 which was deleted due to a broken leg failed at minimal load. Examination of the area surrounding the implant revealed that most of implant was adjacent to calcified tissue. Thirty day implants at 42% and 52% SiO_2 in which the tibiae had broken and had partially healed were found still to be bonded strongly enough to pass the mini push out test. Examination of the area about the implant in the case of 42% SiO_2 composition revealed that only about half of the implant was surrounded by calcified tissue. The distal half was enclosed in soft callus tissue. The passing of the mini push out test by this implant and the failure of the 55% SiO_2 implant under similar conditions indicates that the strength of the bond of 55% SiO_2 glass to be less than the bond strengths of the glasses of lower SiO_2 content.

This was further substantiated by a second qualitative observation.

After mini push out testing, the tibia was sectioned just above and below the implant (see Fig. 2). In some cases the cuts were made so close to the proximal and distal edges of the implant that the bone on either side of the implant was not directly connected to the other, but only through the intervening implant. After such sectioning the integrity of the bond was again challenged. Considerable force was applied by hand in an attempt to separate the bone from the glass. In all the samples tested the SiO_2 content was 52% or less, the bone was not separated from the glass either by sectioning or by applying manual force. The 55% SiO_2 implant tested in this manner was found to easily separate from the enclosing bone. Again this indicates that the strength of the bioglass-bone bond of the 55% SiO_2 is less than the bonds formed with implants of lower SiO_2 content.

Tibia Top (anterior) view

Proximal-

--- Implant

.... Plane of saw cut

Distal-------

Tibia Side View

Proximal-

- Plane of saw cut

Figure 2

36
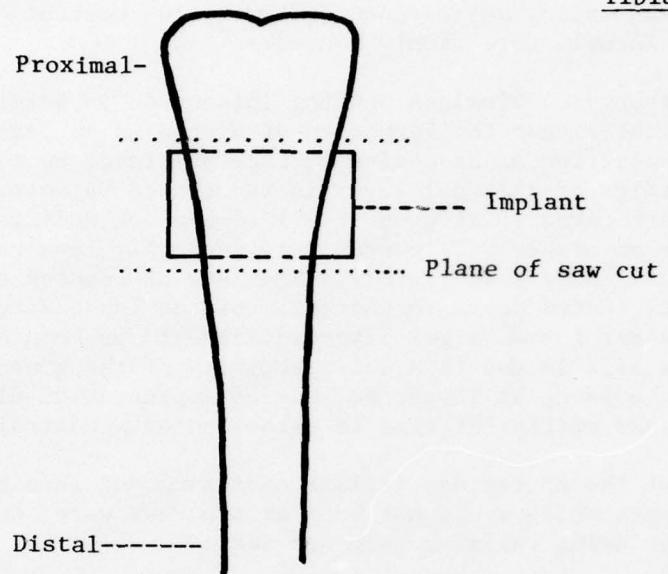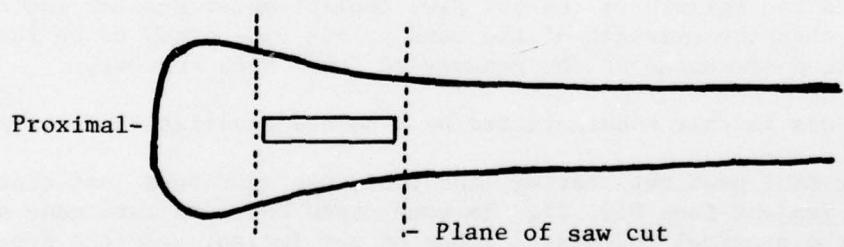
Further tests are underway to determine if increasing the SiO_2 content above 55% will reduce the bond strength even more and thereby produce bond failure under the mini push out test. Increasing the applied load of the mini push out test by using the Instron testing machine is planned for further work so as to further delineate the dependence of bond strength on SiO_2 content.

To further delineate the composition range of bonding dependence, the ratio of CaO/Na_2O has also been varied (see triaxial plotting, Fig. 1) in our recent work. The compositions are as follows:

Table VII

Mole % Composition

Glass #	Glass Code	SiO_2	P_2O_5	CaO	Na_2O
13	46S 6.7	46.1	2.6	34.9	16.4
14	46S 5.9	46.1	2.6	30.9	20.4
15	46S 4.4	46.1	2.6	22.9	28.4
16	46S 3.6	46.1	2.6	18.9	32.4

Expressed in wt %:

Table VIII

wt % Composition

Glass #	Glass Code	SiO_2	P_2O_5	CaO	Na_2O
13	46S 6.7	45.4	6.0	32.0	16.6
14	46S 5.9	45.2	6.0	28.2	20.6
15	46S 4.4	44.8	6.0	20.8	28.4
16	46S 3.6	44.6	6.0	17.1	32.4

Each sample was tested in triplicate (labeled A,B,C) 10 and 30 days after implantation. The results are shown in Table IX.

The results of the 10 day implants of the series in Table IX show that bonding will occur over a large range of CaO/Na_2O ratios. As shown on the triaxial plot the molar percent of SiO_2 and P_2O_5 are held constant while CaO and Na_2O are varied relative to each other.

It is known that calcium silicate glasses are much less reactive than sodium silicate glasses in aqueous solutions. Through increasing the CaO content at the expense of Na_2O it is thought that a less corrosive glass will result. Eventually this reactivity should be so low as to prevent

Table IX

Mini Push Out Results

Glass #	Glass Code		10 Days	30 Days
13	46S 6.7	A	Passed	Passed
		B	Passed	Passed
		C	Passed	Passed
14	46S 5.9	A	Passed	Passed
		B	Passed	Passed
		C	Passed	Passed
15	46S 4.4	A	Passed	Passed
		B	Passed	Passed
		C	No Test Leg Broken	Passed
16	46S 3.6	A	Passed	Passed
		B	Passed	Passed
		C	Passed	Passed

the formation of a gel layer and hence, bonding. Apparently this limit was not reached in the compositional series listed in Table IX. Future work will extend this work and test glasses of higher CaO contents.

A previous investigation during the last couple of years (5) also examined the effect of varying P_2O_5 over a range of 0-12 weight percent. Previous progress reports of this contract have discussed some of the results of the P_2O_5 dependence. To summarize, it was found that bone bonding was more favorable within the range of 3-6 w/o P_2O_5. At 0%, there was a tendency for a bond to form but it did not mature. At 12% excessive calcification appeared to induce a pathological response to the implants. Very large variations in the thickness of the reaction calcium phosphate films were found by AES as the P_2O_5 content was varied. A correlation between film thickness and histological results was reported (5). As a consequence of this previous study our animal prostheses evaluations are based upon a series of bioglass compositions with the P_2O_5 content maintained at 6 weight percent (2.6 mole percent).

References

1. L. L. Hench, T. K. Greenlee, and W. C. Allen, Reports #1, #2, and #3, August 1970, 1971 and 1972; U.S. Army Medical Research and Development Contract #DADA-17-70-C-0001.

2. L. L. Hench, H. A. Paschall, W. C. Allen and G. Piotrowski, Reports #4, #5, and #6, September 1973, 1974 and 1975; U.S. Army Medical Research and Development Command #DADA-17-70-C-0001.

3. G. J. Miller, D. C. Greenspan, G. Piotrowski, and L. L. Hench, 8th Annual International Biomaterials Symposium, held in Philadelphia, Pennsylvania, April 1976.

4. C. Rappaport, "Some Aspects of Growth of Mammalion Cells on Glass Surfaces," in the Chemistry of Biosurfaces, Vol. 2, Ch. 9, Hair, M. L. Ed., Marcel Dekker, Inc., New York, 1972.

5. A. E. Clark and L. L. Hench, in Report #5 (Ref. 2), September 1974, U.S. Army Research and Development Contract #DADA-17-70-C-0001.

B. Electron Microprobe Technique for Evaluating Bioglass-
    Bone Interfaces, D. E. Clark, S. R. Bates, M. S. Harrell
    and W. A. Acree

Introduction

This section reports procedures developed for compositional
analysis of bone-bioglass interfaces using the electron microprobe
(EMP). Compositional analysis of most glasses using electron bombard-
ment requires special techniques. During electron beam impingement on
the specimen surface local compositional changes occur due to diffusion
of mobile alkali species (1-3). The actual change in the glass compo-
sition exposed to the electron beam is dependent on beam current,
accelerating potential, bulk glass composition and the length of
exposure time. Several methods have been proposed in the literature
for minimizing glass compositional variations during analysis (3-5).
Clark et al. (4) developed an EMP technique for analyzing soda-lime-
silica glasses employing a defocussed 100 μm beam diameter and scanning
the surface at 150 μm/min. This is an excellent technique for macro-
scopic analysis of glass surfaces. However, for compositional inter-
facial analysis, the large beam size and rapid scanning procedure greatly
reduce the spatial resolution. Pantano et al. (6) have used a low temp-
erature Auger electron spectroscopy technique for glass analysis. During
analysis the specimen is maintained at liquid nitrogen and the alkali
ion mobility is significantly decreased. However, under the high current
densities normally encountered in EMP analysis the low temperature
technique is not very effective for reducing alkali mobility.

The objective of this study was to develop a reliable EMP method
for routine compositional analysis of bone-bioglass interfaces.

Experimental Procedure

The model used for this investigation was a 45S5 bioglass chip
(4 mm x 4 mm x 1 mm) which had been implanted in rat tibia for one year.
At sacrifice the tibia were sectioned to give specimens containing
bioglass bonded to bone. These were fixed in cold buffered qlutaralde-
hyde, dehydrated in alcohol and embedded in epoxy resin. The samples
were then ground to 600 grit SiC paper and polished through 1 μm diamond
paste exposing the bone-bioglass interface. Prior to analysis the
samples were coated with ∿100 Å carbon.

EMP* analyses were obtained at three locations on each sample using
both scanning and point counting techniques and accelerating potentials
of 10 KV and 20 KV. A 1 μm diameter electron beam maintained at 10^{-7} amps

---

*MS-64 Electron Microprobe, Acton Laboratories, Acton, MA.

40

was used and the X-ray intensities in counts per second (cps) were recorded. Scanning was performed by translating the sample under a stationary electron beam at a constant rate of 20 μm/min, starting in the bulk bioglass and moving perpendicular across the interface into the bone. The silicon and calcium X-ray intensities were continuously monitored on a strip chart recorder. A total of six scans was made; three scans at 10 KV and three scans at 20 KV. Fixed time point counts were taken in the tracks caused by the electron beams impinging on the surface of the specimen during scanning. Ten second point counts were obtained at 10 μm intervals in the scan tracks across the interface.

Results and Discussion

Compositional data obtained at 20 KV using both scanning and point counting techniques are shown in Figure 1. There is a wide scatter in the X-ray intensities for each element using the scanning versus the point counting technique. This scatter is more pronounced in the glass and interfacial layers than in the bone. Ideally, the X-ray intensities obtained for a specified current and accelerating potential should be the same for both point counting and scanning. However, as already discussed, alkali ion diffusion from under the electron beam yields a time dependent compositional analysis for most glasses. In the bulk glass, the silicon and calcium X-ray intensities are higher for point counting than for scanning, while in the interfacial layers the X-ray intensities of these elements are lower for scanning than for point counting. These trends are due to the fact that beam remains in one location for 10 seconds and during scanning the electron beam impinges on any 1 μm spot for only ~3 seconds. The 10 second impingement time causes more alkali diffusion from under the beam in the bulk glass than does the 3 second impingement. This effectively produces greater relative concentrations of silicon and calcium during point counting than during scanning. However, in the interfacial layers, relatively little alkali species is present and the variation in concentration of other species in the layers are dependent upon the beam damage since more beam damage is encountered with point counting. The concentration of all species appear lower in the interfacial layer when point counting is used instead of scanning.

Figure 2 presents compositional data obtained with the EMP employing a 10 KV accelerating potential. These data were taken in approximately the same location on the specimen as those shown in Figure 1. The relative X-ray intensity for each element at 10 KV is approximately one half the intensity for the same elements at 20 KV. Significantly, at 10 KV the variations in X-ray intensities between point counting and scanning are within the error bounds normally expected with EMP analysis. These results suggested that both the alkali diffusion problem and electron beam damage to the specimen
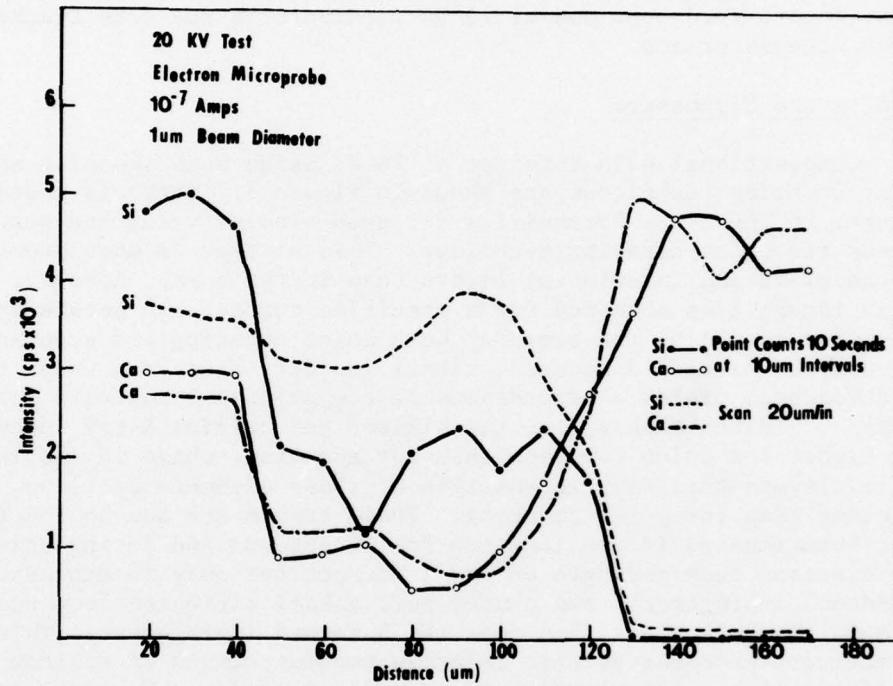
Figure 1.   Elemental X-ray intensities across a 1 year implant
bioglass-bone interface. Data was obtained at 20 KV
using both scanning and point counting techniques.
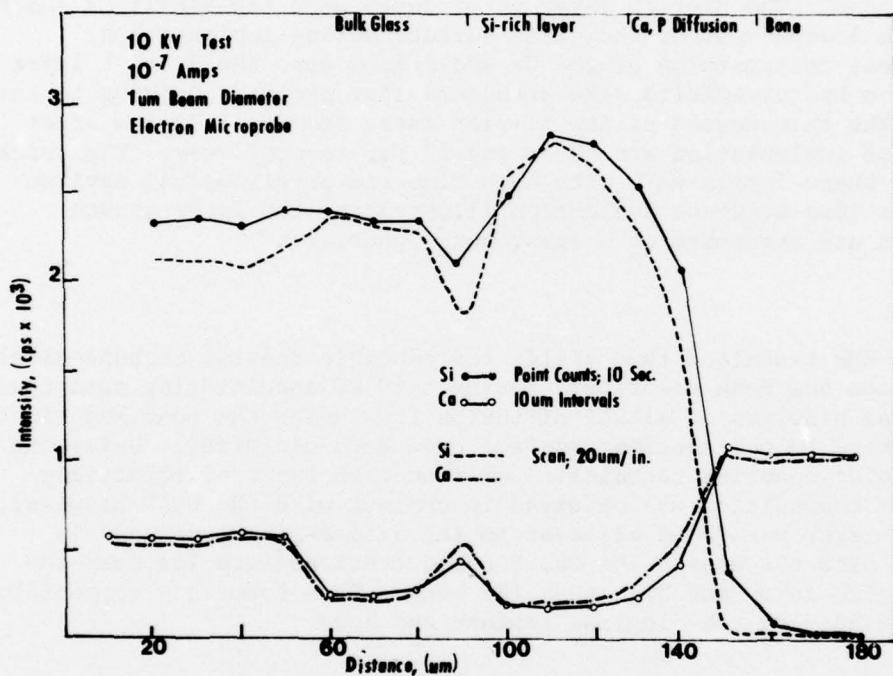
Figure 2. Elemental X-ray intensities across a 1 year implant
          bioglass-bone interface. Data was obtained at 10 KV
          using both scanning and point counting techniques.

surface are much less at 10 KV than at 20 KV. The scanning electron micrograph* in Figure 3 shows a typical interfacial area scanned and point counted at both 30 KV and 10 KV. The beam damage to the specimen is much less at 10 KV than at 20 KV. Furthermore, the beam damage to the bone is not as great as to the bioglass and interfacial layers.

Four distinct compositional regions are illustrated in Figure 2; 1) bulk bioglass, 2) a Si-rich layer, 3) a Ca, P diffusion layer, and 4) bone. The Si-rich layer is produced when the alkali Ca and P ions are leached out of the glass surface during implantation. Subsequent redeposition of the Ca and P ions onto the Si-rich layer creates a hydroxyapatite like structure that promotes bonding to the bone. The thicknesses of the Si-rich layer and Ca, P layers after 1 year of implantation are 60 μm and 30 μm, respectively. The thickness of these layers vary with both time and physiological environment. A time-sequence evaluation illustrating the layer growth kinetics are presented in a subsequent paper (7).

Summary

An EMP technique that yields reproducible results of bone-bioglass interfaces has been described. Using a 10 KV accelerating potential, the usual problems of alkali diffusion from under the beam and electron beam damage to the specimen surface have been minimized. Using the 10 KV point counting technique a silicon-rich layer of relatively constant composition was observed in contact with the bulk bioglass. A Ca, P layer was found adjacent to the silica-rich layer and in contact with the bone. The Ca, P concentrations were low near the silica-rich layer and high near the bone. Thus forming a compositional gradient between the bioglass implant and bone.

References

1. J. L. Lineweaver, "Oxygen Outgassing Caused by Electron Bombardment of Glass," J. Appl. Phys., 34 [6], 1786-1979 (1963).

2. M. P. Borom and R. E. Hanneman, "Local Compositional Changes in Alkali Silicate Glasses During Electron Microprobe Analysis, J. Appl. Phys., 38 [5], 2406-2407 (1967).

3. A. K. Varshneya, A. R. Cooper and M. Cable, "Changes in Composition During Electron Microprobe Analysis of $K_2O-SrO-SiO_2$ Glass," J. Appl. Phys., 37 [5], 2199 (1966).

*Cambridge stereoscan scanning electron microscope, Kent Cambridge Scientific, Inc., Morton Grove, Ill.

4. D. E. Clark, L. L. Hench and W. A. Acree, "Electron Microprobe Analysis of $Na_2O-CaO-SiO_2$ Glass," J. Amer. Ceram. Soc., <u>58</u> [11-12], 531 (1975).

5. L. F. Vassamillet and V. F. Caldwell, "Electron-Probe Microanalysis of Alkali Metals in Glass," J. Appl. Phys., <u>40</u> [4], 1637-1643 (1969).

6. C. G. Pantano, Jr., D. B. Dove and G. Y. Onoda, Jr., "AES Analysis of Sodium in a Corroded Bioglass Using a Lower-Temperature Technique," Appl. Phys. Lett., <u>26</u> [11], 601-602 (1975).

7. M. S. Harrell, W. A. Acree, M. A. Keane, S. R. Bates, D. E. Clark, A. E. Clark and L. L. Hench, "Effects of Time on the Thickness of Bioglass Bonding Layers," Report #8, U.S. Army Medical Research and Development Command, Contract #DAMD17-76-C-6033 (1977).

Figure 3. Scanning electron micrograph (550X) of the 1 year
implant bioglass-bone interface. The extent of
electron beam damage at both 10 KV and 20 KV can
be observed.

C. Effects of Time on the Thickness of Bioglass Bonding
    Layers, M. S. Harrell, W. A. Acree, M. A. Keane,
    S. R. Bates, D. E. Clark, A. E. Clark and L. L. Hench

Introduction

Development of new analytical means for investigating the
chemical bonding of bioglass to bone has recently been an area of
major accomplishment. Previous reports have described the develop-
ment of various transmission electron microscopy (TEM), scanning
electron microscopy (SEM) with energy dispersive X-ray analyses (EDXA),
and Auger electron spectroscopy methods applied to the bioglass-bone
interface.

The bonding of bioglass to bone has long been well established (1,2).
The mini-push out test has shown that mechanical fixation of the bone-
bioglass bond reliably occurs by 1 month in rat tibia (3). Auger spectro-
scopic studies (4) have shown that the formation of reaction layers
begins within the first hours after surgical implantation. Transmission
electron microscopy and analytical scanning transmission electron
microscopy (ASTEM) of the bone bioglass junction show ultrastructural
evidence of similar compositional gradients across the interface (5).
The histological integrity of the bone bonded to bioglass is also well
established (6,7).

Methods have been developed for obtaining ground and polished 100 μm
thick sections for transmitted light microscopy without loss of the
bonding interface during specimen preparation. The reflected light micro-
graph samples are especially suited for quantitative analysis of the
compositional changes occurring across the bonding interface using the
electron microprobe analyzer (EMP). EMP analysis of the development of
the bonding layers between bioglass and bone has been completed.

This paper reports results of work done to investigate in vivo the
reaction layers formed on the surface of bioglass implants in rat tibiae.
Metallographic techniques were adapted for the preparation of biological
specimens so that the specimens can be studied by reflected light micros-
copy, electron microprobe, scanning electron microscopy with energy
dispersive X-ray analysis, and finally by transmitted light microscopy on
sections of approximately 100 μm thickness.

The techniques developed for this study enable us for the first time
to see a cross section of the whole implant in its interrelationship with
the rat tibia both by reflected light microscopy and by transmitted light
microscopy. In addition, electron microprobe profiles provide a measure-
ment of the thicknesses of the reaction layers on the bulk glass as well
as the thicknesses of newly formed bone within the medullary canal and on
those surfaces of the implant which protrude through the boney cortex.

Experimental Procedures

45S5 bioglass chips, 5 x 4 x 1 mm, were placed in the left tibia of male Sprague Dawley-Dublin rats weighing approximately 200 g according to the procedure described elsewhere (7). The animals were sacrificed after 1, 3, 6, 12, and 28 months. Samples harvested at sacrifice were fixed in cold buffered glutaraldehyde, dehydrated through a series of alcohols, and embedded in epoxy resin. One sample from each time period was sawed with a jeweller's saw through the bone and the bioglass implant in order to yield a cross-sectional view (Fig. 1) showing the implant in contact with cortical bone. These samples were polished through 600 grit SiC paper and with the 1 μm diamond paste. Reflected light micrographs were taken using the Research II Metallograph. Each sample was coated with a thin layer of carbon (∿100 Å), placed in the electron microprobe, and analyzed for silicon, calcium, and phosphorus across the bone/bioglass interface for a distance of about 150-200 μm while moving from bulk glass into bone. A 1 μm electron beam diameter maintained a 10^{-7} amps was used for each specimen evaluation. The accelerating potential was 10 KV and the samples were point counted for 10 seconds at 5 μm intervals. Scanning electron microscopy (SEM) - energy dispersive X-ray analysis (EDXA) was performed on the one month specimen to corroborate the EMP and light microscopy results.

The one month and 28 month samples were sectioned with a low speed diamond saw yielding a section about 300 μm thick. This section was thinned with SiC papers to a thickness of about 100 μm and polished with 6 μm and 1 μm diamond paste for transmitted light microscopy.

Results

The electron microprobe profiles and energy dispersive X-ray data confirm (8-10) the presence of a silicon-rich reaction layer on the bulk bioglass and a clacium phosphorus-rich layer between the Si-rich layer and the bone. The composition of the Si-rich layer appears to be relatively constant while the region referred to as the Ca, P-rich layer resembles a typical interfacial diffusion profile.

Microprobe data were obtained on regions extending from bulk bioglass into cortical bone. The EMP profile for the one month sample (Fig. 2) shows a Si-rich reaction layer of about 37 μm and a Ca, P-rich layer of about 42 μm thickness. Energy dispersive X-ray data for this sample (Fig. 3) provides confirmation of these areas, showing a high Si peak in Area 2 (the Si-rich layer), increased Ca and P in Area 3 (the Ca, P-rich layer), and the absence of silicon in bone (Area 4). For comparison, a scan was obtained from bioglass into new medullary bone (Fig. 4).

Electron microprobe profiles for 3, 6, 12, and 28 months (Figs. 5, 6, 7 and 8) show thicknesses of 45 μm, 54 μm, 60 μm and 190 μm respectively for the silicon rich layer. For the Ca, P-rich layer the thicknesses are 28 μm, 29 μm, 30 μm and 30 μm for 3, 6, 12 and 28 months, respectively.
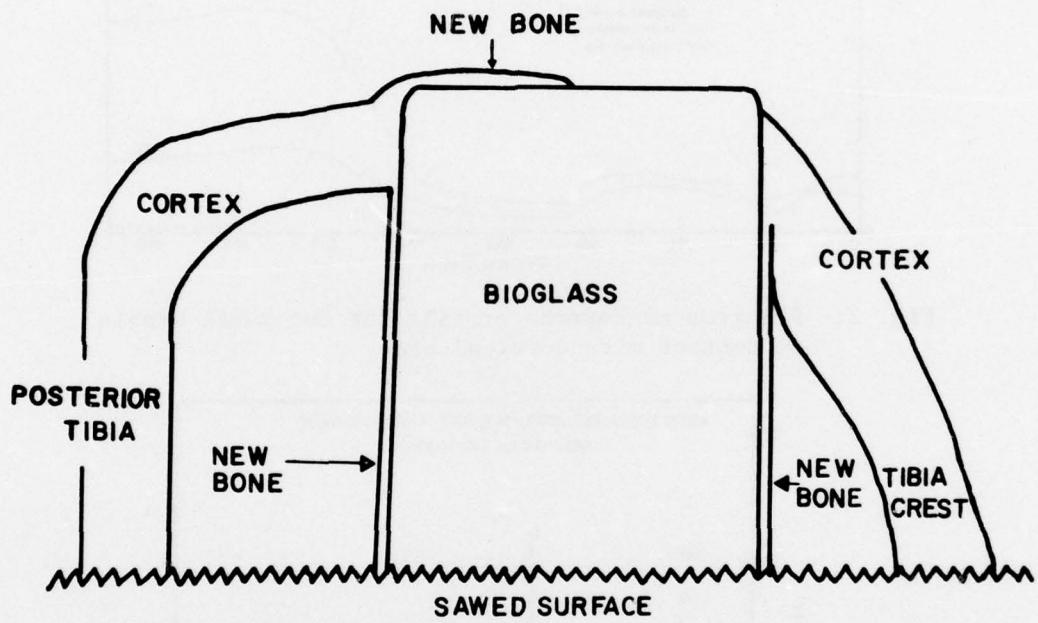
Fig. 1. Schematic drawing showing cross sectional view of
bioglass implant in the rat tibia.
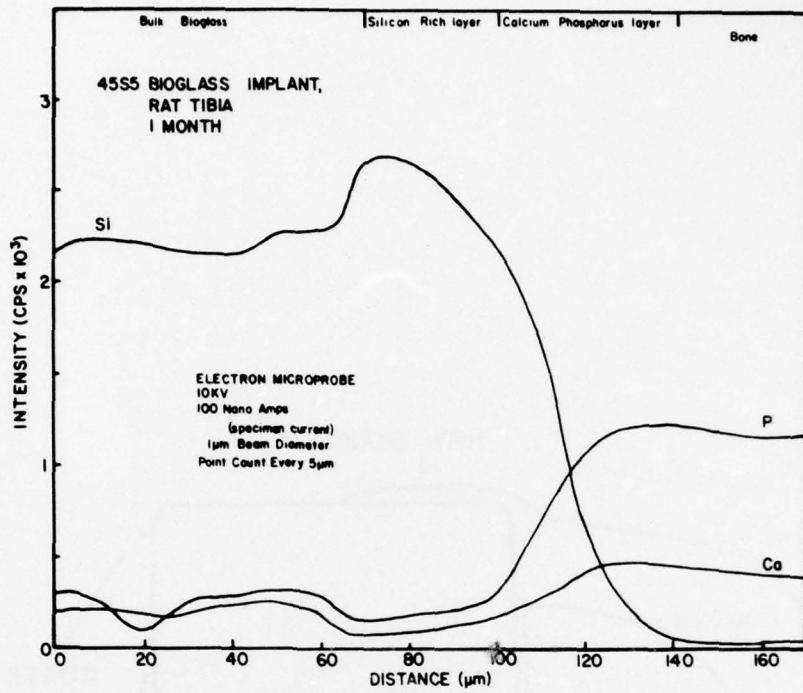
Fig. 2. Electron microprobe profile for one month sample on contact with cortical bone.
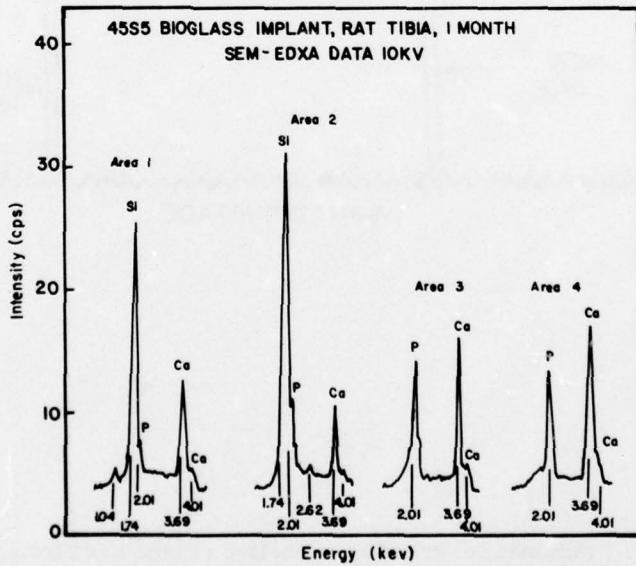
Fig. 3. SEM-EDXA data for one month sample. Areas 1,2,3 and 4 are also labelled in the micrographs (Figs. 8 and 10) and correspond to 1) bulk bioglass, 2) Si-rich layer, 3) Ca, P-rich layer and 4) bone.
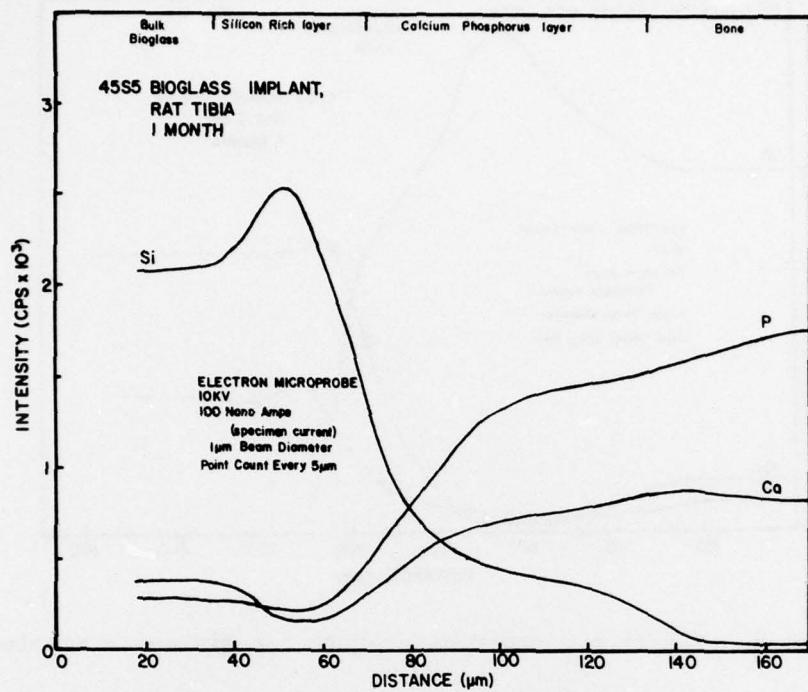
Fig. 4.   Electron microprobe profile for one month sample
          (into medullary bone).
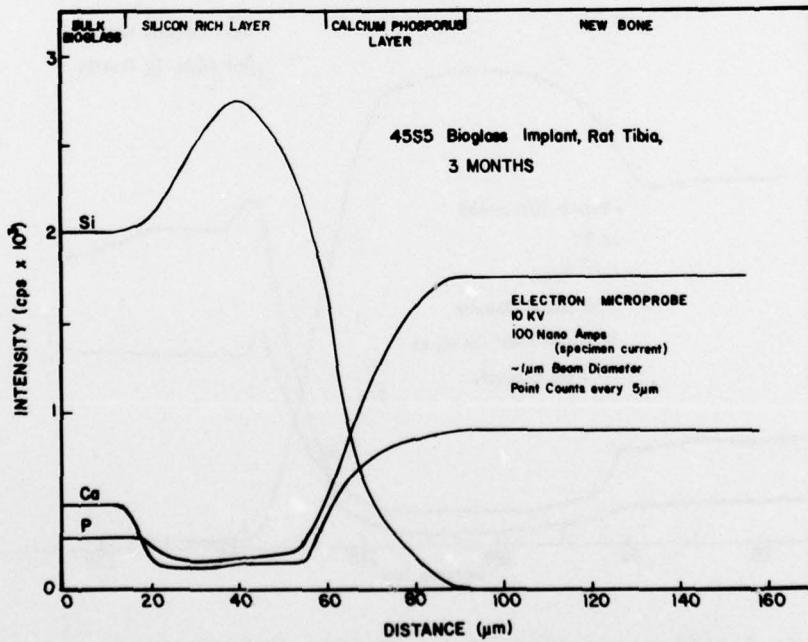
Fig. 5.   Electron microprobe profile for three month sample.
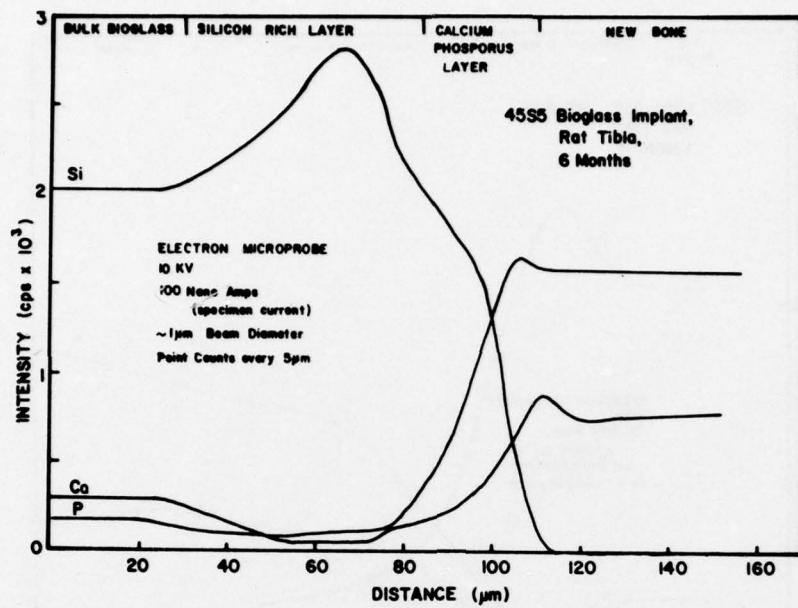
Fig. 6. Electron microprobe profile for six month sample
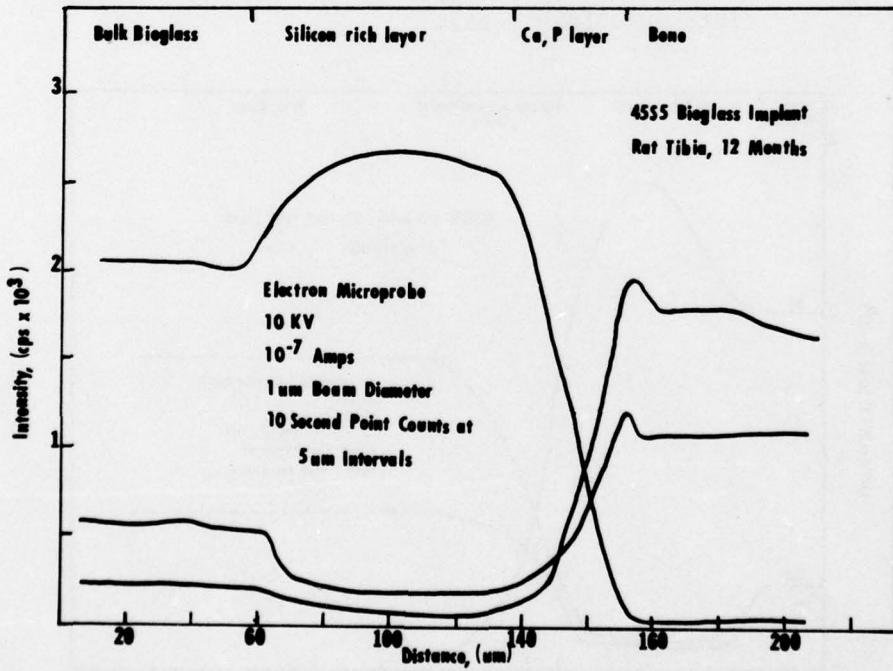
Fig. 7. Electron microprobe profile for one year.
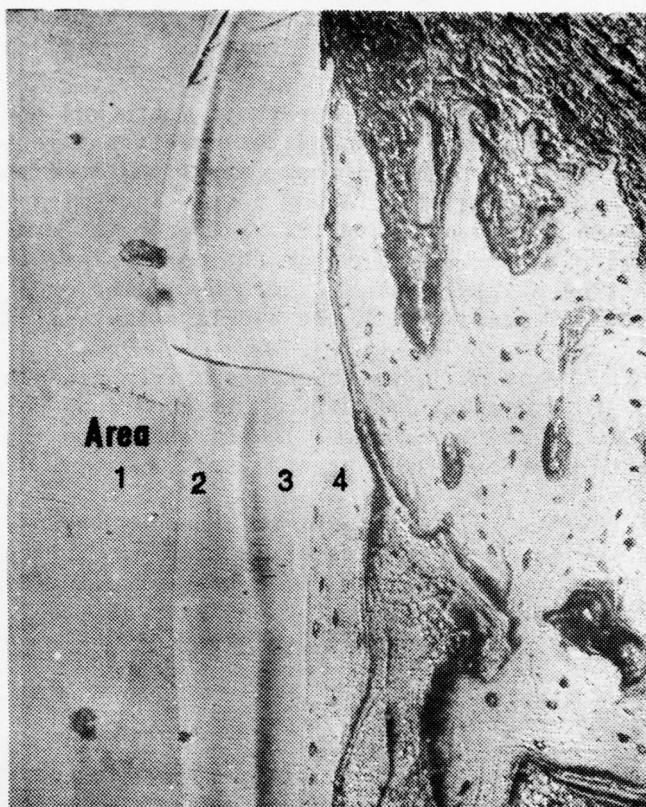
Fig. 8. (a) Research II Metallograph picture of one month sample, and (b) of one year sample. Areas 1,2,3, and 4 are, respectively, bulk bioglass, silicon rich layer, calcium-phosphorus layer, and bone. Both micrographs are 200X.

53

Refelected light micrographs for the 1 month and one year samples (Fig. 8) provide visual comparison of the reaction layers formed at the bone interface. Layer thicknesses determined from the micrographs agree with the microprobe data. A low power light micrograph of the three month sample is shown in Fig. 9. New bone is forming along the bioglass surface which extends through the cortex into the area external to the tibia. Transmitted light micrographs of the one month sample show healthy bone in contact with the bioglass implant (Fig. 10).

The measured reaction layer thicknesses from all microprobe data on all samples are presented in Table I. It should be noted that these measurements were taken from various locations around the cortex - bioglass interface for each implant analyzed.

A plot of average reaction layer thicknesses versus time (Fig. 11) indicates that the Ca, P surface layer is stable. This plot was constructed from graphs similar to those presented in (Figs. 2, 5, 6, 7 and 8). By three months the Ca, P-rich layer is stable at about 30 μm, while the Si-rich layer continues to thicken to ∿240 μm after 28 months.

Discussion and Conclusion

Comparison of the thickness of bioglass bonding layers between the rat model described above and canine and baboon tooth implants show similar results. Bulk 45S5 bioglass implants after 6 months in the canine mandible, reported by Cook et al. (11), were used for EMP analysis of the bonding layers. A 70 μm Si-rich layer on the bulk implant and a 45 μm Ca, P-rich layer between the Si-rich layer and the bone were measured.

In a separate study conducted by Stanley et al. (12) single tooth bioglass implants were fabricated to match the anatomical shape of teeth in adult female baboons. The bioglass teeth were bracketed into the natural tooth socket as described previous (13). Several implants fractured coronally producing an open wound in the oral cavity. Subsequently osseous tissue filled in over the remaining root portion of the implant, and epithelial tissue overgrowth sealed the site. The resulting buried roots remained in place for a total implantation period of 2 years. The EMP profiles and reflected light microscopy show a Si-rich layer 120 μm thick on the surface of the bulk glass and a Ca, P-rich transition layer 70 μm thick between the Si-rich layer and bone.

These results indicate that the bioglass bone bond stabilizes within a 3 month period of time and remains relatively unchanged for 2+ years in various species.
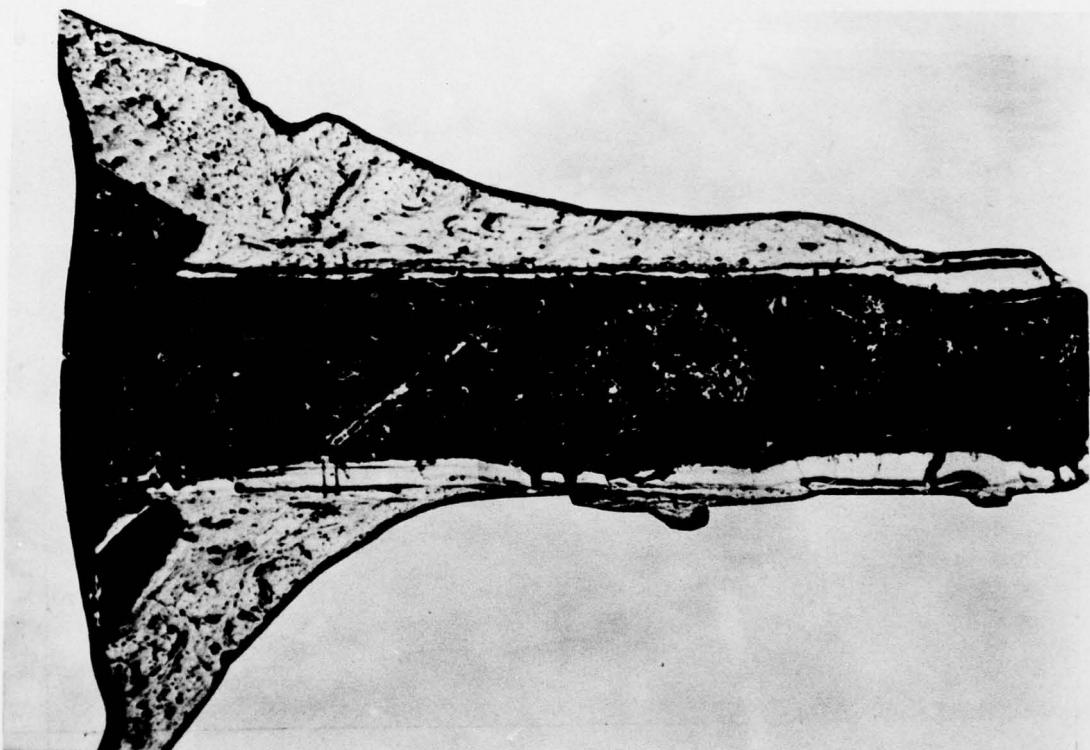
Fig. 9. Lower power reflected light micrograph of a three
months sample. New bone is forming along the
bioglass surface which extends through the cortex
into the area external to the tibia.

(a)

(b)

Fig. 10. (a) Low power transmitted light micrograph of one month
bioglass implant in rat tibia. Note formation of new bone
on implant surfaces in medullary canal as well as along the
surface exterior to the tibia. Cracking seen in the implant
is due to sawing and grinding. A higher magnification of
the boxed area is shown in Fig. 8b. (b) High power trans-
mitted light micrograph of one month bioglass implant in rat
tibia showing healthy bone bonded to implant. Area 1 = bulk
bioglass, area 2 = silicon-rich layer, area 3 = calcium
phosphorus layer, area 4 = bone. Cracking is artifact.

Table I

Reaction Layer Thicknesses (µm)

Implantation Time	Si-rich Layer	Ca, P-rich Layer
1 month	35	45
	40	40
	50	40
	35	25
	40	90
	30	40
	35	25
	40	70
	35	25
	45	35
	27	30
	25	25
	45	45
	25	30
	45	45
	25	55
	31	55
	45	40
	50	30
3 month	55	30
	40	25
	55	30
	30	30
6 month	60	25
	50	32
	60	24
	45	30
12 month	75	35
	80	35
	55	32
28 month	330	20
	345	25
	115	40
	125	25

Fig. 11. Average Ca, P and Si layer thicknesses and ratio of
these layer thicknesses as a function of time. The
Ca, P-rich bonding layer stabilizes after 3 months.

58

References

1. Hench, L. L., Splinter, R. J., Allen, W. C. and Greenlee, T. K., Jr., "Bonding Mechanisms at the Interface of Ceramic Prosthetic Materials," J. Biomed. Mater. Res. Symp., No. 2, Interscience, New York, 117-141 (1972).

2. Piotrowski, G., Hench, L. L., Allen, W. C., and Miller, G. J., "Mechanical Studies of the Bone-Bioglass Interfacial Bond," J. Biomed. Mater. Res. Symp., No. 6, Interscience, New York, 47-61 (1975).

3. Miller, G. J., Greenspan, D. C., Piotrowski, G., and Hench, L. L., "Mechanical Evaluation of Bone-Bioglass Bonding," 8th Annual Int. Biomater. Symp., April 9-13, Philadelphia, Pa. (1976).

4. Clark, A. E., Pantano, C. G., and Hench, L. L., "Compositional Analysis of the Formation of Bone-Implant Bond," in Report No. 6, An Investigation of Bonding Mechanisms at the Interface of a Prosthetic Materials, U.S. Army Medical Research & Development Command, Contract No. DADA 17-70-C-0001 (1975).

5. Hren, J. J. and Johnson, P. F., Private communications.

6. Hench, L. L. and Paschall, H. A., "Direct Chemical Bond of Bioactive Glass-Ceramic Materials to Bone and Muscle," J. Biomed. Mater. Res. Symp., No. 4, 25-42 (1973).

7. Hench, L. L. and Paschall, H. A., "Histo-Chemical Responses at a Biomaterials Interface," J. Biomed. Mater. Res., Not. [Part 1] 49-64 (1974).

8. Pantano, C. G., Clark, A. E., and Hench, L. L., "Multilayer Corrosion Films on Bioglass Surfaces," J. Amer. Ceram. Soc., $\underline{57}$, [9] 412-413 (1974).

9. Clark, A. E. and Hench, L. L., "The Influence of P^{5+}, B^{3+} and T^{-} on Corrosion of Invert Soda-Lime-Silica," accepted by J. Amer. Ceram. Soc. (1976).

10. Clark, A. E., Pantano, C. G., and Hench, L. L., "Auger Spectroscopic Analysis of Bioglass Corrosion Films," J. Amer. Ceram. Soc., $\underline{59}$ [1-2] 37-39 (1976).

11. Cook, S. E., et al., 9th Annual Biomaters. Symp., New Orleans, La., April 15-19, 1977, paper 101.

12. Stanley, H. R., et al., "A Two-Year Study of Natural Tooth Form Bioglasses in Baboons," to be published.

13. Stanley, H. R., et al., Oral Surgery, Oral Medicine, Oral Pathology, $\underline{42}$, No. 5, 339-356 (1976).

D. Evaluation of Bioglass Canine Fibula Grafts, G. Piotrowski,
   T. Carr, M. Ferrari, and W. Petty

Introduction

A study was performed to study the feasibility of bioglass as a
viable component in an artificial bone graft material system. Such
a system would involve a substrate of alumina, surgical stainless
steel, or other suitable load carrying material, and a bioglass
coating for providing fixation of the graft to the bone. Since the
ability of bioglass to bond to bone had previously been demonstrated
(Annual Reports 1 through 7) such a feasibility study was indicated
as the next logical step in the progression toward clinical utiliza-
tion of the bone-bonding ability of bioglass.

Materials and Methods

The canine fibula model described by Enneking et al. (W. F.
Enneking, H. Burchardt, J. J. Puhl, and G. Piotrowski, Physical and
Biological Aspects of Repair in Dog Cortical-Bone Transplants,
J.B.J.S. 57-A:237-252, 1975) was employed. This model involves the
replacement of a 40 mm long segment of dog fibula with an implant
which, in our study, was either an autogenous bone graft or artificial
graft coated with bioglass.

Two types of implants were fabricated. Rods of 316L stainless
steel 3 mm in diameter and 39 mm long were coated with about 0.5 mm of
bioglass by two applications of the immersion process described by
Buscemi and Hench in Annual Report #7, pp. 55. The bulbous ends were
then ground down such that there was a flat spot with a diameter of at
least 2.5 mm at each end of the implant. Similar sized rods of high
density 99% alumina were coated by the process outlined by Greenspan
and Hench (J. Biomed. Maters. Res., 10, No. 4, 503-509, 1976). Since
the coating on the alumina was very thin and followed the contours of
the substrate, no further processing of the implants were performed.

Each batch of bioglass used for these implants were tested for
bonding ability. Small chips of the same pair of materials used for
the fibular grafts, but much smaller in size, were made and implanted
in rat tibias, following the protocol of Ferrari et al. (M. G. Ferrari,
T. Carr, and G. Piotrowski, Standard Method of Test for Ability of a
Biomaterial to Bond to Bone, Report No. 7, pp. 40-49, 1976). Only after
each batch of coated materials passed the in vivo screening test were
they utilized in the canine fibula experiment.

Twenty-four adult mongrel dogs weighing 15 to 18 kg were used.
On one side, the excised 40 mm long segment of fibula was inverted

proximal to distal and reinstalled in the defect, thereby acting as the autograft. On the other side, the excised segment was replaced with one of the artificial "grafts" described above. Animals were sacrificed at 12 and 24 weeks; the distribution of materials and durations is outlined in Table I. No internal or external fixation was used.

Table I

Number of Dogs Used in the Artificial Bone Graft Study.

Duration	Implant Materials	
	45S5 Bioglass on 316L Stainless Steel	45S5 Bioglass on High Density Alumina
12 Weeks	7	5
24 Weeks	6	6

X-rays were routinely taken at two week intervals to monitor the radiographic features of repair and remodeling of the bone-graft junctions. At sacrifice, the fibulas were carefully excised and manually tested for bonding of the grafts.

Results

Three types of responses were seen in the X-ray sequences, and their frequency of occurrences outlined in Table II. A type A response exhibits very little radiological evidence of any changes at or near the bone-implant interface. A Type B response involves formation of bone between the radiodense material between the original bone and the end of the implant, which may have moved slightly after implantation. Bridging of the bony gap was classified as a Type C response. The frequency of these responses did not appear to depend on the material involved.

Most of the radiological changes appeared between 4 and 8 weeks post-operatively, and only gradual changes were apparent after 12 weeks. These late changes were of the form of a gradual remodeling, almost a 'streamlining', of the bony ends where they adjoined the implants.

A typical sequence of X-rays for a Type A response is shown in Figure 1. Small amounts of radiodense material may form in the vicinity of the bone ends, but typically the bone ends remodel, with the proximal end of the distal fragment becoming very slender and pointed.
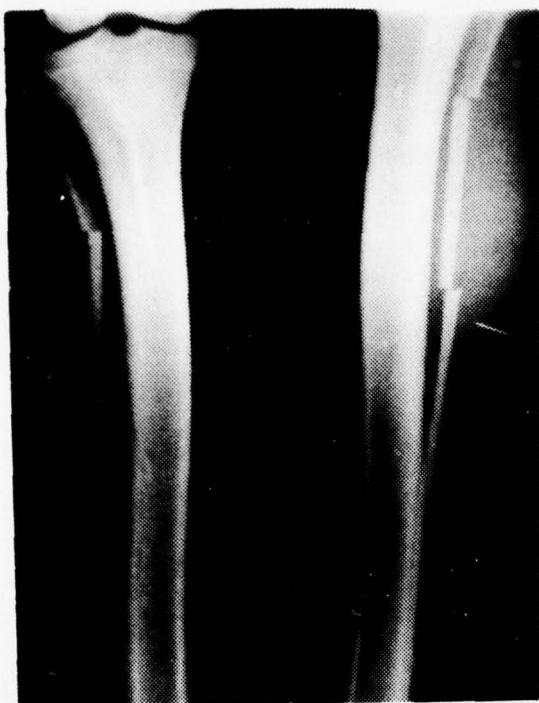
A. Post-op

B. 6 Weeks

C. 7 Weeks

D. 24 Weeks

Fig. 1. Sequence of X-rays illustrating minimal response to canine fibula implant (Type A response).

Table II

Frequency of Occurrence of the Three
Types of Responses to the Implant

Duration	Implant Materials	
	45S5 Bioglass on 316L Stainless Steel	45S5 Bioglass on High Density Alumina
12 Weeks	A – 3 B – 4 C – 0	A – 1 B – 3 C – 1
24 weeks	A – 1 B – 4 C – 1	A – 2 B – 4 C – 0
Totals	A – 4 B – 8 C – 1	A – 3 B – 7 C – 1
	A – 7 B – 15 C – 2	

Two kinds of Type B responses are shown in Figures 2 and 3. In the first of these, radiodense material appears in the space between the host bone and the implant, which has tilted and migrated distally to a slight extent. This new material seems to have an affinity for the implant, but does not form a bond with it. As this material re-models, it appears to do so in a fashion which maintains the area of the interface between it and the implant. Figure 3 shows a similar response, but one that involves an implant which has not migrated. In this case, the new material appears to form end caps around the bone, and frequently no radioluscent space can be seen between parts of these caps and the implant. However, no bond takes place here, as in the previous example. In both cases, the implant appears to become captured within the first few weeks after implantation, and little if any of the implant relative to the bone is evidenced after the second week.

This Type B response is by far the most common observed response, and in many cases combines the features shown in Figures 2 and 3. The distal end of the implant will shift laterally, and the implant will

A. Post-op

B. 4 Weeks

C. 10 Weeks

D. 12 Weeks

Fig. 2. Sequence of X-rays illustrating how radiodense material fills
in the space between bone and canine fibula implant
(Type B response).
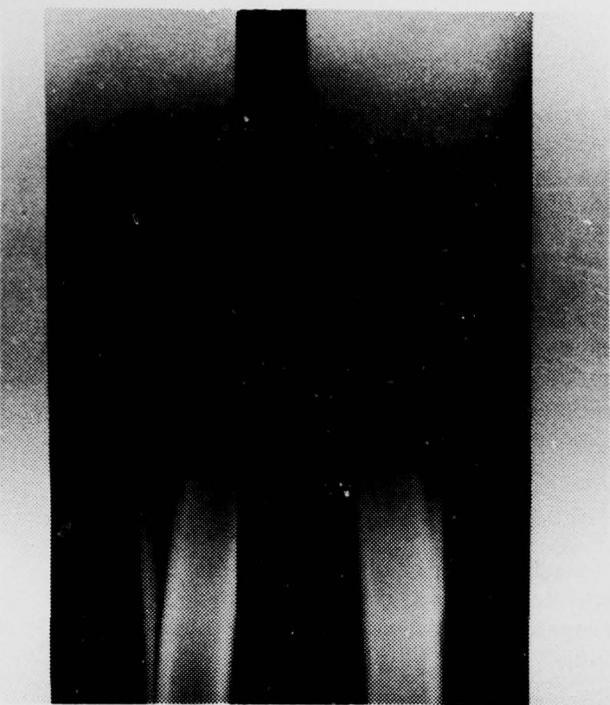
A. 3 Weeks
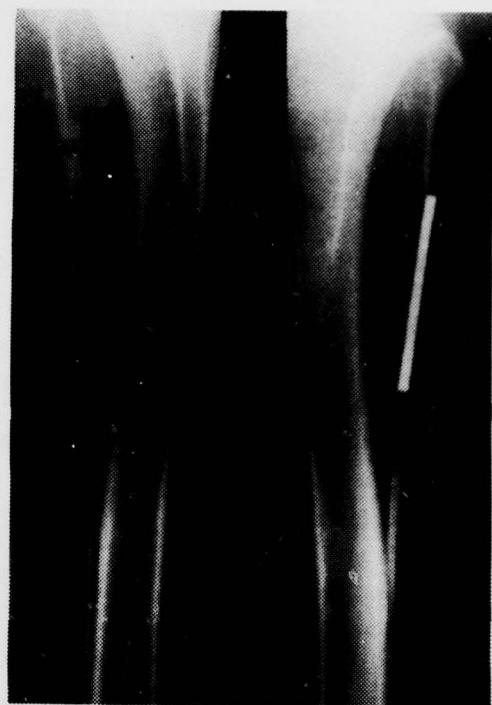
B. 6 Weeks
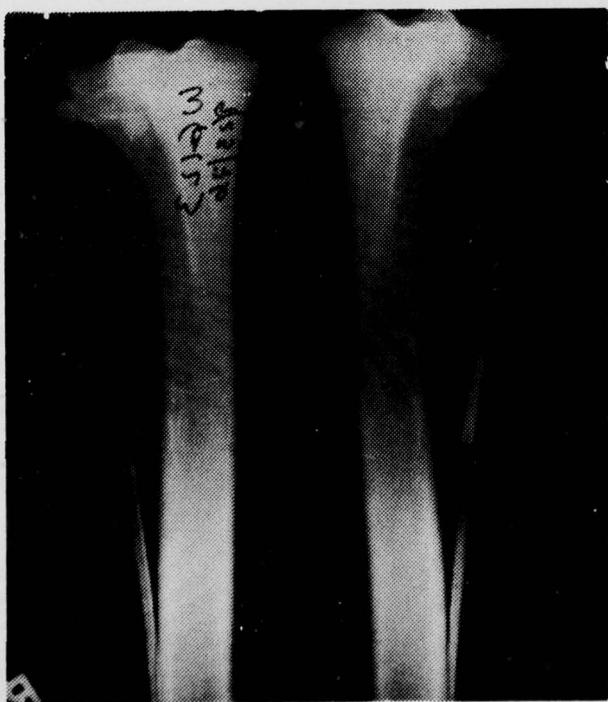
C. 10 Weeks

D. 12 Weeks

Fig. 3.   Sequence of X-rays illustrating how radiodense material forms
          caps around the ends of the artificial canine fibula graft
          (Type B response).

slip distally by about 3 to 5 mm. The proximal bone fragment extends itself distally, and forms an end cap about the proximal end of the implant. At the same time, the distal fragment of the bone extends itself laterally to meet the distal end of the implant.

In two cases, the gap created at surgery was completely bridged, with the radiodense material subsequently remodeling to essentially reconstitute the fibula, and with the implant captured within it. Again, however, the implant is not bonded. The events associated with this type of response are illustrated in Figure 4. (In one case which was classified Type B the radiodense material lacks 2 mm of forming a complete bridge next to the implant.)

Discussion

The total lack of bonding of the bioglass coated implants was quite unexpected, and has generated further studies into its probable causes. Two hypotheses have been developed to shed some light on the significance of the results of this study.

The implants were not fixed rigidly to the cortical bone, but were free to move for some time after implantation. The formation of the bone-bioglass bond occurs through a well-characterized sequence of events. One hypothesis states that the motion of the implant in the immediate post-operative period interfered with one or more of the steps in the bond-formation sequence, or mechanically interfered with the formation or persistence of one of the several surface layers formed in the bonding process.

Another hypothesis is based on the fact that the dob fibula is completely made of cortical bone, and that there is no cancellous bone near the bioglass. This, coupled with the fact that cortical bone is metabolically less active than cancellous bone, may be an important factor in the disruption of the bond-formation process.

These two hypotheses have resulted in the design and initiation of further studies, which have the ultimate aim of increasing the reliability of the formation of the bond between bone and bioglass.

66
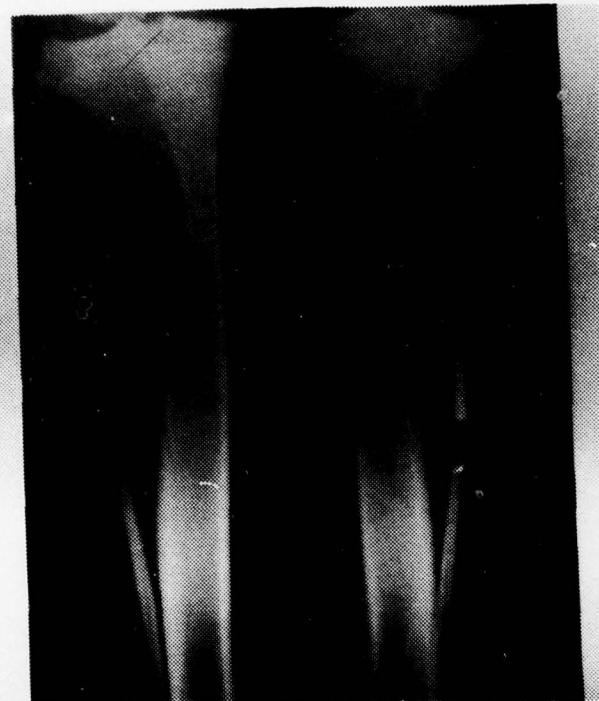
A. Post-op
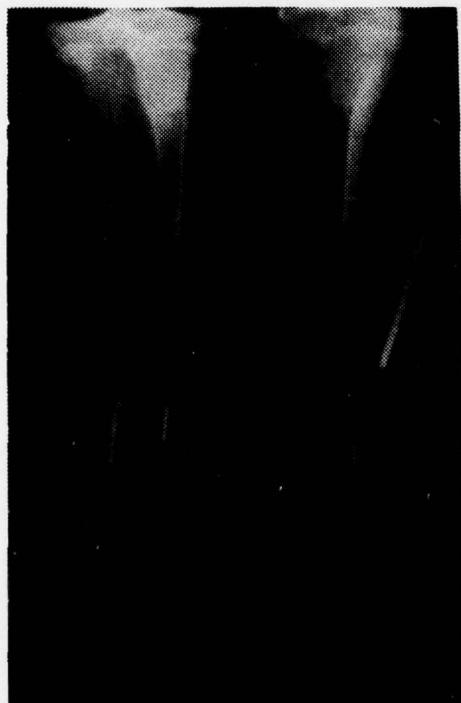
B. 4 Weeks

C. 10 Weeks
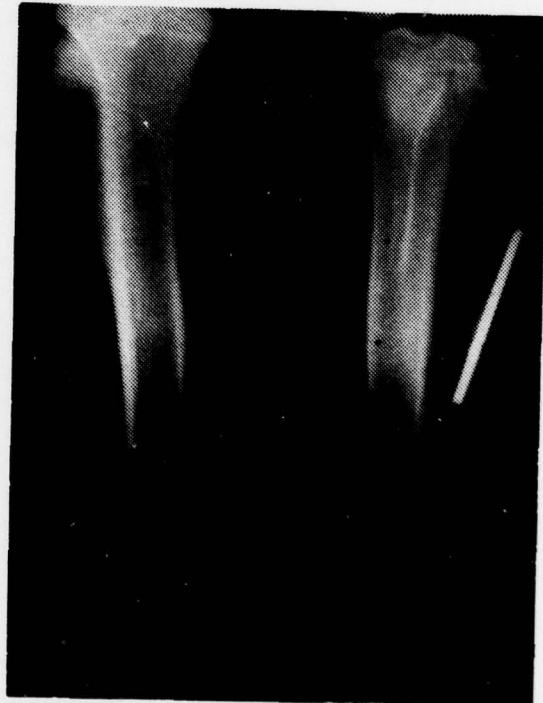
D. 24 Weeks

Fig. 4. Sequence of X-rays illustrating the formation of a bony bridge across the gap and around the canine fibular implant (Type C response).

67

E. Development of Bioglass Coatings for Vitallium Prosthetic
    Devices, D. E. Clark, M. C. Madden and L. L. Hench

Introduction

Bioglass and bioglass-ceramics have received wide acclaim over
the last several years for their ability to promote the formation of
a bond at the material-bone interface (1-3). The chemical bonding
of these nonporous materials is accomplished by incorporating into
the bioglass-ceramic structures soluble sodium, calcium and phosphate
ions in ratios which can influence osteogenesis. Walker and Hench (4)
have found that there is a definite compositional bonding with respect
to SiO_2, Na_2O and CaO content within the glass which will bond to bone.
Outside the compositional limit bonding does not occur either because
the glass is too soluble or is too inert.

In many instances the strength of bioglass is below the structural
requirements of weight bearing prostheses. One solution to the problem
is to use a composite bioglass coated metal prostheses. The bare
metal would provide the necessary structural stability while the bio-
glass coating would provide the biocompatability with the physiological
environment and enhance fixation of various orthopedic devices. A
technique for coating vitallium specimens with a closely adhering bio-
glass and bioglass-ceramic coating has been developed, involving the
rapid immersion of the preoxidized metal into the molten glass (5).
The objective of this investigation was to evaluate the in vivo
response of vitallium specimens coated with selected glasses that are
within the bone bonding compositional boundaries.

Experimental Procedure

Six bioglass compositions (Table I) were prepared by melting
reagent grade raw materials in 15 cc Pt crucibles placed inside an
electric muffle furnace. The glasses were homogenized for 24 hours
at 1350°C prior to being used for immersion coating. Vitallium
slabs ∿0.030" thick, 0.150" wide and 1" long were oxidized in a
resistance heated furnace at 800°C for 10 minutes. This oxidation
treatment produces a chromium oxide-rich surface that promotes glass
metal bond formation. Immediately upon removal from the oxidation
furnace, the vitallium slabs were immersion coated with the molten
bioglasses. Prior to coating, the glasses were removed from the
furnace and allowed to cool to ∿1200°C. Actual immersion time for
each vitallium slab was ∿3 sec. Three vitallium slabs were coated
with each 15 cc batch of glass. Contamination levels of metal ions
in the glass melts after immersion coating were below the detection
limits of the electron microprobe (i.e., <100 ppm). The coated
specimens were annealed at 500°C for 6 hours.

TABLE I

Bioglass Compositions that have been Immersion
Coated onto Vitallium and Evaluated In Vivo

	Composition (mol %)			
Glass Code	SiO_2	P_2O_5	CaO	Na_2O
49S4.6	49.1	2.6	23.8	24.5
50S4.6	50.1	2.6	23.8	23.5
51S4.6	51.1	2.6	23.8	22.5
52S4.6	52.1	2.6	23.8	21.5
52S4.1	52.1	2.6	21.5	23.8
52S3.75	52.1	2.6	19.5	25.8

The glass coating thickness on the vitallium specimens after
immersion was 1 mm. The bioglass on four sides of the slabs were
ground to a thickness of ∿125 μm using SiC paper. Specimens 4 mm in
length were wafered from each slab producing standard rat chips
4 mm x 4 mm x 1 mm with glass coatings on 4 of the 6 sides. During
implantation this geometry presents a metal-bioglass interface for
the body fluids and thus permits interfacial durability evaluation.
Three bulk bioglass specimens 4 mm x 4 mm x 1 mm were also prepared
from each composition and used for controls.

The partially coated specimens were placed in the left tibia of
male Sprague Dawley-Dublin rats weighing ∿200 g according to the
procedures described in detail in a prior report (6). The rats were
sacrificed after 30 days and the extent of bone bonding was checked
using the standard mini-pushout test. This involves excising the
tibia containing the implant and subjecting it to a push-out force
of 30N. An implant which can sustain this push-out force without
loosening is assumed to be bonded. Although this test does not yield
quantitative bond strength data, it does provide a qualitative minimal
bond strength.

Samples harvested at sacrifice were fixed in cold buffered
glutaraldehyde, dehydrated through a series of alcohols, and embedded
in epoxy resin. One bulk and one coated specimen from each composi-
tion were prepared for electron microprobe analysis and light micros-
copy using the techniques reported by Harrell et al. (7) and Clark
et al. (8).

Results and Discussion

All six glass compositions adhered firmly to the vitallium substrates using the immersion coating process. The sensitivity of the physical properties of the materials system to both glass composition and processing parameters will be discussed in a future publication.

Using the 30N mini-pushout procedure all specimens (both coated and bulk) were found to be bonded to the rat tibia after 30 days. This test procedure provides only a minimal value for the bone-bioglass interfacial strength. The actual strength may be dependent on the bioreactivity and mechanical properties of the glass composition. A quantitative mini-pushout test is presently being developed that will permit the actual bone-bioglass bond strength to be determined.

The electron microprobe (EMP) compositional profile for the 30 day 52S4.6 bulk glass is shown in Figure 1. This profile was obtained by traversing the specimen with the electron beam perpendicular to the bone-bioglass interface. The characteristic X-ray intensity for Si, Ca and P were measured using the fixed time technique (10 sec), starting as 40 μm into the bulk bioglass and moving at 5 μm intervals across the interface into the bone. The X-ray intensity for each element is proportional to the concentration of that element in the specimen. Four distinct compositional regions can be seen in the EMP profile: 1) bulk bioglass; 2) silicon-rich, Ca, P layer; 3) Ca, P-rich layer, and 4) bone. During implantation the soluble ions in the glass (Na, P, Ca) are selectively leached into the surrounding environment producing a silicon-rich layer on the surface of the bioglass. The Ca and P concentrations are minimal in this layer and the Ca/P ratio is slightly lower than in the bulk. Simultaneously, the Ca, P layer begins to deposit on top of the silicon-rich layer thus leading to a gentle gradient of composition from the natural bone to the bioglass implant. The relative thicknesses of these interfacial layers are dependent on the time of implantation as discussed by Harrell et al. (7) After 30 days the average thicknesses of the silicon-rich layers and Ca, P-rich layers on the bulk glass are 34.5 μm (±10 μm) and 2.5 μm (±5 μm) respectively.

Figure 2 presents the EMP profile of the 30 day implanted bioglass coated (52S4.6) vitallium rat chip. The same distinct compositional regions observed in the bulk glass are also found in the bioglass coated vitallium specimens. In addition, the bioglass-vitallium interfacial compositional profile is also shown. The metal-glass interfacial reaction zone is ∿15 μm thick. None of the major constituents of vitallium (i.e., Co, Cr) have penetrated to the bone-bioglass interfacial region. The total thickness of the glass coating including the
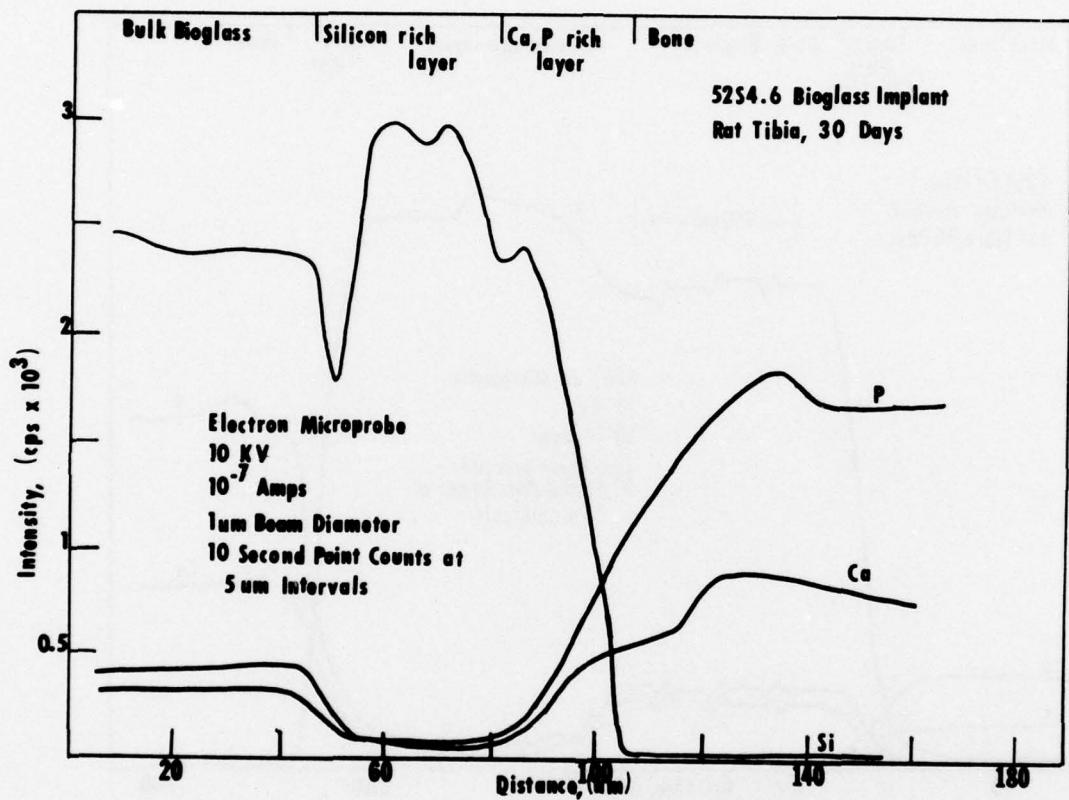
Figure 1. Electron micrograph interfacial compositional profile
of bulk bioglass (52S4.6) implanted for 30 days in a
rat tibia.
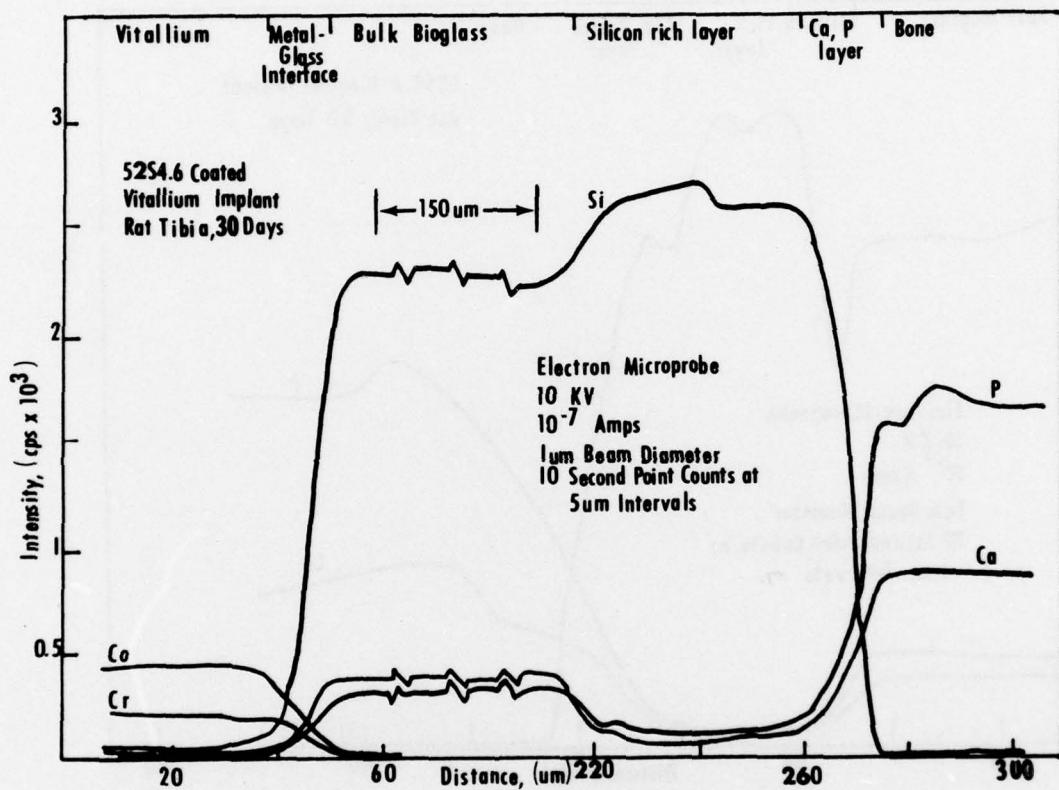
Figure 2.   Electron micrograph interfacial compositional profile
of bioglass coated (52S4.6) vitallium implanted for
30 days in a rat tibia.

reacted region is ∿200 μm. Approximately 150 μm of unreacted bioglass remains on the vitallium substrate after 30 days. The thicknesses of the silicon-rich and Ca, P-rich layers are 51.7 μm (±10 μm) and 21.7 μm (±5 μm), respectively. Statistically, there appears to be no difference in the bioreactivity, judged on compositional profiles, between the bulk bioglass coated vitallium for the 52S4.6 composition.

Table II lists the layer thicknesses for other bioglass compositions for both bulk and coated vitallium rat tibia specimens. As with the 52S4.6 composition, there is no significant difference in interfacial layer thicknesses between bulk and coated vitallium specimens. Furthermore, the thickness of the Si-rich layer does not appear to be sensitive to the glass composition in the range investigated (45 mol % SiO_2 – 52 mol % SiO_2). The Ca, P diffuse layer thickness does appear to depend on the glass composition. However, no definite trends in Ca, P layer thickness versus glass composition have been established at this time.

TABLE II

Si-Rich and Ca, P-Rich Layer Thickness for Both Bulk
Bioglasses and Bioglass Coated Vitallium After 30
Days of Implantation in Rat Tibia

Sample	Si-Rich Layer Thickness (μm)	Ca, P Layer Thickness (μm)
52S4.6 (bulk)	35	22
52S4.6 (coated)	52	16
49S4.6 (bulk)	40	30
49S4.6 (coated)	40	28
52S4.1 (coated)	50	35
52S3.75 (bulk)	41	37
50S4.6 (coated)	40	24
45S5 (bulk)*	35	38

*Reported by Harrell et al. (8)

Light micrographs of the interfacial areas used for EMP analysis are shown in Figures 3 and 4. The various interfacial features presented in the EMP profiles are correspondingly illustrated on the micrographs. The cracks in the glass are thought to be due to the stresses applied with the mini-pushout test prior to analysis. The scan tracks left by the interaction of the electron beam with the specimen can also be seen. These scan tracks are perpendicular to the bioglass-bone interface.
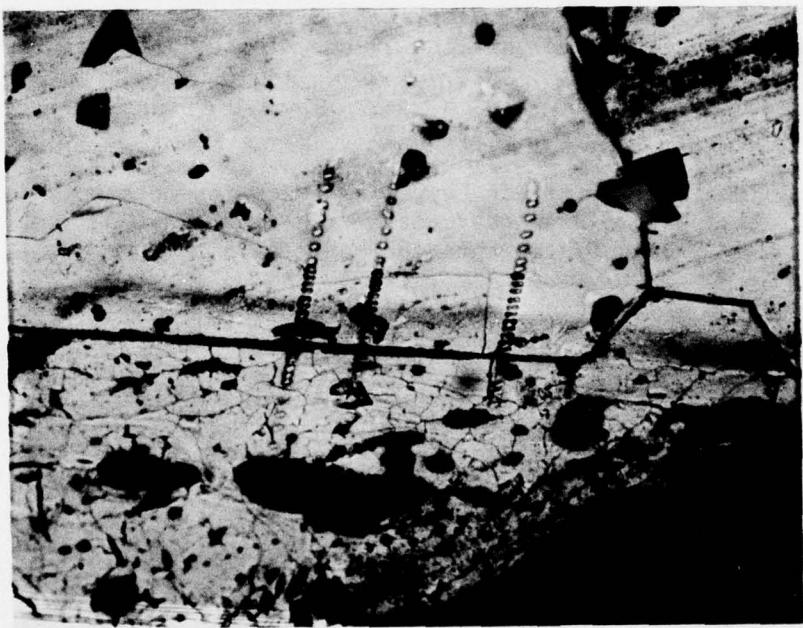
Figure 3. Light micrograph of a bulk bioglass (52S4.6)-bone
interface. Specimen was implanted for 30 days in
a rat tibia (200X).
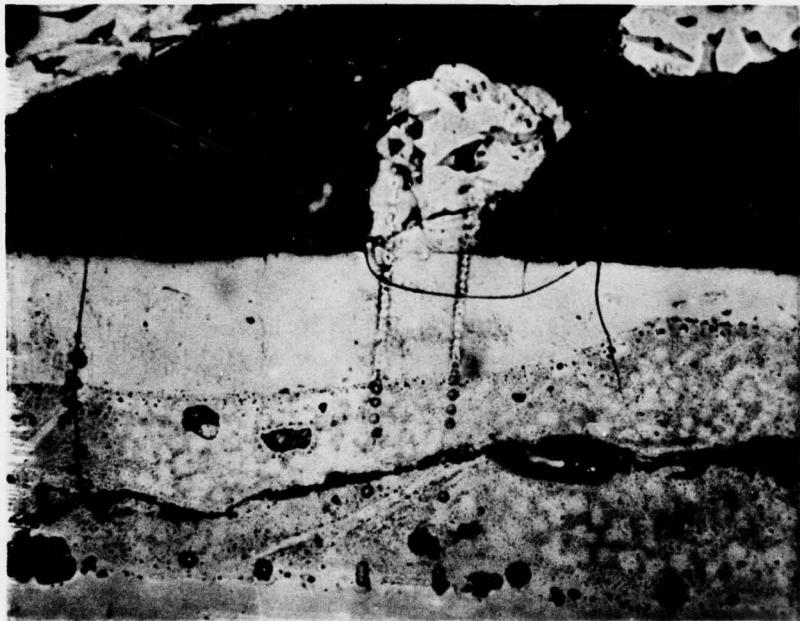
Figure 4. Light micrograph of a bioglass (52S4.6) coated Vitallium
bone interface. Specimen was implanted for 30 days in a
rat tibia (200X).

Summary

    A technique of coating bioglass onto vitallium substrates has
been developed. Using the rapid immersion process, six bioglass
compositions within the bone bonding region were coated onto
vitallium slabs. All of the glass compositions adhered very well to
the metal. Furthermore, all the glasses bonded to bone after being
implanted for 30 days in tibia of young rats. Electron microprobe
analysis of the bone-bioglass interfaces indicated similar composi-
tional profiles for the bulk bioglass-bone and bioglass coated
vitallium-bone interfaces.

    The thickness of the silica-rich layer that develops during
implantation appears to be insensitive to glass composition. After
30 days the thickness of this layer was 35 μm to 52 μm for the
compositions investigated. Furthermore, the composition of the silica-
rich layer is relatively constant with only small concentrations of
Ca and P. A Ca, P-rich layer forms on top of the silica-rich layer.
The composition of this layer resembles a typical diffusion profile
with the concentrations of Ca and P increasing gently from the glass
to the bone. This layer apparently forms the structural linkage
between the glass and the bone.

    Applying a bioglass to a metal prostheses in order to achieve
both strength and fixation appears to be a viable approach to
prostheses improvement. The _in vivo_ response obtained with such a
coated system using a rat tibia model is equivalent to that obtained
for bulk bioglass.

References

1. L. L. Hench, R. J. Splinter, W. C. Allen and T. K. Greenlee, Jr.,
    J. Biomed. Maters. Res. Symp., No. 2, Interscience, New York,
    1972, pp. 117-143.

2. L. L. Hench and H. A. Paschall, "Direct Chemical Bond of Bioactive
    Glass-Ceramic Materials to Bone and Muscle," Symposium on Materials
    and Design Considerations for the Attachment of Prostheses to the
    Musculo-Skeletal System, Clemson University, April 1972.

3. L. L. Hench, T. K. Greenlee, Jr., W. C. Allen and G. Piotrowski,
    "An Investigation of Bonding Mechanisms at the Interface of a
    Prosthetic Material," Reports #1 and #2, U.S. Army Medical Research
    and Development Command, Contract No. DADA17-70-C-0001 (1970,1971).

4. M. M. Walker and L. L. Hench, "Compositional Dependence of the Bone-
    Bioglass Bond," Report #8, U.S. Army Medical Research and Development
    Command, Contract No. DAMD17-76-C-6033, 1977.

5. P. Buscemi and L. L. Hench, "An Immersion Process for Coating
    Metal Implants with Bioglass," Report #7, U. S. Army Medical
    Research and Development Command, Contract No. DAMD17-76-C-6033,
    1976.

6. L. L. Hench and H. A. Paschall, "Histo-Chemical Responses at a
    Biomaterials Interface," J. Biomed. Mater. Res., No. 5 (Part 1)
    49-64 (1974).

7. M. S. Harrell, W. A. Acree, M. Keane, S. R. Bates, D. E. Clark,
    A. E. Clark and L. L. Hench, "Effects of Time on the Thickness
    of Bioglass Bonding Layers," Report #8, U.S. Army Medical Research
    and Development Command, Contract No. DAMD17-76-C-6033, 1977.

8. D. E. Clark, S. R. Bates, M. S. Harrell and W. A. Acree, "Electron
    Microprobe Technique for Evaluating Bioglass-Bone Interfaces,"
    Report #8, U.S. Army Medical Research and Development Command,
    Contract No. DAMD17-76-C-6033, 1977.

F. Bioglass Coated Monkey Hip Prostheses - A Progress Report,
    G. Piotrowski, M. Ferrari, and W. Petty

Introduction

     Previous publications have described the development of a monkey
femoral head replacement as a model for testing the bonding of hip
prostheses by means of bioglass coatings (1,2). Most of the previous
data was obtained using 45S5F bioglass applied by flame spray coating.
Lack of control over the flame spray coating process led to a consider-
able number of failures due to corrosion between the metal and glass
coating and spalling of the glass.

     Due to development of the new rapid immersion process for
applying bioglass coatings to metal devices, described in Annual
Report #7, we have been able to produce 45S5 bioglass coatings on 316L
stainless steel femoral head prostheses with high reliability. Progress
in implantation and mechanical testing of the bonding between stem of
the prostheses and the medullary canal is reported herein. As before,
our objective is to achieve short term immobilization of the device with
a tight mechanical fit at surgery. Bonding between bioglass and bone
develops with several weeks to provide long term fixation. No polymer
cements are used.

     Duration of this series of implants was restricted to eight weeks
because a prime objective is to determine how rapid a strong mechanical
bond is achieved. A second objective is to determine the tensile
strength of the bond by use of a pull out test of the device post
sacrifice. A third objective is to evaluate the effect of bioglass
on the stability of the articulating cartilage in the hemi-arthoplasty.
Because of the synovial-like membrane that develops in contact with
bioglass when placed in cartilageneous tissue it is possible that
preservation of the joint capsule may be enhanced with the use of bio-
glass coatings on the head of Moore-type prostheses. This hypothesis
is tested as part of the femoral head prostheses experiment by completly
coating the prostheses with bioglass.

     Monkey 5A-21 was implanted on September 14, 1977 with 45S5 bioglass
coated prosthesis #A-20. After drilling of the marrow cavity the bio-
glass coated prosthesis was hand pressed into position. The immediate
post-op X-ray revealed that the implant was properly located in the
acetabulum. There was no gap between the implant and bone which
indicates the prosthesis was well fixed. The 4 week X-ray revealed
that the implant was located in the same position as initially implanted.
No boney reaction at the distal end of the stem was noted, indicating
that the implant was not loose. An 8 week X-ray was taken prior to
sacrifice and it was noted that the monkey moved relatively normally.
The X-ray again showed that the implant was still located in the aceta-
bulum. The post-op, 4 week and 8 week X-rays are shown in Figure 1.

Fig. 1. X-rays of 5A21 monkey femoral head prostheses of bioglass coated 316L stainless steel.

    A. Immediate post-op
    B. 4 weeks post-op
    C. 8 weeks post-op
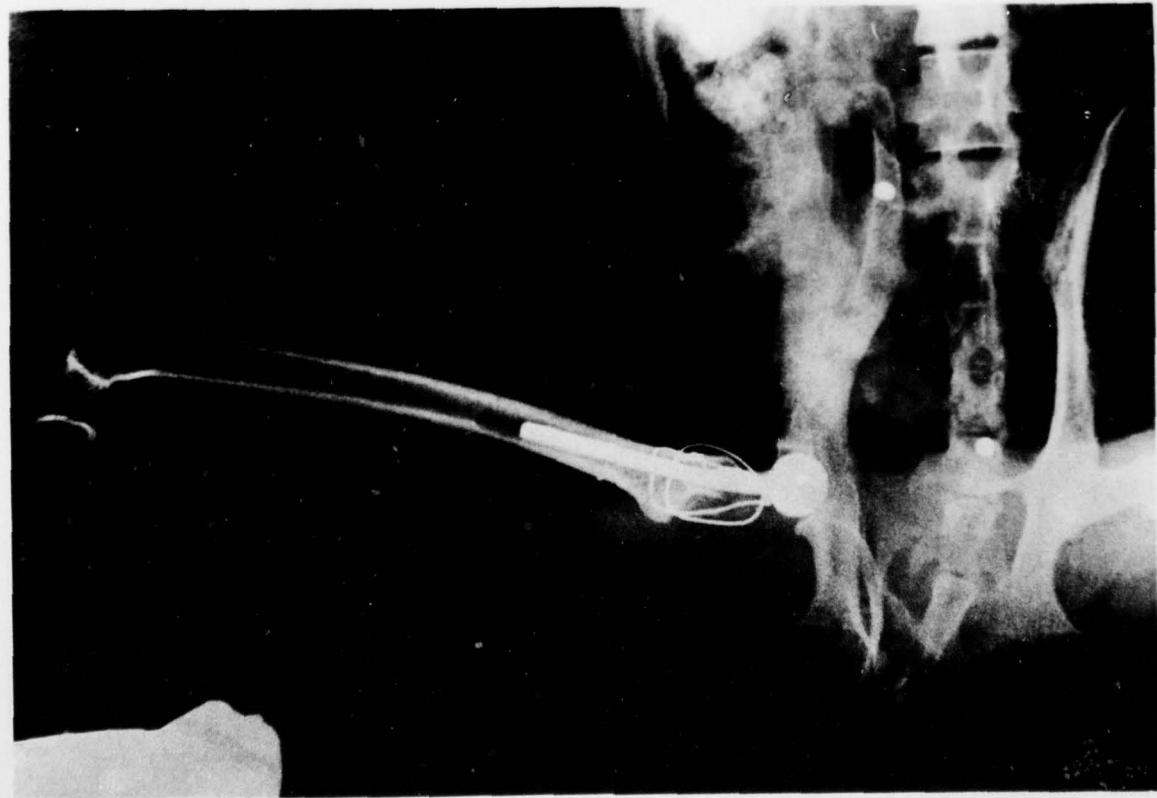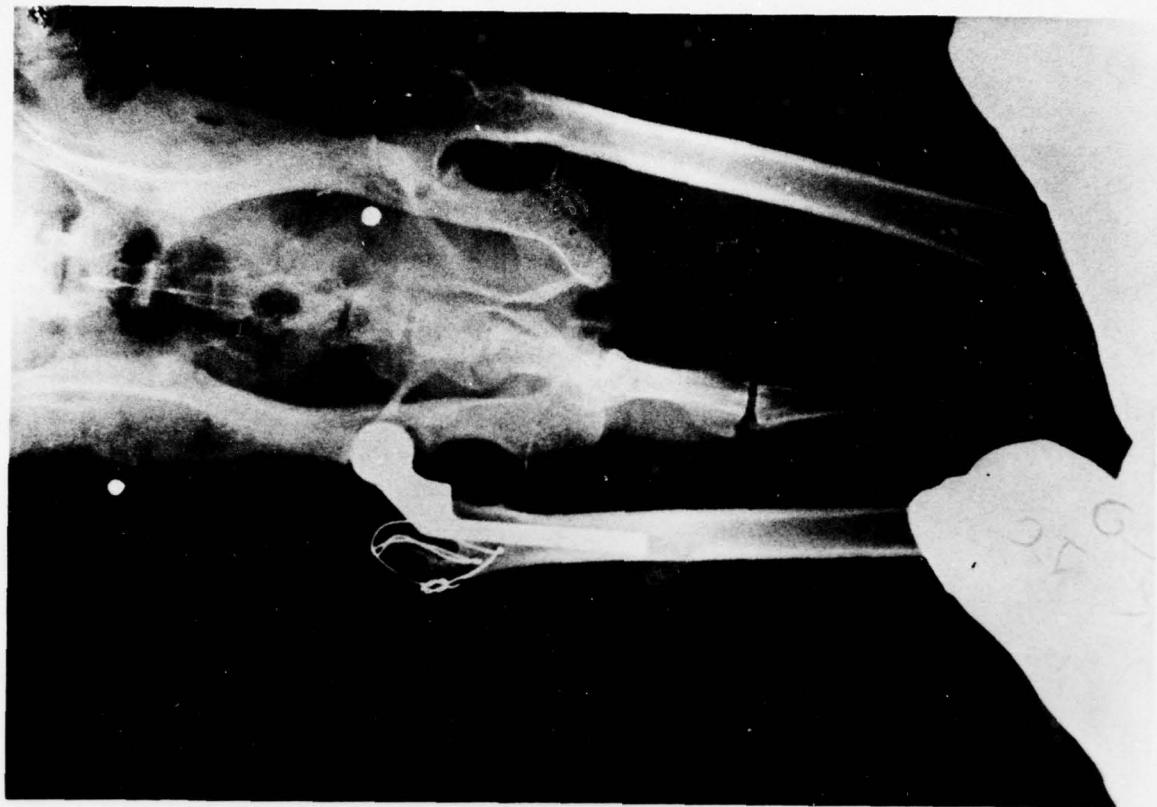
GAINESVILLE FLA
521

B.

81
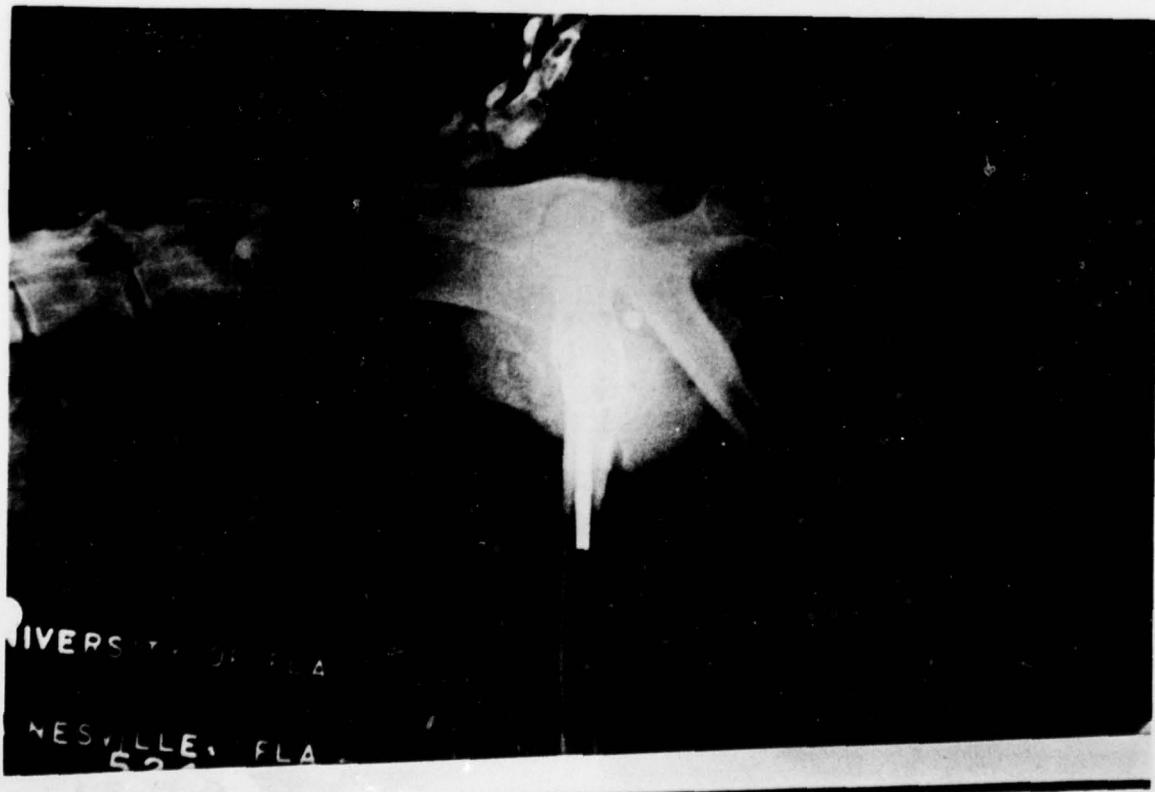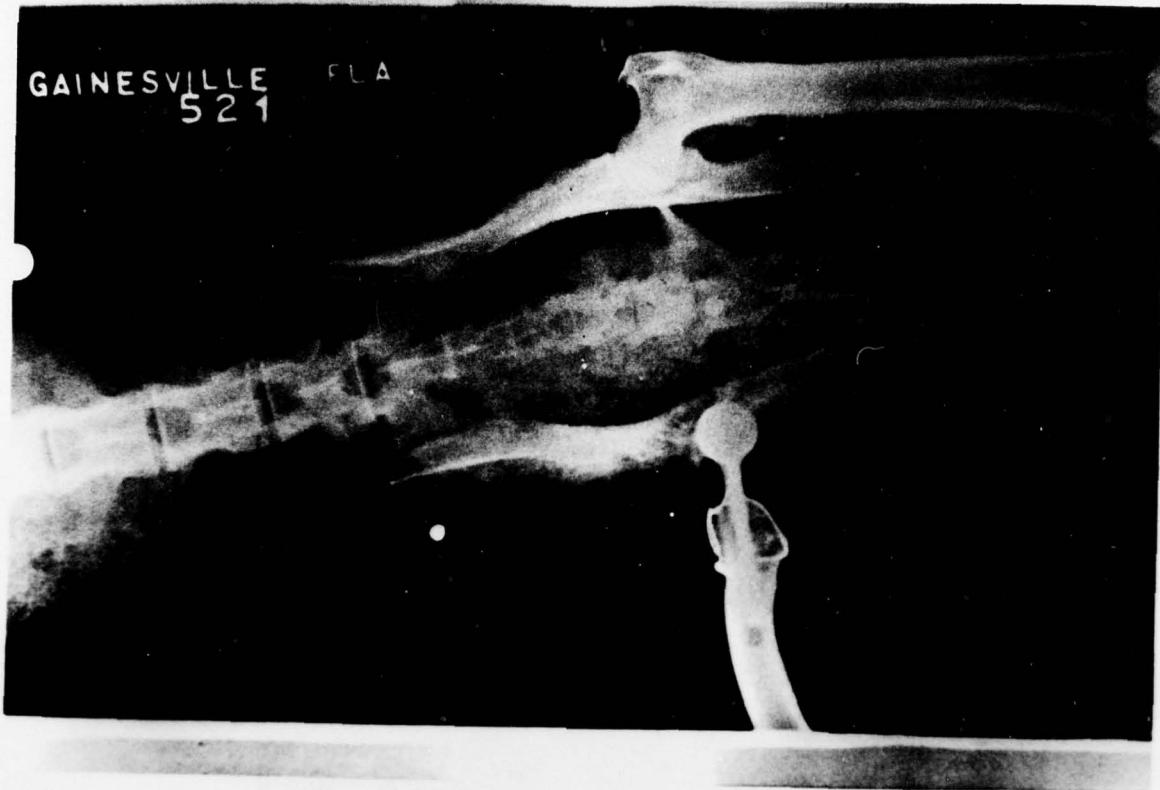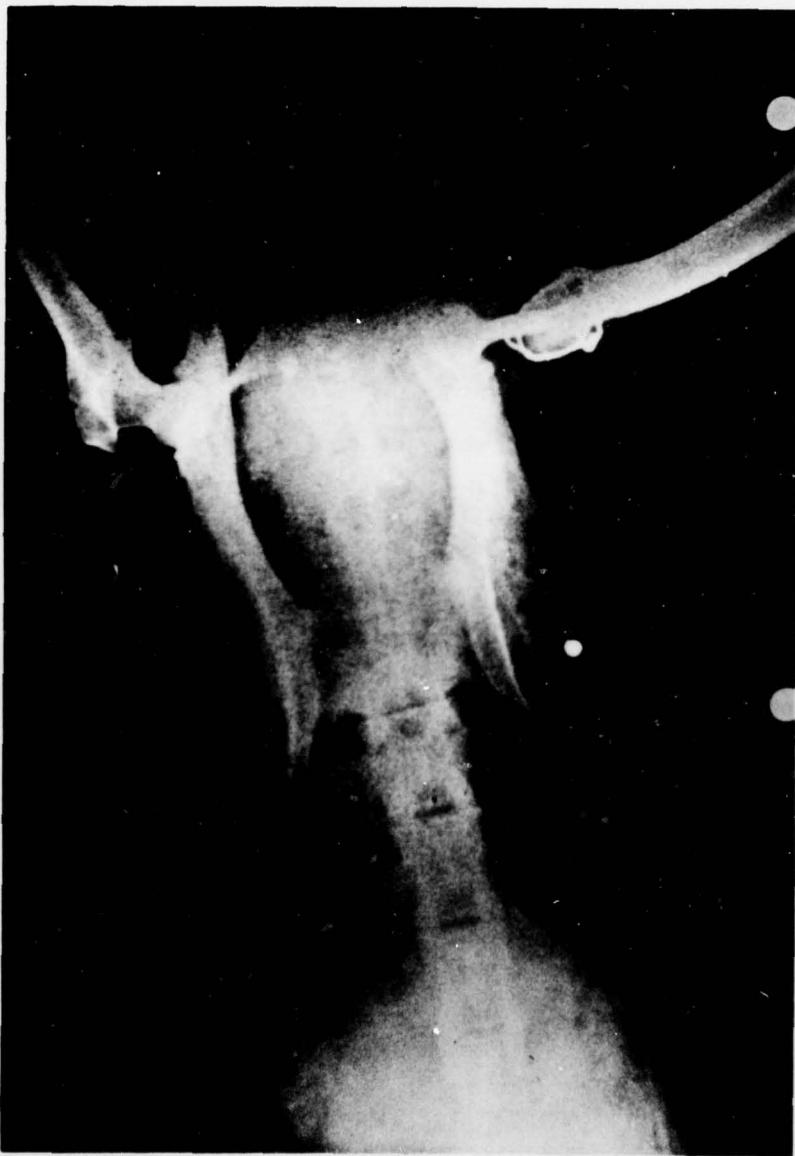
At the time of sacrifice the range of motion was examined. There appeared to be normal flexion in both legs; it lacked 80° of extension in the right leg, 30° of internal rotation of the left leg and 5° for the right, and both legs had an internal rotation of 50°.

The implant was found to be in the acetabulum and all surrounding areas of the femur seemed to be normal. The bioglass coating on the head of the prosthesis was intact. The implant appeared to be fixed in the marrow cavity so the entire femur was placed in saline solution for transportation to the laboratory for testing.

The distal end of the femur was embedded in plastic alumina for mounting in the test fixture. A tension test was performed and a maximum force of 60 lbs was developed before the implant was dislodged. This data is presented in Figure 2.

Monkey 5A-22 received femoral head replacement A-22, immersion coated with 45S5 bioglass, on June 28, 1977.

The monkey was anesthetized and surgery performed on the right leg in the usual manner.

A posterial lateral approach was used to expose the hip. Following good hemostasis of the femoral head, the femoral shaft was notched on the medial side to accomodate and locate the neck of the prosthesis. In order to rigidly maintain the prosthesis in place it is desired to achieve a press fit with a femoral shaft. The rectangular cross sectional diagonal of the stem measured .158 in. The femoral shaft was reamed using a .149 in and .152 reamers. After drilling the marrow cavity the prosthesis was pounded in place using an impact absorbing tool. A visual inspection revealed that the integrity of the glass coating on the prosthesis head has been maintained. The prosthesis was then reduced into the acetabulum and surgery was concluded in the usual manner. An immediate post operative X-ray of the anterior-posterior and lateral views confirmed the implant to be firmly situated in the marrow cavity and well located in the acetabulum as shown in Fig. 3.

Four weeks post operative the monkey was visually inspected in his open run. It appeared the animal did not favor either leg and normal activity had been resumed. At that time an X-ray was taken suggesting a union between the greater trochanter and proximal femur. The prosthesis was located as initially implanted.

An eight week X-ray revealed no loosening and some slight periosteal reaction taking place on the medial aspect of the proximal femur.

This monkey was sacrificed on August 31, 1977, nine weeks post op. The ranges of motion of both legs were the same and apparently normal. The operative scan was well healed and difficult to locate. The capsule appeared normal, as did the acetabular cartilage.
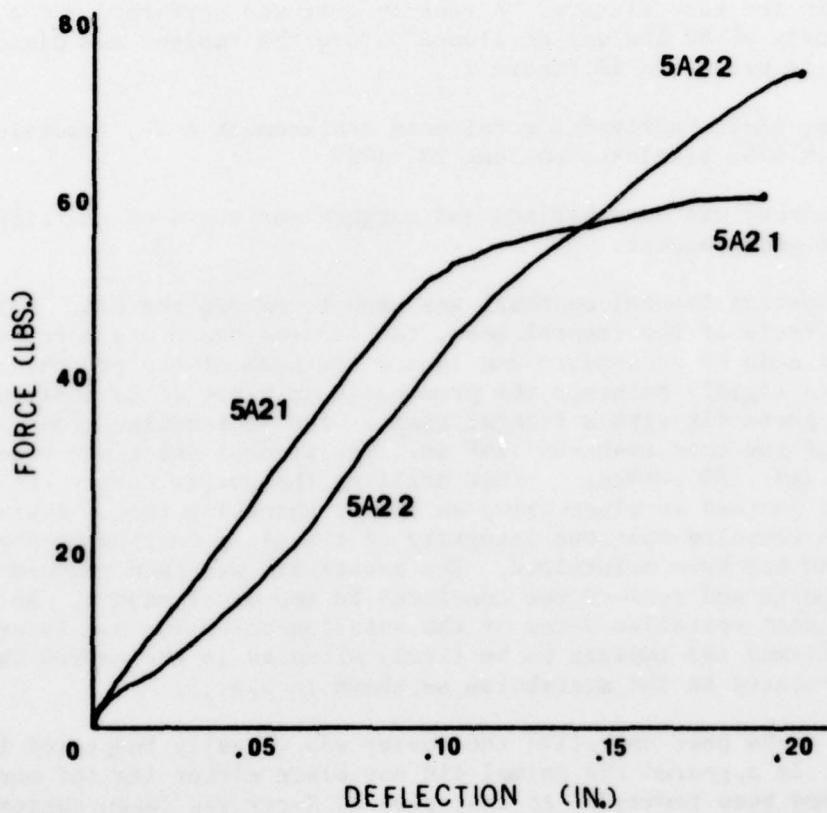
Fig. 2. Force deflection curves for tensile testing of femoral head prostheses with bioglass bonding.

Fig. 3. X-rays of 5A22 monkey femoral head prostheses
of bioglass coated 316L stainless steel.

A. Immediate post-op
B. 4 weeks post-op
C. 8 weeks post-op

B.

87

88
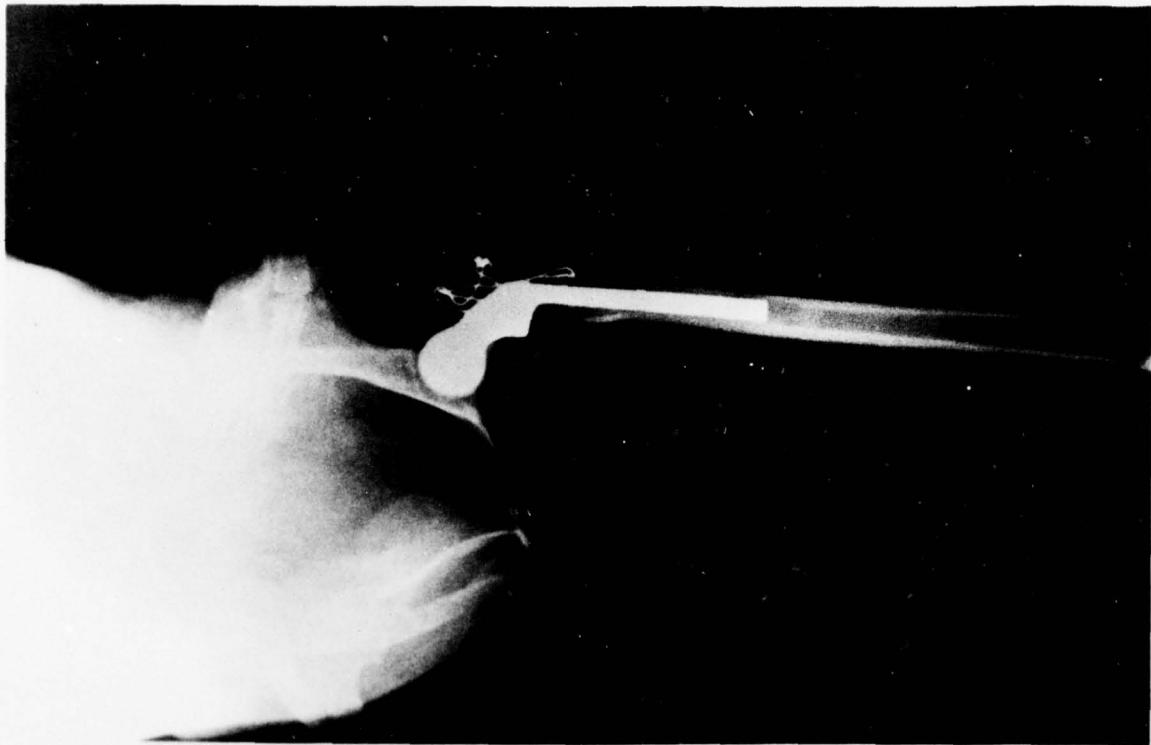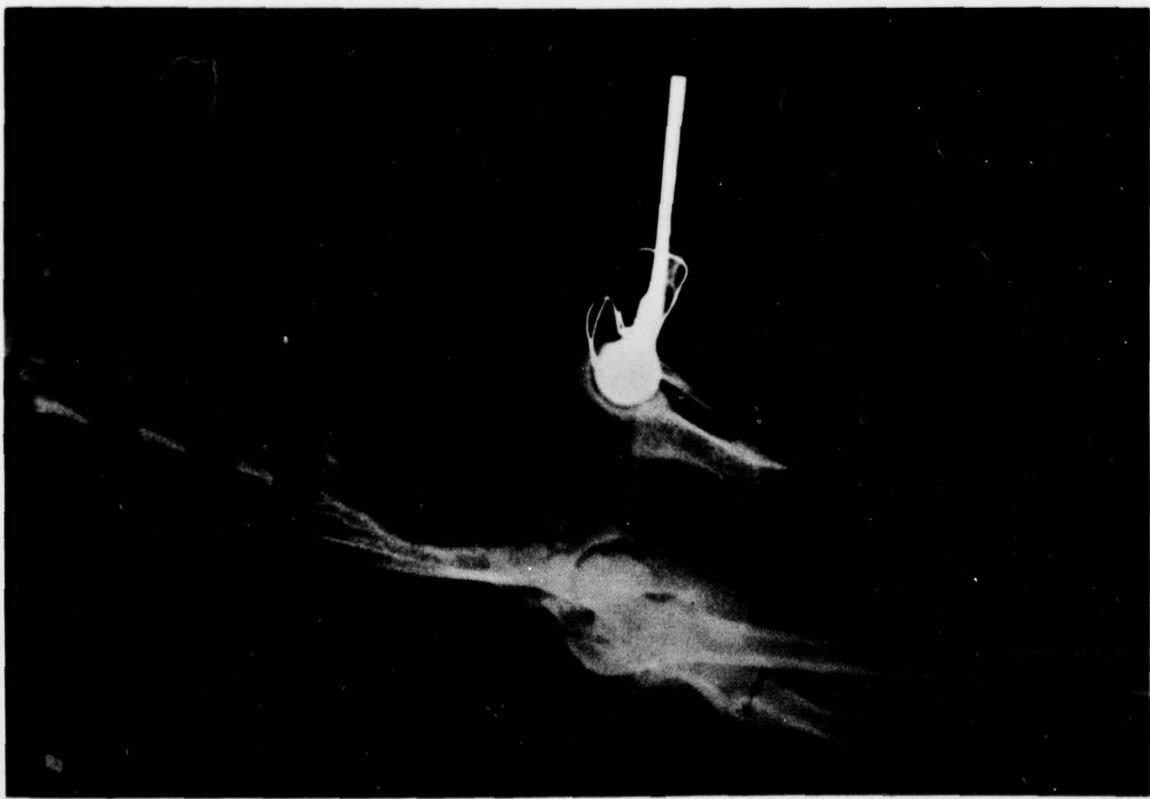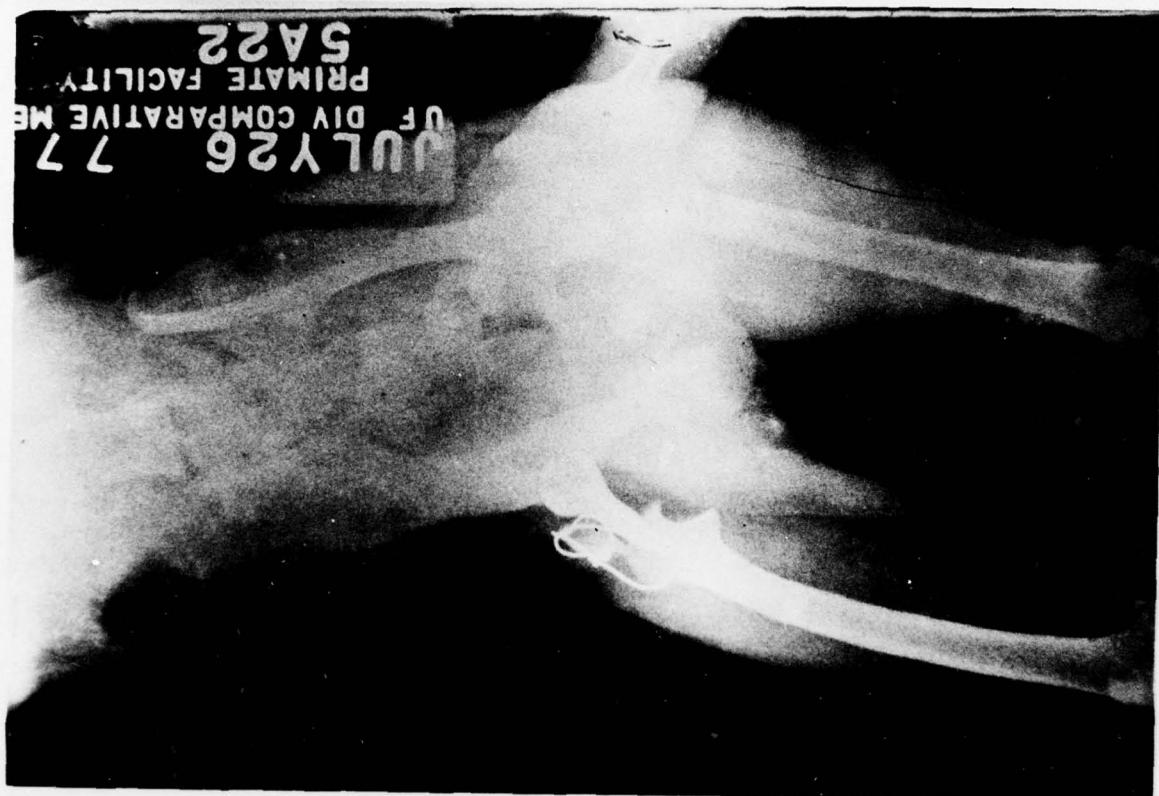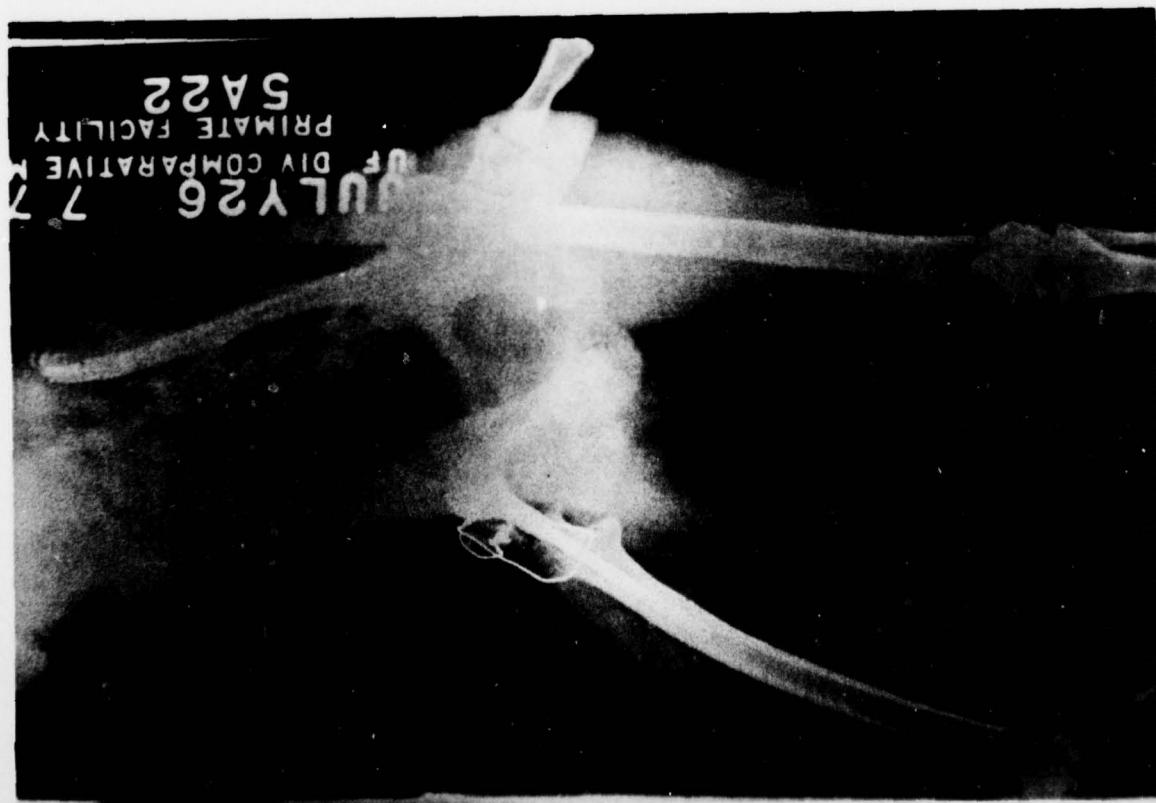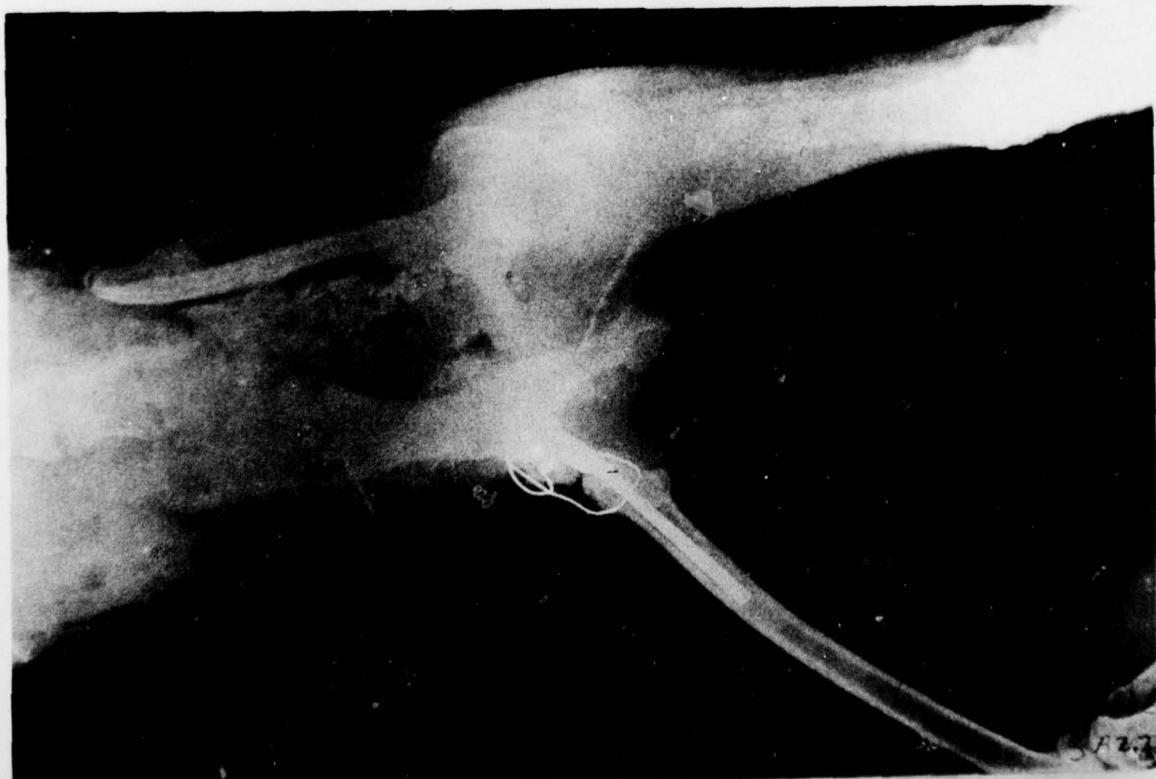
The implanted femur was removed and the distal end embedded in plastic aluminum in preparation for testing in tension. The femur pulled out of the plastic aluminum at 196N (44 lbs). The distal femur was repotted in PMMA and retested. A sudden slip occurred at 329N (74 lbs), and a maximum load of 609N (137 lbf) was developed before the test was terminated. The implant was extracted about 5 mm from the bone, and the stem appeared to be bare. This suggests that the glass was sheared from the stem at the high loads, and that the bone-bioglass bond is still intact. The specimen was frozen in saline to preserve it for future studies such as electron microprobe analysis of the bonded interface.

This monkey was not caged post-operatively, but allowed into a run. It is felt that this was an important factor in the succes of the implant, since it allowed the monkey to recuperate in an undisturbed manner.

Conclusion

Tensile loads as high as 137 lbf have been withstood by the femoral stems before failure occurred. Even at this high loading the bone-bioglass bond remained intact and the coating came off the metal prostheses.

The bone-bioglass bond develops in primate in the monkey femoral head prostheses model with 8 weeks or less.

References

1. L. L. Hench, H. A. Paschall, W. C. Allen, and G. Piotrowski, "Interfacial Behavior of Ceramic Implants," NBS Special Publication 415, May 1975, pp. 19-35.

2. L. L. Hench, C. G. Pantano, Jr., P. J. Buscemi, and D. C. Greenspan, "Analysis of Bioglass Fixation of Hip Prostheses," J. Biomed Maters. Res., 11, No. 2 (1977) 267-281.

G. Transmission Electron Microscopy of Bone Cell Culture
    Samples on Bioglass, L. L. Hench, P. F. Johnson, E. J.
    Jenkins, R. Grant* and R. Stevens*

Introduction

A line of stable bone cell cultures have been developed by
Dr. Grant and colleagues at Pfizer, Inc. research laboratories. The
cell cultures were derived from the calveria of mouse embryo. A
series of histo-chemical experiments of the bone cell cultues in
contact with bioglass is being conducted by Drs. Grant and Stevens
through support of other agencies. The purpose of the experiment
reported herein was to conduct a preliminary evaluation of the use
of the analytical scanning transmission electron microscope (ASTEM)
in conjunction with energy dispersive X-ray analysis (EDXA) to
identify chemical compositional variations at the cell-bioglass inter-
face. Hopefully, if such compositional analyses are possible with
sections from these in vitro bone cell culture studies the results
can be correlated with the in vivo experiments performed within this
contract.

Experimental Procedure

EM thin sections were prepared by Dr. Stevens from two week,
six week, and eight week cell cultures exposed to 45S5 bioglass
substrates. An effort was made to preserve the bioglass bonding
layers in contact with the cell layers. Some sections were stained
with uranyl acetate and lead citrate following normal EM histology
procedure. Other sections were left unstained in order to minimize
the background fluorescent X-radiation from the sample when performing
the compostional analyses. Specimens were placed on copper EM grids.
A subsequent experiment is planned using newly developed carbon grids
which will eliminate most of the background radiation from the grids.

A Phillips EM 301 ASTEM was used for the experiment. This instru-
ment has been specially modified by our laboratory to optimize EDXA
analysis of biological TEM specimens (1,2). The aluminum sample holder,
cold finger, and EM stage greatly decreases back-round radiation making
it possible to analyze low atomic number elements in the electron
microscope.

Results

The first experiment was an effort to analyze the intercellular
regions at two weeks to determine whether mineralization had begun.

Stained sections of the two week samples were used. Figures 1 through 5 are electron micrographs taken at various locations along the interface between the bioglass bonding layer (marked BG) and the cells.* Extensive intercellular collagen (marked Co) is seen in all five figures. An adherant BG layer is also seen in all figures. The contrast of Figure 5 has been increased to show additional features of the BG layer-cell interface. Figures 1-4 show that the BG bonding layer is adherant to and contiguous with an amorphous non-cellular substance. In some areas, such as a portion of Figure 1, collagen is also present within the amorphous region. In others, such as Figure 4, collagen formation has not occurred within the BG amorphous zone.

In all BG regions examined, the boundary between the amorphous non-cellular substance and the relic of the bioglass bonding film is delineated by a dark electron opaque line approximately 0.1 μm thick. This line or interfacial bonding zone is especially noticeable in Figure 5 at the higher contrast. In some areas along this zone in Figure 5 contiguity between the cell process and the BG zone appears to exist. Similar "bridges" or adherant cell wall contacts also seem to be present at various sites along the BG layer in Figures 2-4.

Another significant feature seen consistently in Figures 1-5 is the presence of multiple layers of cell bodies. At least seven layers are present or seen in these sections. High activity of the cells in terms of intercellular collagen formation is also apparent in Figures 1-5. Initiation of mineral precipitation within the collagen-amorphous matrix is uncertain

In an effort to identify intercellular mineralization an EDXA scan was performed on a large intercellular region. A spot size of approximately 2 μm was used. Figure 6 shows the TEM of the region analyzed with the large dark spot being the carbon contamination resulting from holding the EM beam stationary for a considerable time to enable the X-ray fluorescent analysis to be performed. The EDXA spectrum obtained is shown in Figure 7. No significant levels of Ca or P were detected. The elements shown were primarily those of the heavy metals used for staining. Thus, the dark spots within the intercellular collagen are concluded to be concentrations of stain rather than the onset of mineralization. Some intercellular silicon did seem to be present, however.

A second EDXA analysis of a different intercellular region with large concentrations of collagen was performed using a 0.5 μm electron beam. No Ca or P was detected. Less Si also seemed to be present in this region.

---

*Recent experiments of Dr. Grant indicates that the bone cells in samples examined in this experiment are not typical of the general behavior of the rat embryo calvaria line of cells. However, the validity of the ASTEM analyses is not compromised by this recent finding.
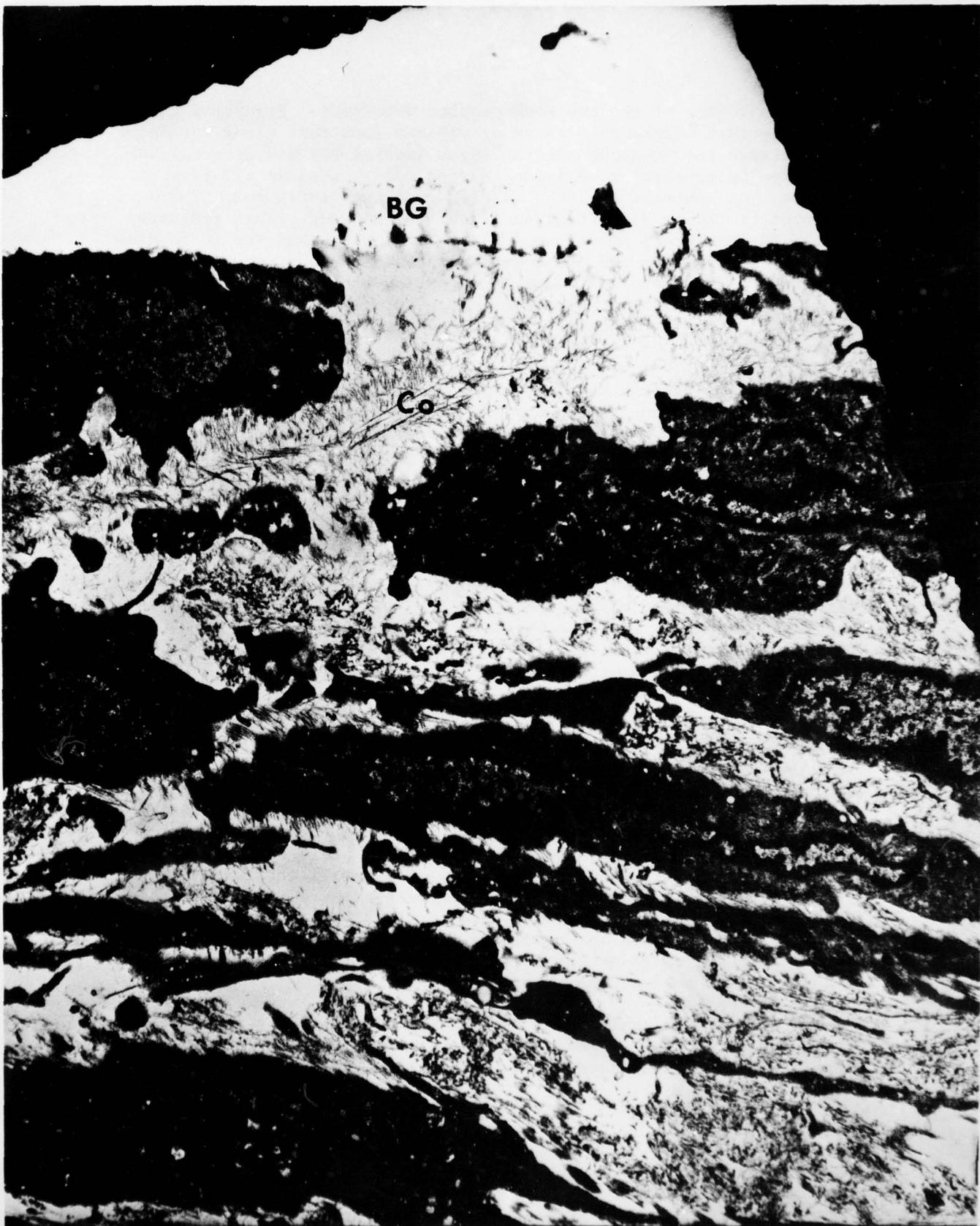
91

Fig. 1. Transmission electron micrograph of bone cell-bioglass interface (10,100X).

MICROCOPY RESOLUTION TEST CHART

NATIONAL BUREAU OF STANDARDS-1963-A
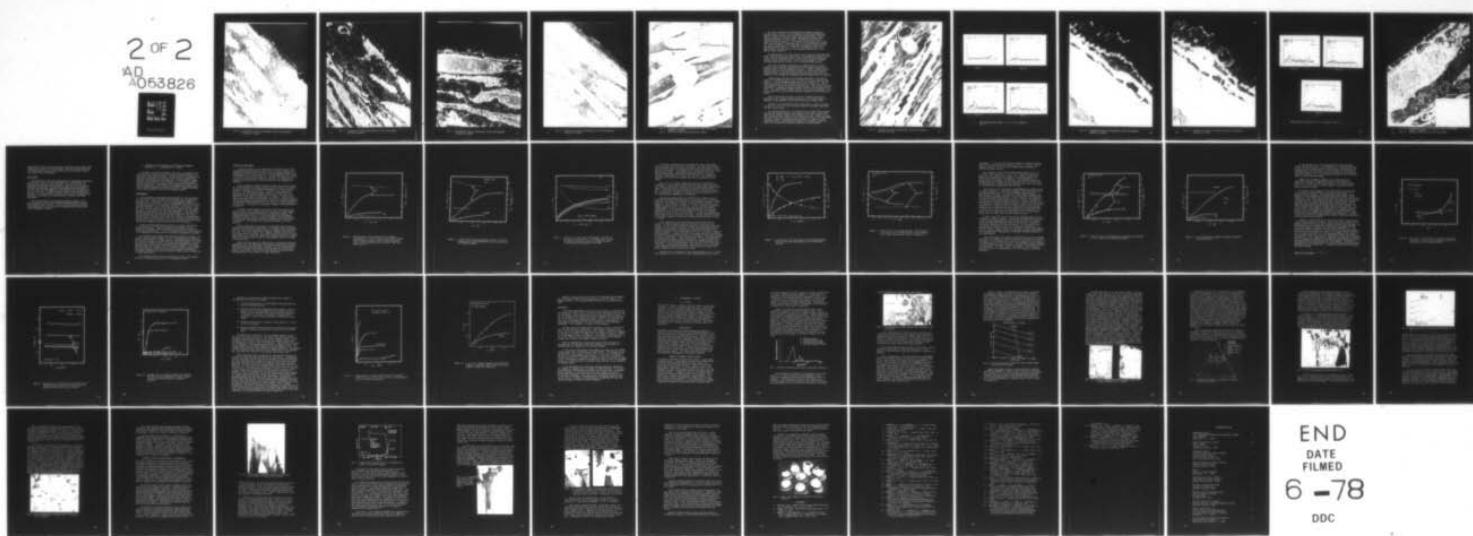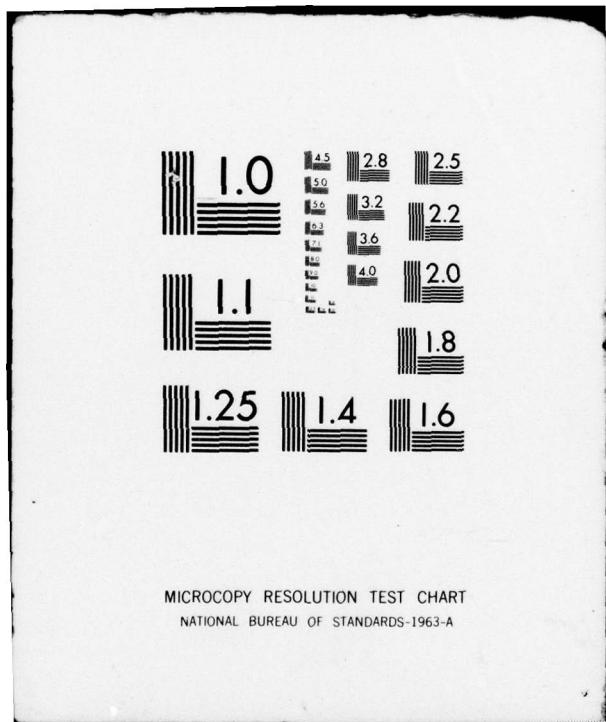
Fig. 2. Transmission electron micrograph of bone cell-bioglass
interface (10,100X).

93
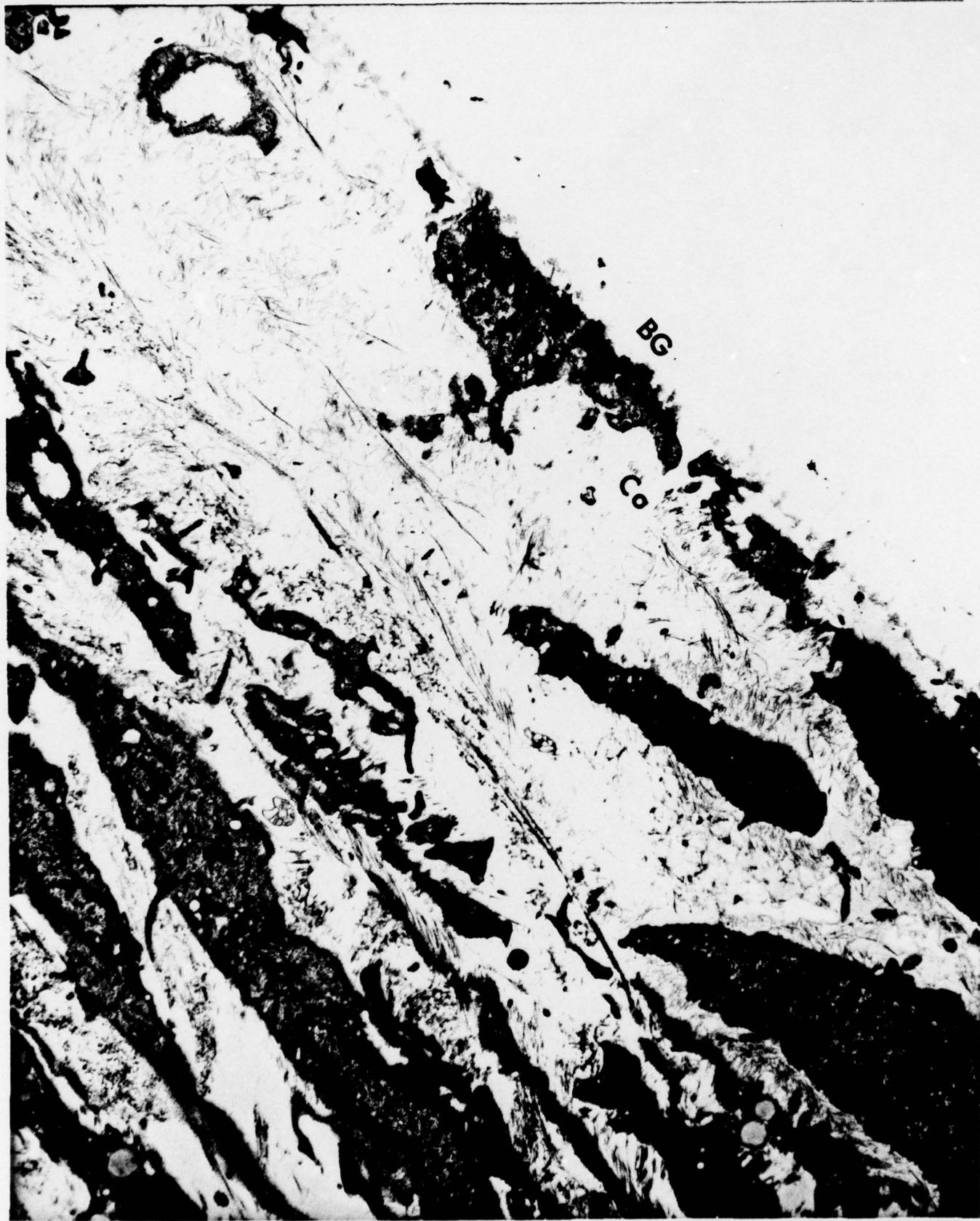
Fig. 3.   Transmission electron micrograph of bone cell-bioglass
          interface (10,100X).

94
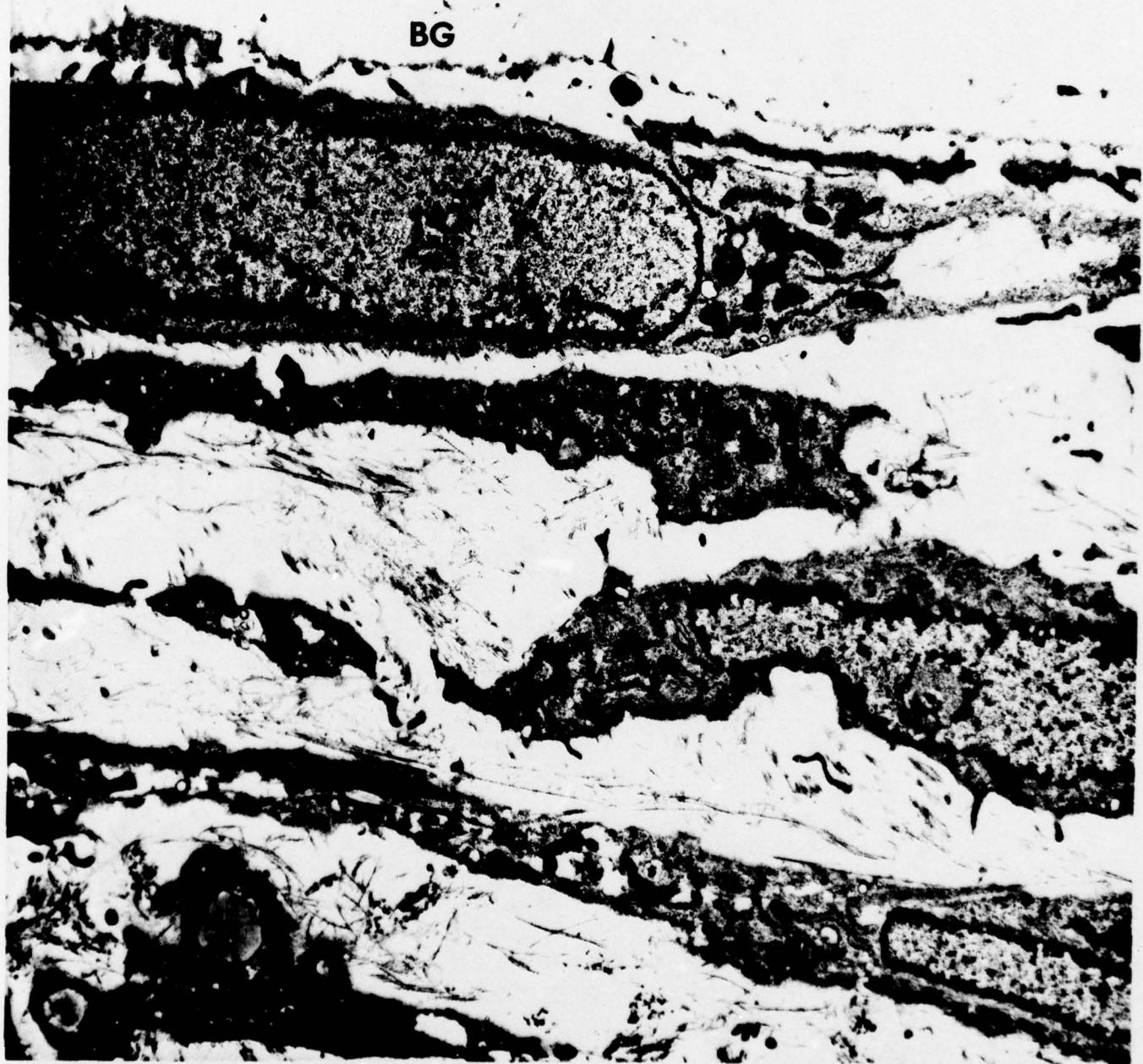
Fig. 4. Transmission electron micrograph of bone cell–bioglass
interface (10,100X).

Fig. 5. Transmission electron micrograph of bone cell—bioglass
interface (10,100X).
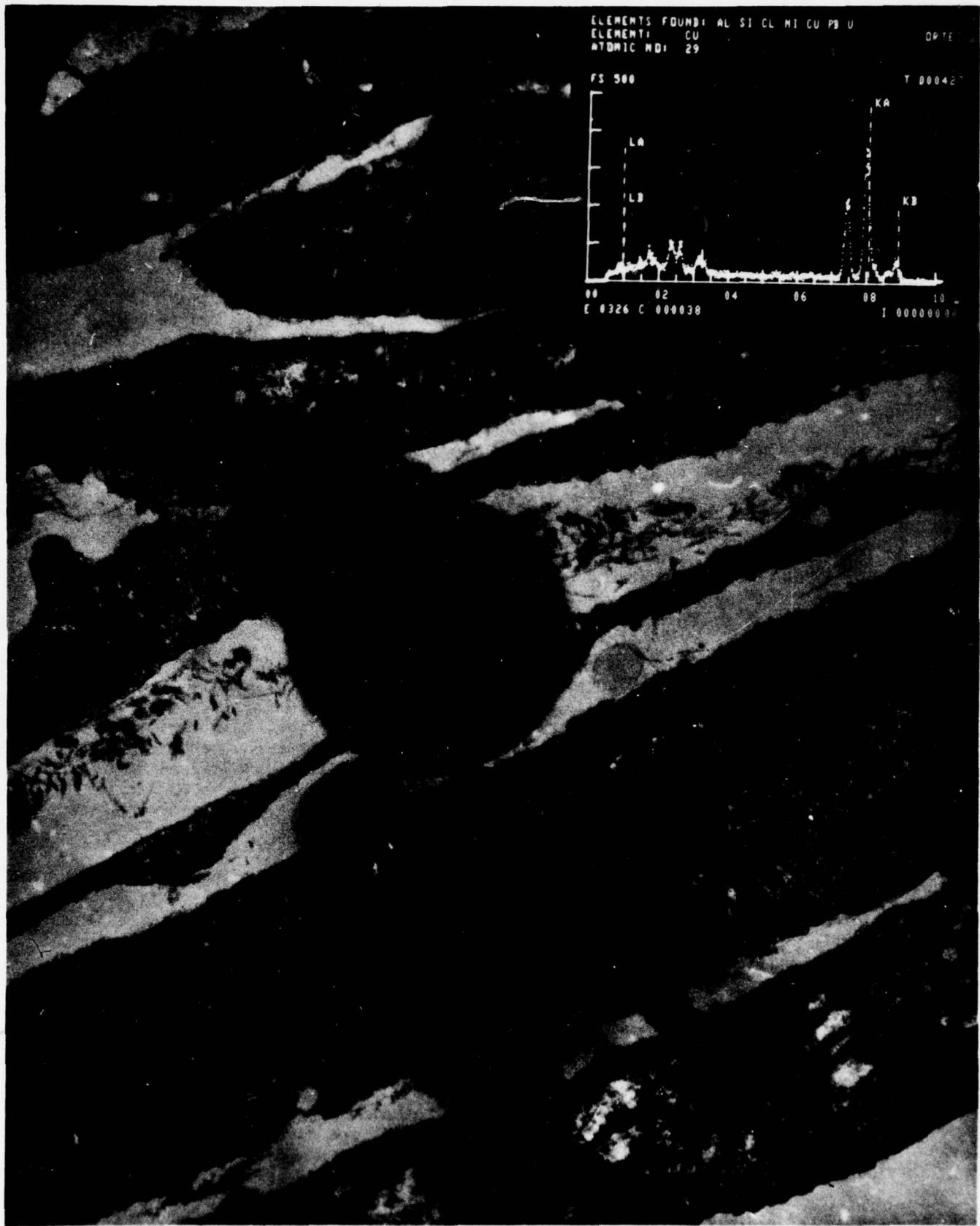
Fig. 6. Transmission electron micrograph of bone cell–bioglass interface (36,400X).

Fig. 7. (insert) is EDXA spectrum from dark region.

The lack of evidence for mineralization prompted changing to stained 6 week bone cell culture samples for the second experiment. Figure 8 shows the TEM of the region after EDXA analysis. Spot #1 was in a region of relatively dense intercellular collagen with a considerable density of dark spots. The EDXA spectrum of this region is shown in Figure 9. A relatively clear region with no dark spots was analyzed for comparison, Spot #2 and EDXA spectrum, Figure 10. Finally analysis of a neighboring cell body was taken, Spot #3, and EDXA spectrum, Figure 11. Spot #4, contamination area not on TEM of Figure 8 because the area was analyzed subsequently, led to EDXA spectrum, Figure 12.

No significant Ca or P was found in any of the four spots analyzed. Large counts from the heavy metal stains and background radiation, such as Zn, from the objective aperature and Cu from the grids compromise making a useful identification. Thus, further attempts to analyze for mineralization will require use of non-stained TEM sections.

The third experiment conducted was an EDXA analysis of the BG bonding layer to attempt identification of the various compositional gradients within the cell-bioglass interface. Figure 13 shows several distinct layers of varying electron opacity at the BG-cell boundary. Identification of these layers might well provide the answers to the identify of the fundamental bonding mechanisms between bone and bioglass.

Compositional analyses were performed using EDXA at the approximately 2 μm diameter Spots #1, #2, #3 shown on the post analysis TEM, Figure 14. The corresponding EDXA spectra are Figures 15-17. Spot #1 shows considerable Si and P present with some Ca. Thus, this region corresponds to the active SiO_2-rich reaction layer that has been reported previously as forming on bioglass samples exposed to physiological solutions. The darker border between the SiO_2-rich region corresponds to the much thinner Ca-P rich film that develops contiguous with the SiO_2-rich region.

Spot #2 shows much lower Si, P, and Ca concentrations and is apparently just a heavily stained portion of a cell process which is adherant to the amorphous intercellular material on either side.

Analysis of the amorphous intercellular region is given in Figure 17, Spot #3. No Ca or P is detected but some Si is present along with the heavy metal stains.

In a fourth experiment, a six week bone cell culture 45S5 bioglass specimen was examined without the presence of the Uranyl acetate and lead citrate stains. However, OsO_4 fixation was used. Figure 18 shows that significant TEM contrast is still present and most of the BG bonding boundary, cellular, and intercellular features are similar to those illustrated above. Compositional analysis of the sample, Figure 19, shows that considerable background radiation is still present.

Fig. 8.   Transmission electron micrograph of bone cell–bioglass
          interface (36,400).
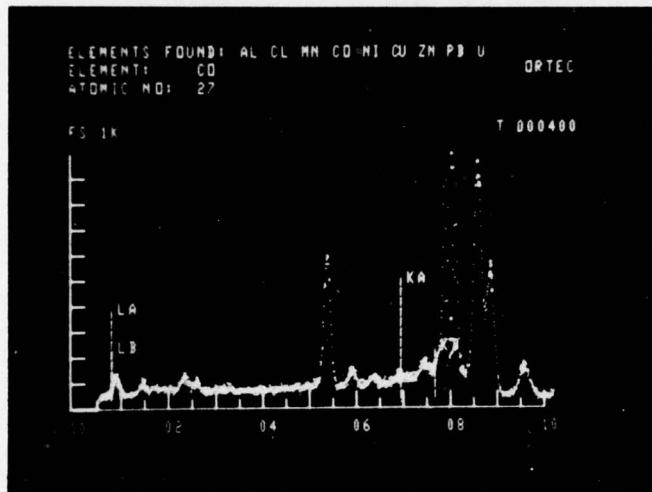
Fig. 9.
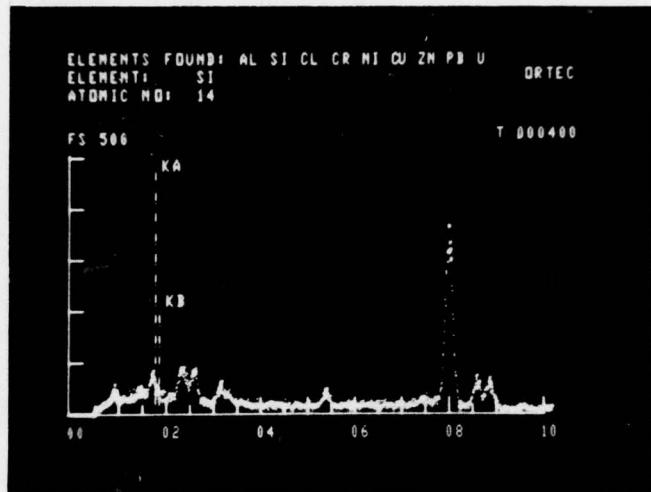
Fig. 10.
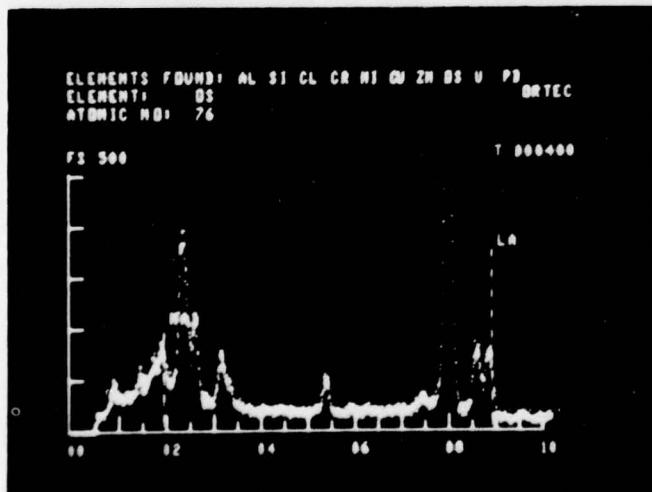
Fig. 11.
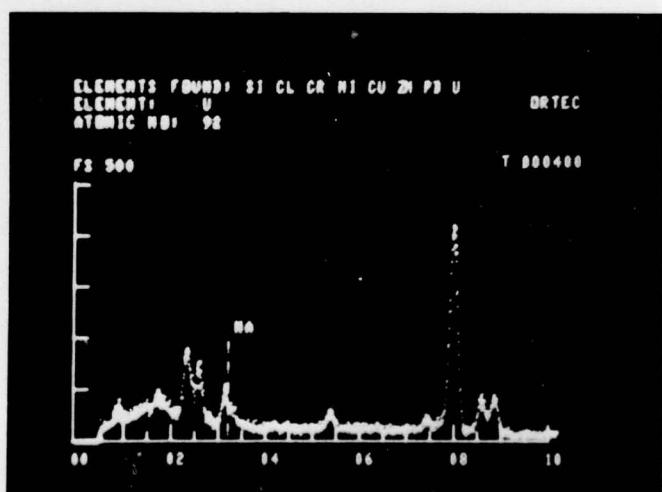
Fig. 12.

EDXA spectrum from region 1 or 2 or 3 or 4 marked in
Fig. 8.
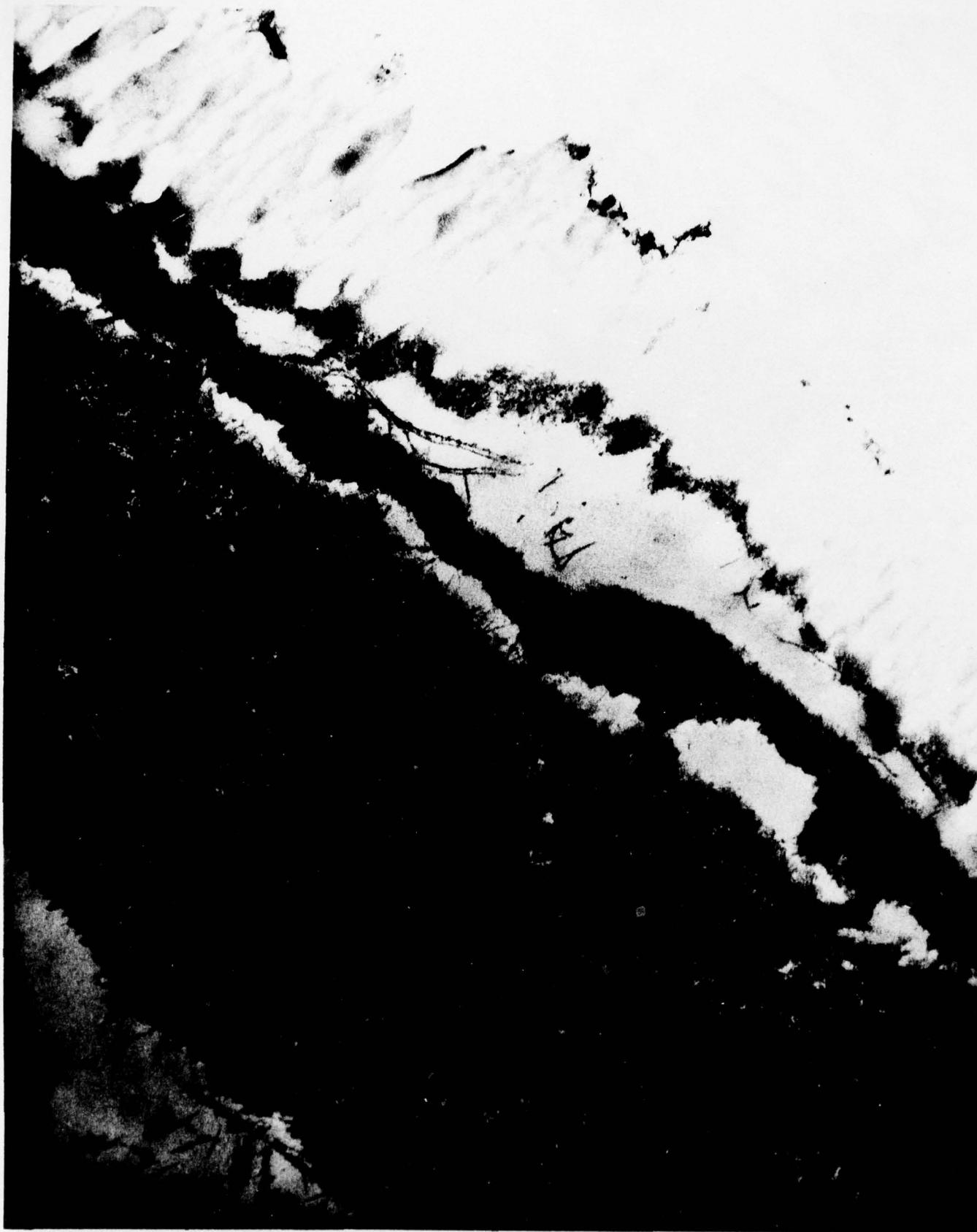
Fig. 13. Transmission electron micrograph of bone cell-bioglass interface (36,400X).

101

Fig. 14. Transmission electron micrograph of bone cell-bioglass
interface (36,400X).

102
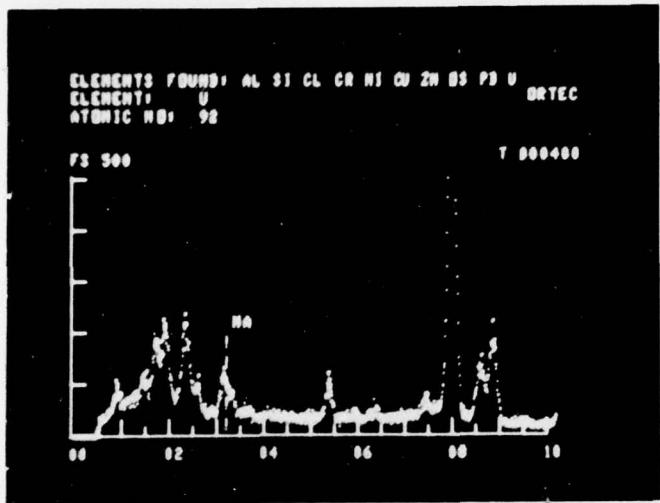
Fig. 15
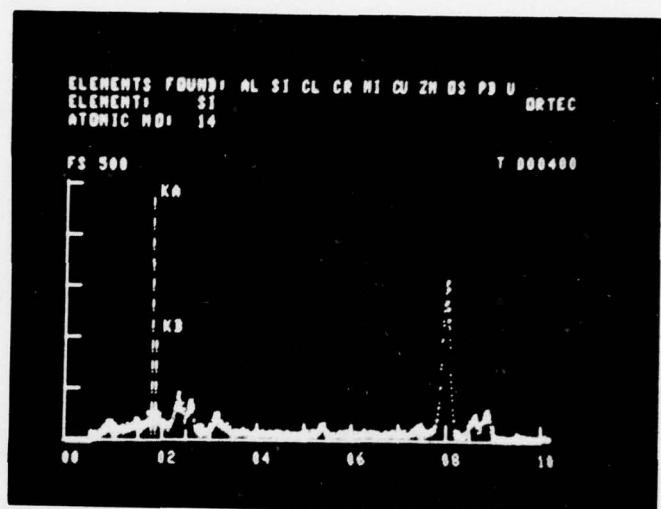
Fig. 16
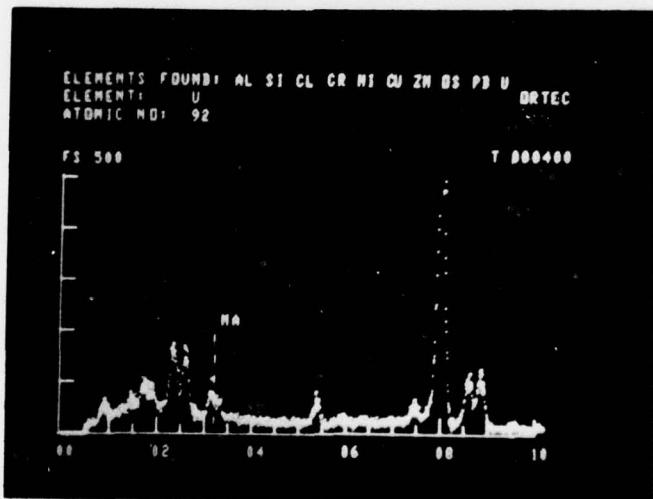
Fig. 17

EDXA spectrum from region 1 or 2 or 3 marked in Fig. 14.

103

Fig. 18. Transmission electron micrograph of bone cell—bioglass
interface (36,400X).

Fig. 19. (insert) is EDXA spectrum from dark region.

Consequently, efforts in this area will be pursued in the future using samples without OsO₄ in the preparation. Use of new carbon grids and a Be sample holder which is now available will also greatly increase the resolution of the analyses.

Conclusions

The presence of a Si-rich bonding layer on the bioglass substrates covered with a thin Ca-P rich layer which is in contact with the physiological milieu has been confirmed. The Ca-P rich layer is separated from the bone cell processes in many areas by an amorphous intercellular substance, probably a sulfonated mucopolysaccharide. In other areas the cell membrane itself appears to be contiguous with the Ca-P rich film. Collagen formation occurs within the amorphous substance but does not seem to attach to the Ca-P rich film even after six weeks. No evidence for mineralization is present from these experiments.

Cell stabilization at the bioglass interface appears to be a critical factor in the culture developing multiple layers of cells which maintain their function. The role of the bioglass interface in mineralization of the intercellular substance will require additional experiments, however.

H. Adsorption of Physiological Constituents on Bioglass Substrates, P. J. Buscemi and L. L. Hench

Although it has been established that there is a chemical bond existing between bioglass and bone, the exact mechanism has not, to this point, been clearly defined. Through the use of calorimetry and adsorption measurements new insights to the initial stages of the formation of the bond have been developed. The binding of collagen and other macromolecules to the surfaces of a well characterized slightly soluble salt, and various oxides demonstrate specific interfacial interactions. When viewed in a systematic way, these interactions strongly suggest the mechanism by which collagen and perhaps other plasma proteins can bind to the bioglass surface.

Experimental

All calorimetric measurements were performed in the same manner. The calorimeter used was a model LKB 10700 batch type equipped with twin gold cells. Each gold cell has two compartments capable of holding 2 and 4 ml of fluid. Into one compartment was placed 2 ml of the reaction solution, the adsorbate, and into the other, 2 ml of the solvent containing .1 gm of the solid adsorbent to be studied. Into the other cell was placed an equal amount of adsorbate in one compartment and 2 ml of solvent into the other compartment. The cells are bounded by thermopiles on two sides through which all heat must flow. The thermopiles are connected electrically opposite so that equal amounts of heat produced in both cells will cancel any voltage output. In this manner the second cell can act as a reference accounting automatically for heats of dilution. The heats of mixing of the solid with solvent were negligably small except in the case of bioglass.

Adsorption measurements were carried out in one of two methods. In one case equal 2 ml volumes containing the adsorbate and the adsorbent were mixed. These determinations were meant to mimic the calorimetric measurements. In the second method the clean solid exposed to the atmosphere was mixed with the solution containing the adsorbate.

All chemicals were reagent grade and were supplied by Sigma[R]. The collagen used, molecular weight 3×10^5 as determined by gel chromatography, was prepared as a soluble mixture. Poly-galacturonic acid (PGA) has molecular weight of 45,000 while the molecular weights of the polypeptides poly-L-lysine and poly-L-arginine were approximately 30,000. Macromolecules were supplied by Aldrich Chemical Company. The alumina used was Linde 'B' .05 micron Al_2O_3 of specific surface area 82 m^2/gm. Tricalcium phosphate (TCP) and silica were prepared by Mallinkrodt and Fisher respectively and were of specific surface areas 57 m^2/gm and .7 m^2/gm respectively.

The solutions used to mix the macromolecules were either Ringers solution or Ringers solution with a .2 M phosphate buffer.

Results and Discussion

It has been shown in this laboratory and elsewhere that if two macromolecules bind strongly as in the case of poly-L-arginine and chondroitin sulfate it does not imply that the monomers making up the macromolecule will bind nor that one of the macromolecules will bind the monomers of the other (Figure 1). In this particular case several factors coerce the two large molecules together. In studying the binding of macromolecules to solid surfaces the same phenomenon is observed.

One such example is shown in Figure 2 where the reaction energy Q, and the enthalpy of binding lysine, and poly-L-lysine (PLL) to SiO_2 are plotted against the original concentration C_o of the adsorbate solution. The solution is at pH 7. The pKa of the lysine is at pH 10.4 so that the carboxyl group should not interfere with its adsorption to the negative surface of the silica. The first K_b is below 10^{-7} so that only one amino group is ionized. There is only the ionized side chain on the polymer. Not only do the reaction heats reflect the greater binding reaction but also the calculated enthalpies. The essential difference between the two molecules in this situation is their size. The surface is oppositely charged to both molecules at this pH [7].

In Figure 3 some examples are given in which the charge of the surface is near zero (slightly positive for this particular sample); and in which the adsorbing molecules are negatively charged. The binding experiments were run in both distilled water and Ringers solution to show the effect of salts on binding. Poly-galacturonic acid (PGA) and galacturonic acid show the same effect as PLL but not as pronounced. The monomer shows increased enthalpy in the salt solution.

Further indications of the effect of the molecular size can be shown by electrophoretic measurements. For example, these demonstrate that PGA will reverse the surface charge of alumina while the monomer will not. This is an indication of specific chemical interaction of the polymer with the surface. This together with the previous observations reveal that a molecular model for a polymer should not be chosen only on the criteria that it has the same monomeric form of the same functional groups.

Results indicate that the binding process is cooperative between charge and size. The difference in potential between the surface and macromolecule must be sufficient to attract it to the surface, while the size of the molecule, because of entropy effects of the solvent, draws it even nearer. This in turn will increase the electrostatic binding because of the decrease in charge separation.
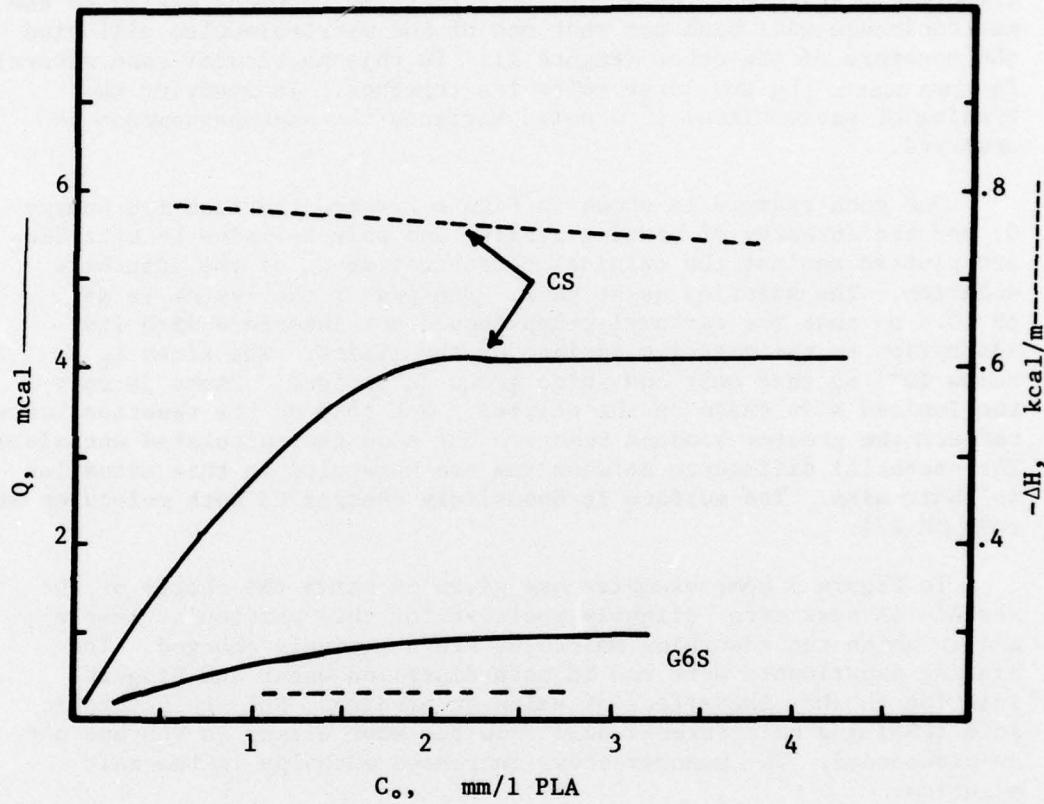
Figure 1. Reaction heat Q and binding heat ΔH vs original
concentration C_o. Heat of binding chondroitin sulfate
(CS) and poly-L-arginine (PLA) in which precipitate
forms. Similar monomer glucose-6-sulfate (G6S) does
not bind to CS.
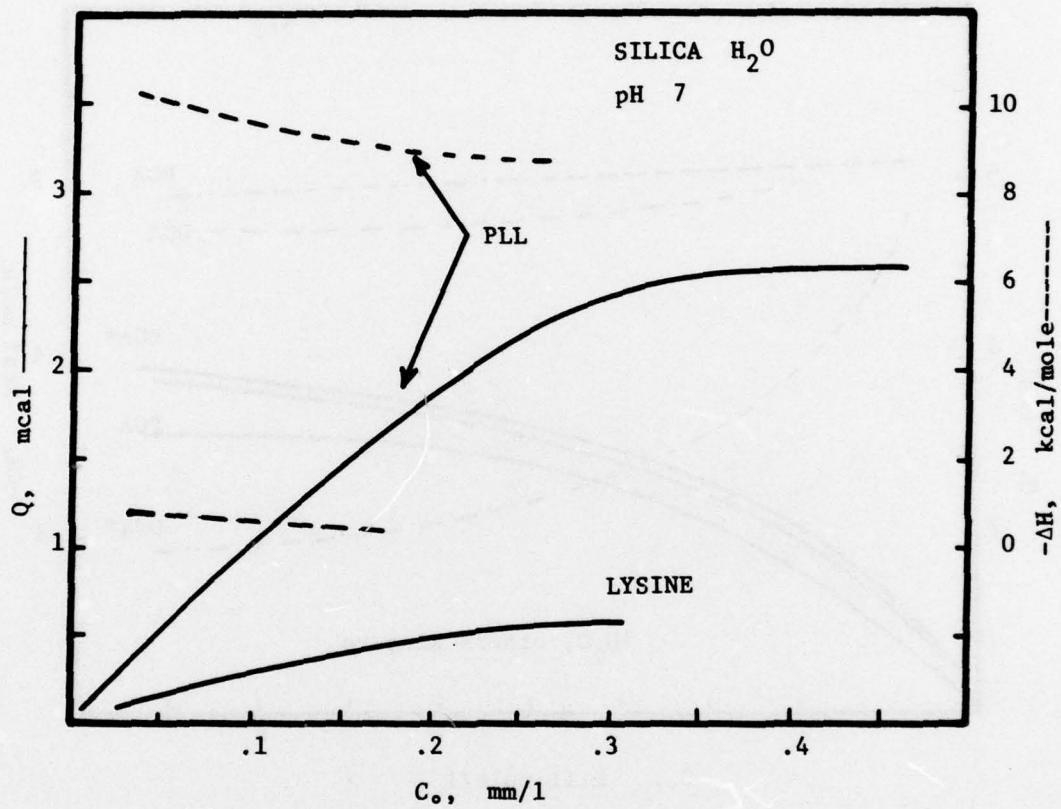
Figure 2. Q and ΔH vs C_o for poly-L-lysine on silica. Only the polymer shows a high binding heat ΔH as in the case of two charged polymers.
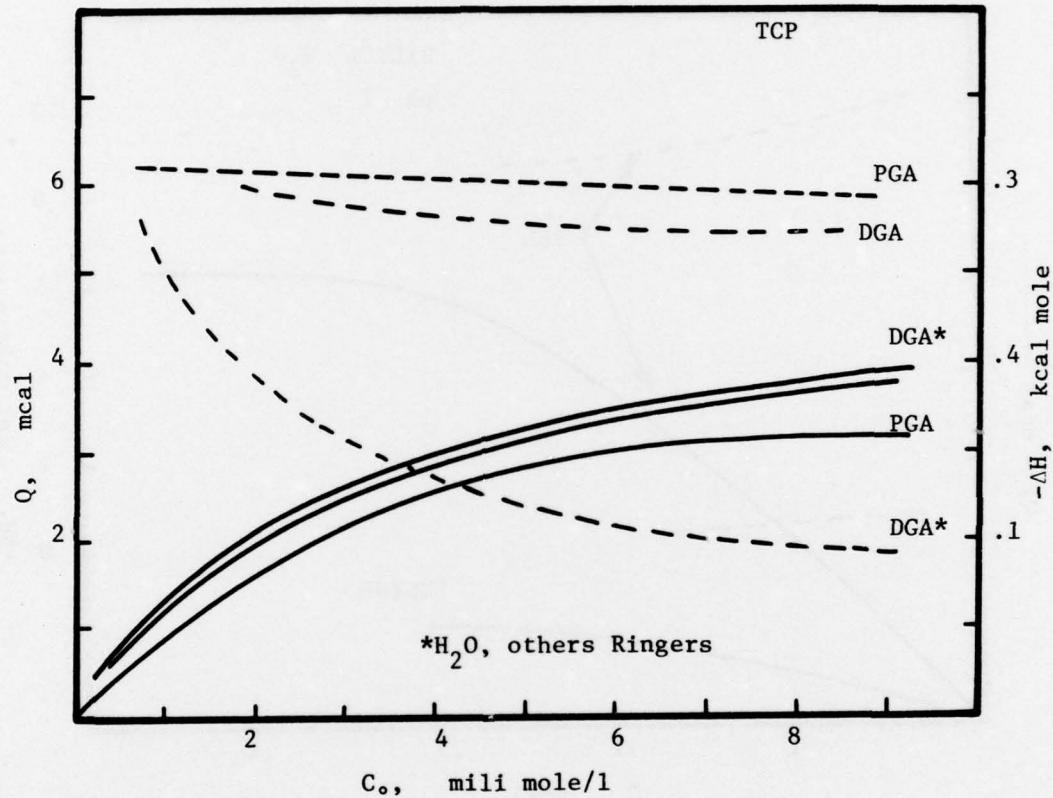
Figure 3. Q and ΔH vs C_o for several saccharides. The heat of
binding is increased for a .1 M concentration of salt.
The polymer poly-galacturonic acid (PGA) has higher
ΔH than monomer D-galacturonic acid (DGA).

As the salt concentration is increased the size of the double layer extending into the solution decreases. The high charge density of this diffuse region is reduced by both polymer and monomer as they approach the surface. The polymers still retain the position of being more strongly bound. An increased salt concentration will also increase the binding of molecules which have neutral to slightly opposite charge relative to that of the surface. For instance the absorption of dextran and collagen onto TCP is increased in this manner.

The effect of a slight charge difference can be detected by calorimetry. Poly-L-arginine (PLA) has a slightly longer side chain (one methyl group) and is slightly more basic than poly-L-lysine (PLL). Figure 4 shows the results of mixing PLL and PLA with solid TCP at pH 7. Even though the reaction heat of the PLA is lower than that of PLL the enthalpy of binding as determined by solution depletion is 5 to 7 times greater depending on concentration.

Thus we have demonstrated that differences in charge, size of molecules and surface characteristics can be depicted by calorimetry. These same differences are visible in the binding of collagen to oxide surfaces. The binding of collagen to silica in distilled water and Ringers solution is shown in Figure 5. At pH 7 collagen is negatively charged having an IP of 5.5 so in water the reaction is negative (endothermic). Solution depletion measurements show that collagen does absorb but it is due to the increase in entropy in releasing solvent into the bulk as stated previously. In water the enthalpy was approximately four to seven cal. per gram. With the addition of salts in the form of Ringers solution the enthalpy became negative at about $-.5$ cal/gm.

It is important to note that several authors report that an increase in ionic strength decreases absorption of proteins onto 'glass'. It has also been shown that high salt concentration denature proteins and cause their unfolding. It has been demonstrated in this laboratory that globular proteins (BSA) adsorb more strongly (more negative enthalpy) in salt concentrations of 10^{-4} M onto Al_2O_3 compared to distilled H_2O. A slight decrease in the amount absorbed is noted at saturation of the surface but there is an increase in the amount absorbed at lower concentrations. These observations indicate that denaturation of proteins cause them to occupy larger areas. If the denaturation is severe enough, profound changes in fraction of proteins absorbed will take place. Low salt concentrations (less than 10^{-4}) will cause only a 'loosening' of the hydrogen bonding. Hence there will be an increase of the available groups to chemically interact with the surface and higher enthalpies of interaction will result.

Collagen will also denature at salt concentrations of 1 to 2 M but only slightly or not at all in the salt concentrations found in these
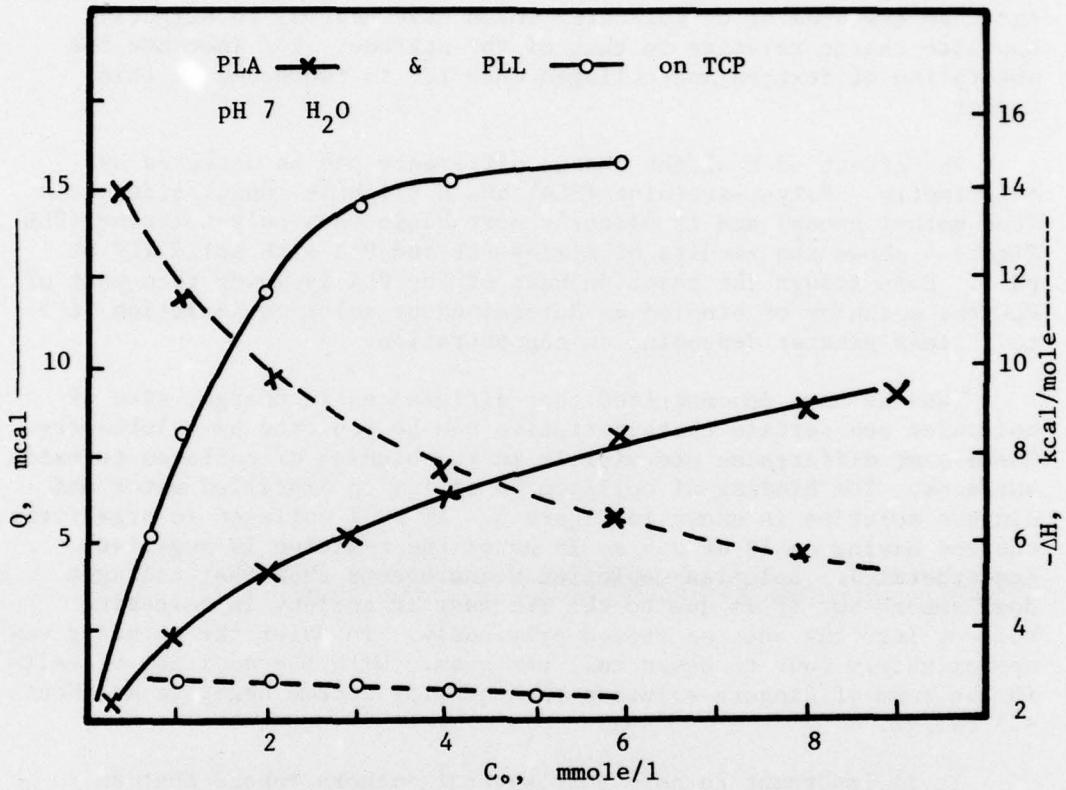
Figure 4. Q and ΔH vs C_o for PLL and PLA on tricalcium phosphate. The more basic PLA shows higher heat of binding, ΔH, than PLL.
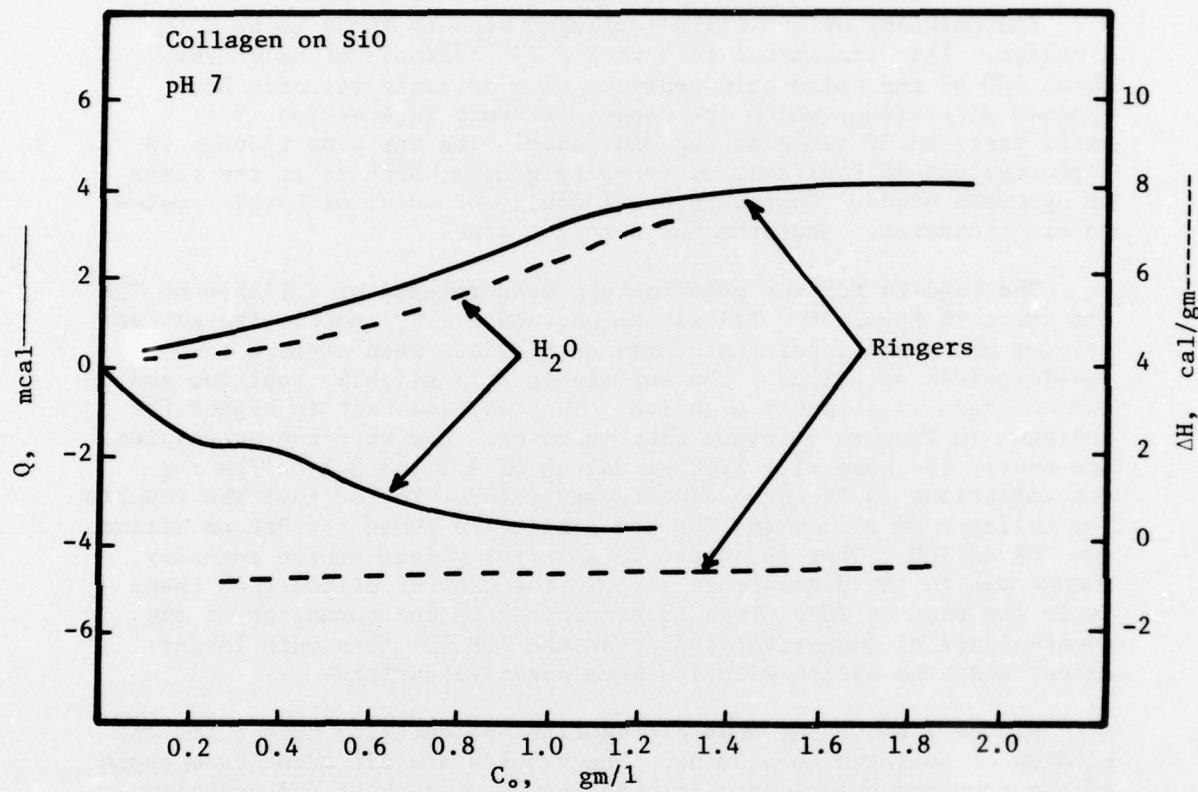
Figure 5. Q and ΔH vs C_o for collagen on SiO_2. The presence of
.1 M solution of salt from Ringer's solution changes
the ΔH value from positive in water to negative.

experiments. It is also found that the amount of collagen adsorbed onto silica increases from a saturation value of .3 mg to ∿.6 mg in Ringers solution. The cause of the higher negative enthalpy is probably hydrogen bonding.

The enthalpy of the silica-collagen bond is found to be 1 to 2 cal/gm. This translates to 3 to 6×10^5 cal/mole of molecules. About 300 of the amino acid residues of a collagen molecule have exposed side groups which are capable of such interaction if a small fraction of these at one end react. The enthalpy reduces to approximately 10 kcal/mole of reacting groups which is in the range of hydrogen bonds. Charge reversal would not occur with this system so electrophoretic measurements were not done.

The results for the calorimetric measurements of collagen on TCP are shown in Figure 6. Tricalcium phosphate (TCP) models the active calcium phosphate layer that forms on bioglass when exposed to physiological solutions. The surface is only slightly positive and the collagen is slightly negative. The reaction heat is higher for collagen in Ringers solution than in water. However, the enthalpies are nearly the same with average values of 4.5 and 4.2 cal/gm for determinations in Ringers solution and water. Notice that the results for collagen on silica and TCP are similar to those for PLL on silica and PGA on TCP. That is, there is a larger effect on the enthalpy change due to the presence of salt in the case of silica than there is in the case of TCP. This is attributed to the formation of the double layer of (negative) ions near the TCP but to a much larger extent near the silica with its more negative surface.

Figure 7 shows the heat of reaction and enthalpy curves for the binding of collagen to alumina. The results are different from those of the previous experiments in that the reaction heat and enthalpy values are quite high reaching values of 80 mcal and a constant 45 cal/gm when Ringers solution is the solvent. In the case of water the results are similar to those of the previous experiments; a maximum value of 8 mcal evolved and a constant 7 cal/gm. The combination of a highly charged surface, an oppositely charged macromolecule and a moderate salt concentration in the bulk solution contribute to the high enthalpy.

Since the surface has a higher potential relative to the collagen than the other surfaces, the salt concentration of (negative) ions will be greater. It is possible that there is an increase in the extent of the denaturation if any occurs at all. The increase in salt concentration will definitely cause a further loosening of the hydrogen bonding in the molecule. The exact amount is not known. In any case the enthalpy value of 45 cal/gm yields 1.35×10^7 cal/mole of collagen molecules.
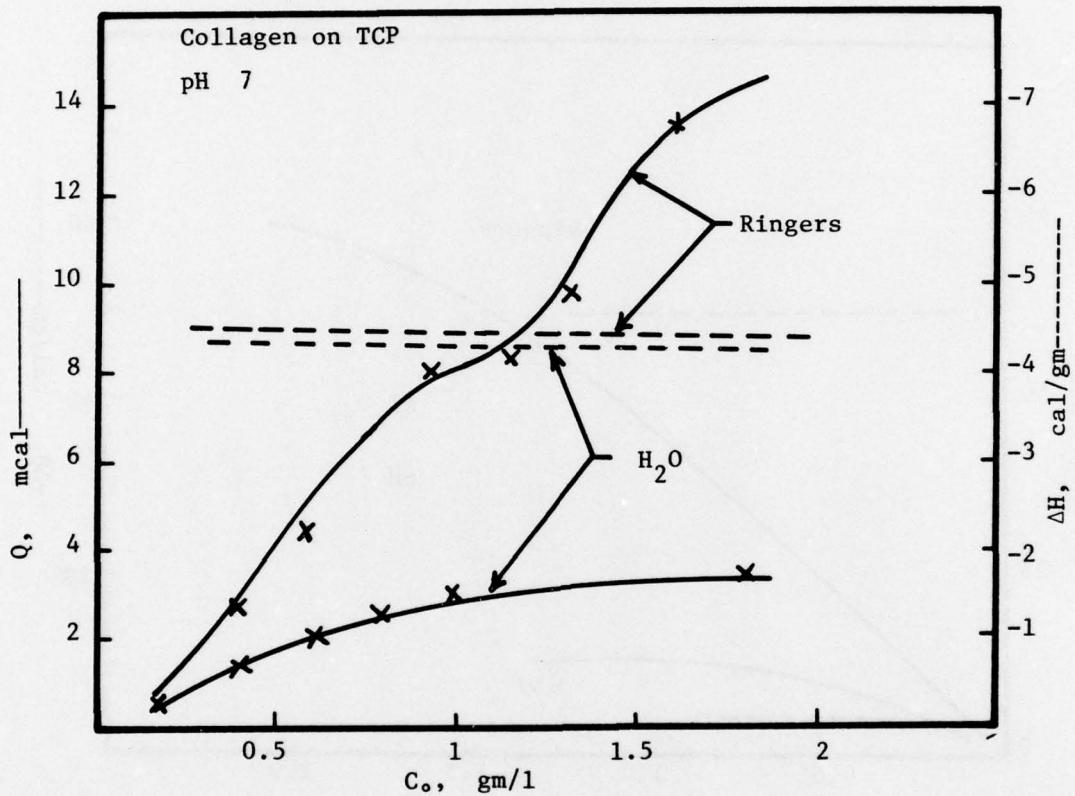
Figure 6. Reaction heat Q and binding heat vs original concentration C_o for collagen onto tricalcium phosphate.
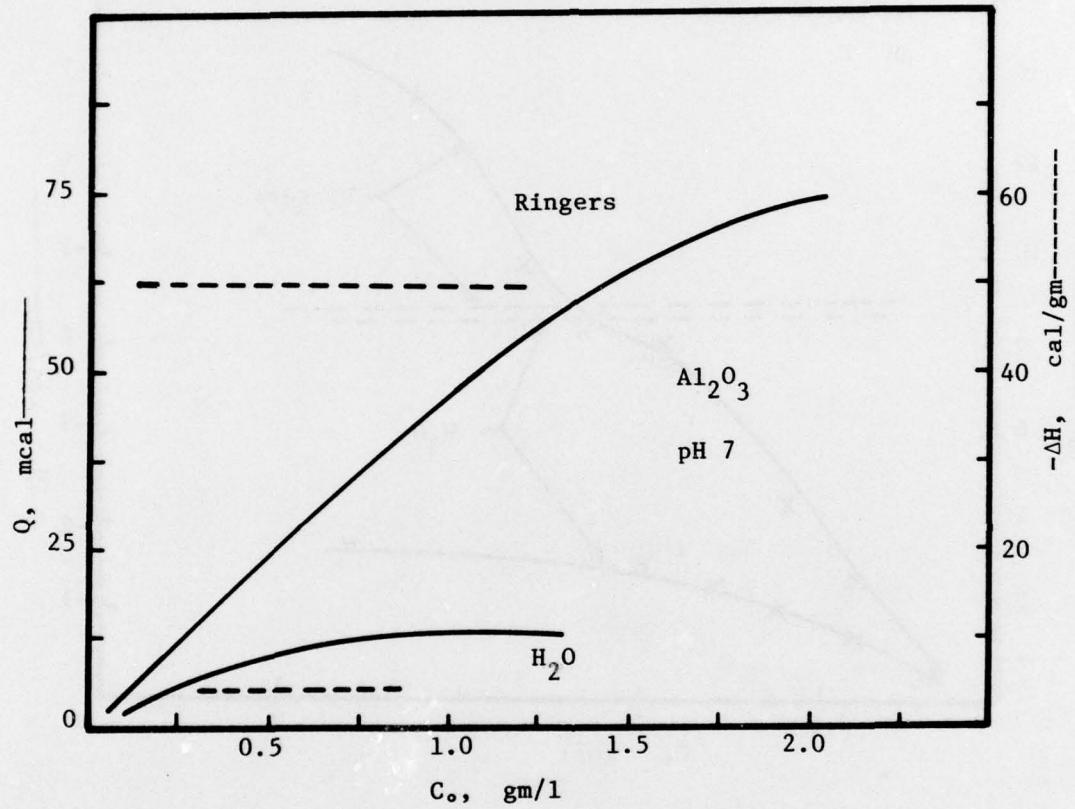
Figure 7. C_o vs Q and ΔH for collagen in alumina in Ringer's solution and water.

In one molecule there are approximately 300 residues which contain active side groups. If the molecule is completely denatured so that all 300 of these residues could interact, the value for the enthalpy would be 45 kcal/mole. If only a portion of the molecule 'unraveled' say a fifth of its 1000 Å length then the value would be about 250 kcal/mole. All these energies are high and are out of the range of purely hydrogen bonding.

Figure 8 is a schematic summary of the results thus far indicating the effect of surface potential in the enthalpy of adsorption. The pzc* of the surface charge for the three surfaces are 3, 7, and 9 for silica, TCP and alumina. The effect of the Ringers solution is seen.

In order to see the effect of the surface area the enthalpies of the reactions were divided by the actual surface areas. A different picture emerges. When normalized in this manner silica appears to bind collagen more strongly than either alumina or TCP (Figure 9). The surface area and ΔH values for silica are low relative to alumina or TCP. The normalization shows then that more collagen is bound per unit area rather than being more strongly bound. This indicates that collagen is adsorbing near or into the positive ions which are physically adsorbed near the negative silica surface. It is not known if this result is actually due to an artifact since the surface areas of the powders are similar only for alumina and TCP. However, it is not thought that increasing the specific surface area of the silica would affect the enthalpy of the adsorption. To help clarify the questions surrounding this analysis, adsorption experiments with silica gel were performed.

Constant .1 gm portions of silica gel were added to collagen solutions of concentrations to 2 mg/ml. One set was run in water, one in Ringers solution and a third set in Ringers in which the silica gel has been dissolved in 4.5 M NaOH and reprecipitated in Ringers solution with several washes to ensure that the pH was stabilized at 7. The results are shown in Figure 10. In the case of the 'dry' silica gel the Ringers solution doubled the amount of collagen absorbed from about .05 to .1 mg at saturation. In the reprecipitated gel, where there was confidence that the surface was completely hydrated, the adsorption increased to 1.5 mg. This result is important in analyzing the adsorption of collagen on bioglass, and in predicting why bioglass if corroded and dried will react differently than fresh bioglass. Calorimetric measurements were not made because of the difficulty of putting the gel suspension into the calorimeter. A comparable experiment with bioglass was then performed.

---

*Point of zero charge.
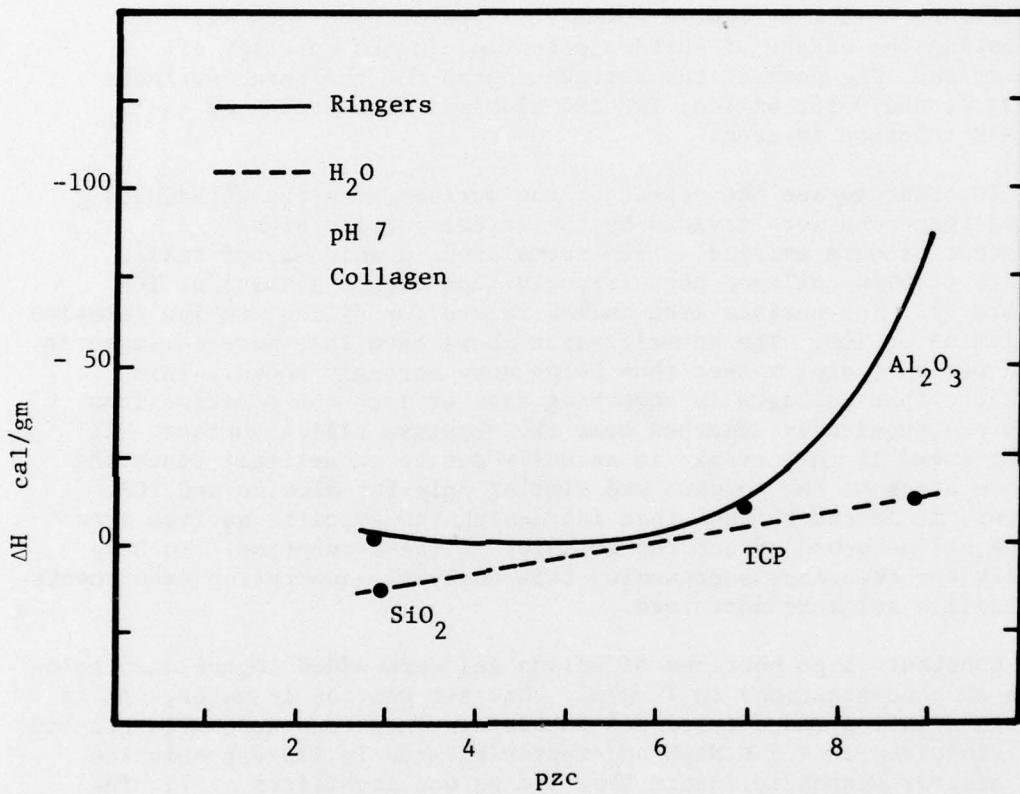
Figure 8. ΔH vs point of zero charge of the three solids used
previously. The effect of the Ringer's solution is
seen as well as the surface potential.
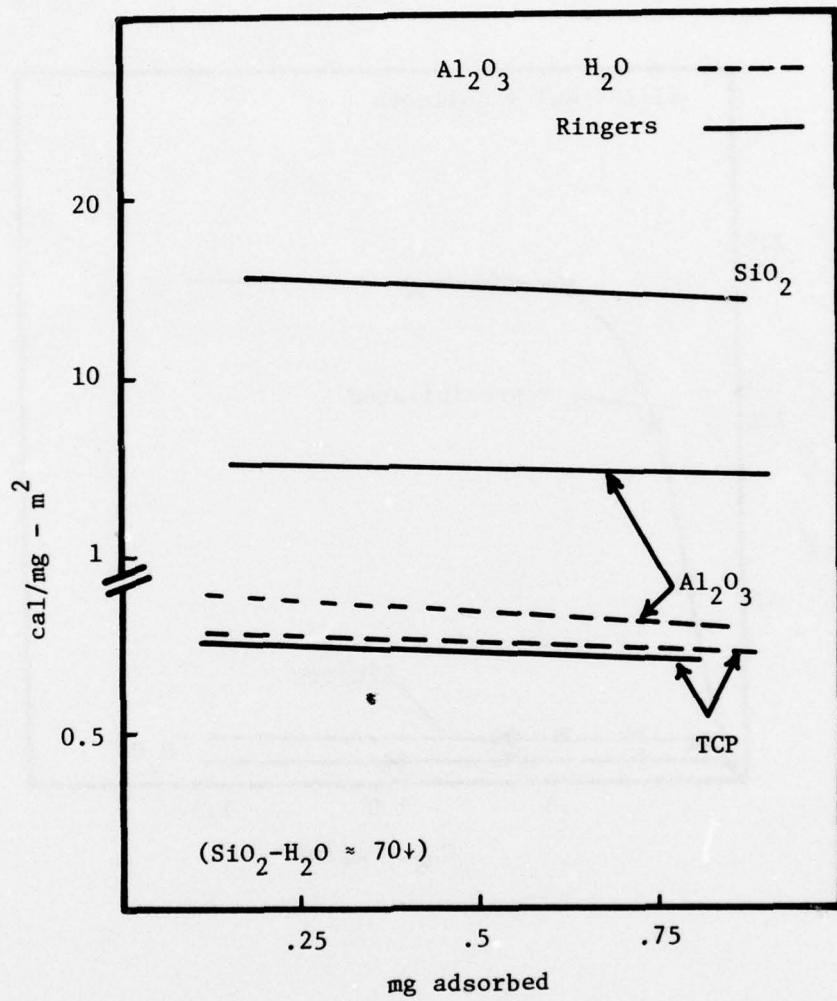
Figure 9. Normalization of binding heat ΔH by surface area shows that silica may adsorb collagen into the diffuse double layer of ions (see text).

119
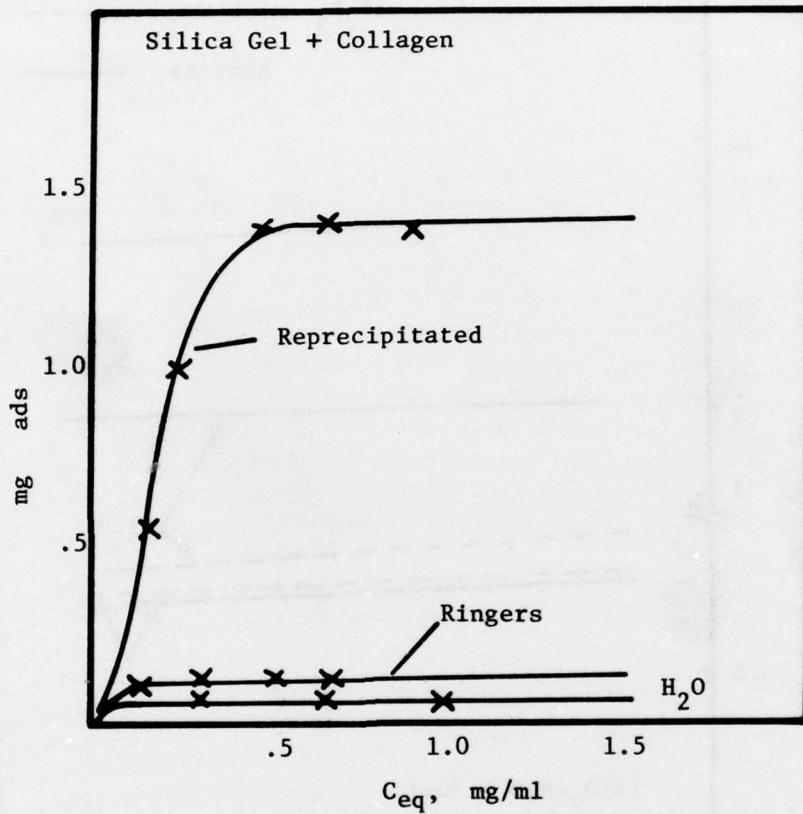
Figure 10. Langmuir plot of collagen adsorbed onto silicon
gel under several conditions; in water, Ringer's
solution and reprecipitated into Ringer's
solution.

Bioglass in four different modes was mixed with collagen to concentrations of 2 mg/m. as follows:

1) Fresh bioglass exposed to the atmosphere was mixed directly with the collagen solution.

2) Bioglass which had been prepared 24 hours earlier, still in the solution (2 ml) was mixed with the collagen solution. Because of the relatively high surface area to volume ratio of the glass to solution, the solution is assumed to be saturated. Corrosion would continue if fresh solution was added.

3) Bioglass was mixed with collagen 24 hours earlier in a total of 4 ml of solution.

4) Bioglass prepared 24 hours earlier was rinsed and then mixed with the collagen solutions with a total of 2.5 ml of solution.

All samples are corrected to 2 ml of collagen solution, at pH 7. The final pH of mode [2] was 8.5. The results are shown in Figure 11. The lowest amount absorbed was by the 'fresh' bioglass sample. In the presence of the solution salts produced by the bioglass dissolution the absorption increased. This is attributed to the increase of surface area of bioglass. The bioglass mixed with the collagen 24 hours prior to measurements showed higher adsorption than the saturated case. The bioglass which had been rinsed showed the highest adsorption. Essentially all the collagen had been adsorbed in each sample with 3.6 mg adsorbed and .4 mg left into solution at the highest concentration used.

There should have been no difference in surface area between mode [2] and [4] since they were prepared in the same manner. Consequently, surface area cannot account for all the increase in collagen adsorption. The salt concentrations of samples [3] and [2] should have been nearly the same, and cannot account for the doubling of the amount adsorbed. Modes [2], [3] and [4] all have greater surface areas than mode [1] so that part of the increase can be attributed to this, just as in the case of silica gel. The one feature that modes [3] and [4] have in common is that collagen was present while the dissolution process was in progress. In case [4] because of the high surface area already present and because the particles were rinsed, the dissolution should proceed at a much higher rate than any of the other modes. Calorimetric measurements show that the adsorption heat is high reaching almost 300 mcal or about 200 cal/mole. In the calorimetric measurements a certain period of time passed before the rinsed collagen in fresh solution could be mixed with the collagen while the calorimeter came to thermal equilibrium. Therefore, this mode is not precisely the same as mode [4]. It was noted that in each case when the bioglass was replaced into solution, that the particles stained red with eosin indicating at least some formation of a calcium phosphate rich layer, Figure 12.
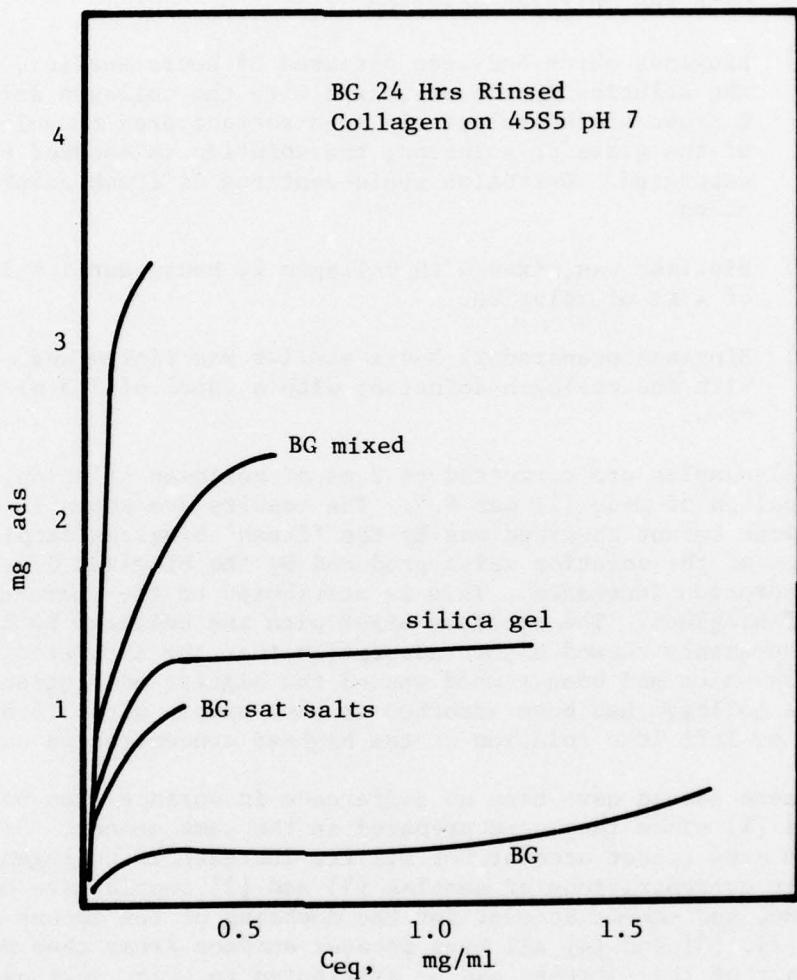
Figure 11. Langmuir plot of collagen adsorbed onto 45S5 bioglass powder with dry specific area .45 m^2/gm. Reprecipitated silica gel shown for comparison.
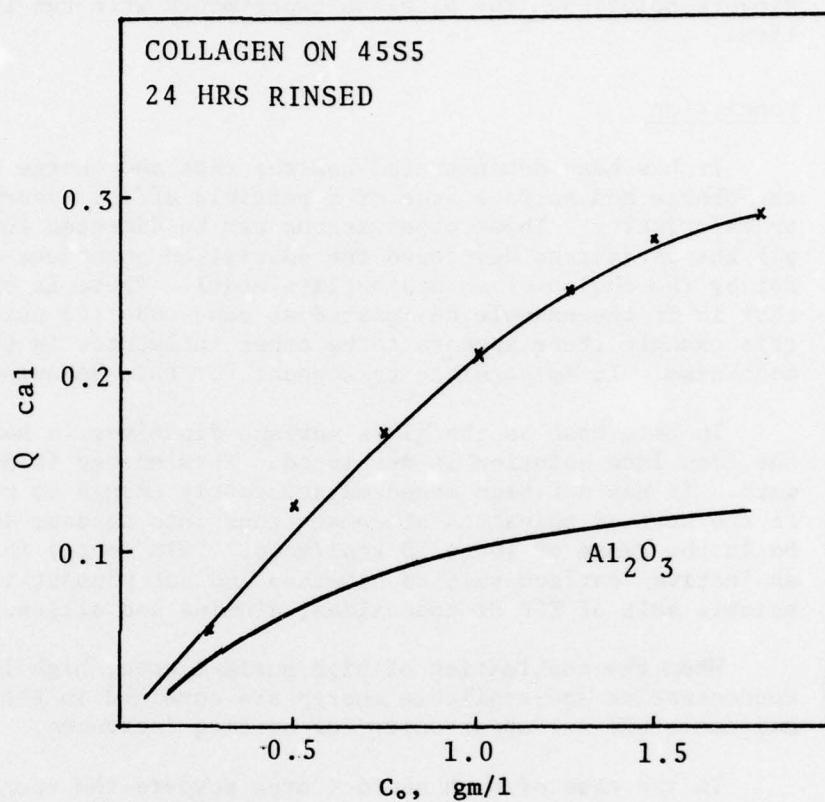
Figure 12.   Q vs C_o for collagen adsorbed onto rinsed 45S5
bioglass in phosphate buffer Ringer's solution.
Alumina is shown for comparison.

123

Finally it was noted that the addition of phosphate buffer reduced the differences between the experiment run in water and those run in Ringers solution. The bioglass experiments were run in buffered solution.

Conclusion

It has been demonstrated how the size and charge of a molecule and the charge and surface area of a particle affect adsorption as reflected by calorimetry. These observations can be directed toward bioglass. In all the parameters developed the adsorption phenomena can be accounted for by the choice of an appropriate model. There is one exception and that is in the example designated as case mode [4] using bioglass. In this example there appears to be other influences in the adsorption mechanism. It is possible to account for this behavior.

In this case as the glass surface dissolves, a heat of solution of the ions into solution is developed. This energy is available to do work. It has not been measured accurately enough to report but compared to the heat of solvation of common ions into aqueous solution it should be in the range of 10 to 20 kcal/mole. This energy is available only to an 'active' surface such as bioglass and not present in the slightly soluble salt of TCP or the oxides, alumina and silica.

When the combination of high surface area, high localized ion concentration and available energy are combined in the presence of a macromolecule the opportunity for binding increases.

In the case of high surface area powders the energy and ion release is much higher than a controlled, polished surface. The possibility for denaturation of the protein increases and in fact this is suspected for the case of bioglass powders and proteins. In the case of a smoother surface such as that of a bioglass prosthetic device the release of ions is not accelerated as compared to powders but there is still the available energy on a localized scale to overcome energy barriers in the formation of chemical bonds.

It has been shown that the energy released during the adsorption of collagen to bioglass is in the range of chemical bonds. It has also been shown that high adsorption energies are not particular to bioglass as with alumina. It has been shown that high surface area plays a particularly important role as in the case of hydrated silica gel and in the case of bioglass. The advantage of the bioglass appears to lie in its ability to combine a charged surface of high specific area and available energy to function in bond formation.

124

I.   BIOCERAMICS: A Review

L. L. Hench

*Bioceramics include: 1) nearly inert materials, such as dense
alumina; 2) totally resorbable ceramics, such as tricalcium
phosphate; and 3) controlled surface reactive ceramics and
glasses. By using coatings of controlled surface reactive
implants that have high strength fatigue resistance and bond-
ing to biological tissues can be achieved. Bonds between
surface reactive bioglasses and tissues involve incorporation
of collagen within a thin film of reactive hydroxyapatite
agglomerates that form on the implant surface. Such bonded
interfaces can be stronger than bone and remain stable for
many years.*

INTRODUCTION

Bioceramics are defined as ceramic materials designed to
achieve a specific biological or physiological behavior. The
first wide spread use of bioceramics was in the form of den-
tal restorative and prosthodontic materials. Dental porcelain
dentures, crowns and inlays represent a high state of art in
restoring oral function to individuals with diseased teeth.[1,2]
Silicate and phosphate cements also play an important role in
dental repair. However, the areas of greatest immediate
interest in bioceramic research are the use of specially de-
signed ceramics as materials to replace missing teeth (tooth
implants) and to repair portions of the musculoskeletal and
cardiovascular system. This paper will review some of the
more important developments in bioceramic implants.

GENERAL BIOCERAMIC DESIGN FACTORS

A successful bioceramic material must satisfy a large number
of design factors. Among others, it must have suitable mech-
anical and biological properties and also be able to be
fabricated into functional devices. These are severe mate-
rials design limitations. It is the general lack of toxic
components in many ceramic materials that has led to the con-
siderable interest in designing ceramics for medical and den-
tal applications. A number of tests have been developed to
examine the biological compatibility of bioceramics. Such
tests usually involve the exposure of small samples to the
soft tissues of small animals such as rodents or to living
tissue cultures in incubators.[3] Of several dozens of ceramic
compositions examined by such means only a few have shown

sufficient compatibility with tissues to justify consideration for future medical and dental implans.[3-6] Additional requirements of sufficient mechanical strength to serve a functional need as an implant and the necessity of fabricating the material into a suitable device further decreases the number of favorable bioceramic compositions. Consequently, at the present time the field of bioceramics can be generally classified into three types of materials.

Figure 1 illustrates the three major types of bioceramics in terms of a relative reactivity index. Nearly inert bioceramics (D) show little chemical change during long term exposure to physiological solutions. Tissue response to this class of bioceramics involves a very thin, several micrometers or less, fibrous membrane surrounding the implant materials. Because fibrous tissues do not chemically bond to nearly inert bioceramics, fixation within the body must be established by a strong mechanical interlock with tissues. High purity alumina and pyrolytic carbons are currently the most acceptable bioceramics of this type. When high strength is required, fully dense alumina or Pyrolite carbon is utilized and the mechanical interlock is provided by large perforations in the implant or threads or steps on the surface.
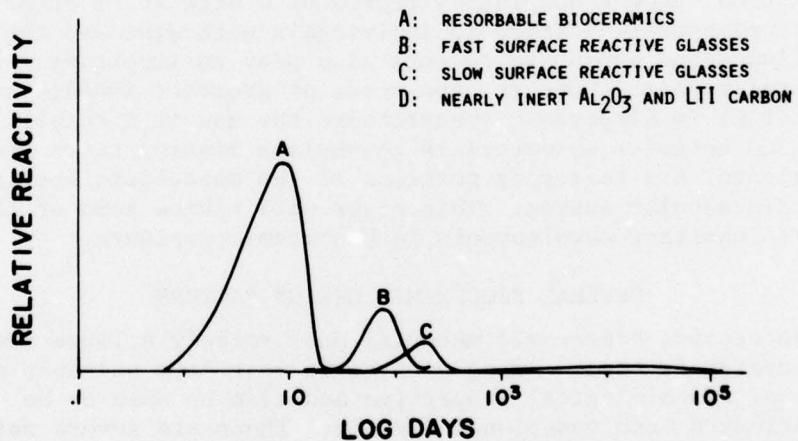
Fig. 1. Relative reactivity spectrum of bioceramic materials.

When strength requirements are sufficiently low, large pores of 50 to 200 μm cross sectional diameters can be utilized to establish mechanical interlocking by tissue ingrowth.[6,7] This approach is shown in Fig. 2 which is a photomicrograph obtained by Klawitter and Hulbert illustrating bone growing into the pores of 200 μm pores of an alumina

ceramic implanted in a rabbit femur for 8 weeks.

Fig. 2. Bone growth into porous alumina (by J. Klawitter and
         S. Hulbert).

A very high degree of control over the size and inter-
connection of the porosity can be achieved by the innovative
replamineform process developed by WHITE, WEBER, ROY and co-
workers at Penn State University.[8] In this process the uni-
form pore skeletal structures of certain marine invertebrates
is replicated in the form of high purity alumina or other
materials or directly converted to hydroxyapatite.

Long term fatigue and wear studies on fully dense alumina
exposed to physiological conditions show there is little
reason for concern for the long term stability of this type of
material.

Recent developments in fracture mechanics by WEIDERHORN,
EVANS[9], and RITTER[10] enable the lifetime of a ceramic device
to be calculated when the stress state and environment is
known. This procedure has been used by GREENSPAN and myself
to evaluate the possible lifetime of fully dense alumina
prostheses under various levels of stress.[11] For stresses of
200 n/mm^2, approximately twice the fracture strength of the
long bones of an adult human, an average lifetime of about
three years can be expected for dense alumina implants. This
prediction is based on a strength value of 340 n/mm^2 for the
alumina tested in liquid nitrogen. If the alumina strength
is increased to 400 n/mm^2 by improved processing which is
easily achieved, the predicted lifetime would be about 140
years under the same applied stress.

Figure 3 shows a lifetime prediction diagram determined by Greenspan for alumina samples, provided by Dr. Heimke of Friederschsfeld GMBH, exposed to a buffered aqueous environment. The above predictions are based on average values. If lifetime predictions are to be meaningful, the weakest specimens must be eliminated by use of a proof test which destroys the weakest samples without severely damaging the survivors. Using fracture mechanics theory and data from dynamic fatigue tests, a lifetime prediction diagram can be constructed. As an example, for an applied stress (σ_a) of 100 n/mm^2 and a required implant lifetime of ten years, a prooftest stress (σ_p) of 190 n/mm^2 (corresponding to a prooftest ratio (σ_p/σ_a) of 1.9) would be necessary to eliminate all weak specimens and still allow the survivor to withstand ten years of service at 100 n/mm^2. A similar procedure can be used to guarantee any given lifetime for the implants.
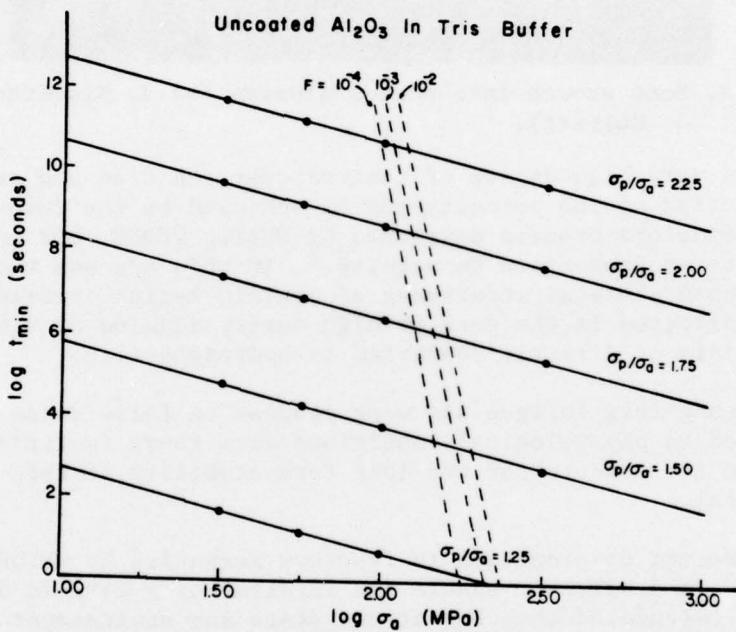
Fig. 3. Lifetime prediction diagram for dense alumina based upon fracture mechanics.

Aging and fatigue studies of porous implants conducted by BROWN and KENNER[12,13] indicate that there may be considerable concern for the long term strength of porous bioceramics. Strength reduction of porous calcium-aluminate bioceramics with load and implantation is particularly severe with fracture stresses decreasing to a range of only a tenth of that of normal bone.

Consider again Fig. 1; at the other extreme of the bio-
ceramic reactivity spectrum (curve A), are totally resorbable
bioceramics. Such materials must have compositions that con-
tain only elements that are easily processed through normal
metabolic pathways such as calcium, phosphorous, H_2O, and CO_2.
With time, such reactive bioceramics are totally resorbed by
the body and replaced by tissues. Consequently, the function
of totally resorbable bioceramics is merely to serve as a
scaffolding or filler of space permitting tissue infiltration
and replacement. This is a similar function to that provided
by bone grafts from the host. However, a major advantage of
the use of resorbable ceramics over host bone grafts is a
ready supply, controlled variations in size, and elimination
of a second surgical procedure. However, a disadvantage of
this type of bioceramic is the serious strength reduction that
occurs during the resorbtion process. Consequently, mechan-
ical design factors must be seriously considered to eliminate
fracturing of the tissue and resorbable ceramic structure
during the intermediate stages of healing. One material, tri-
calcium phosphate, developed by DRISKELL and co-workers[14] and
PEELEN, REJDA, VERMEIDEN, and DEGROOT[15] appears to be the most
outstanding success of a bioceramic of this type. Calcium
aluminate-phosphate compositions also show promise in monkey
models. Micrographs, courtesy of GRAVES, et al.,[16] Figs. 4
and 5, show the resorbtion of the microstructure after this
period of time is readily apparent in Fig. 5. This is due to
slow dissolution of the tracalcium phosphate in body fluids.
There is a strong compositional dependence of the rate of re-
sorption in the various systems of this type.
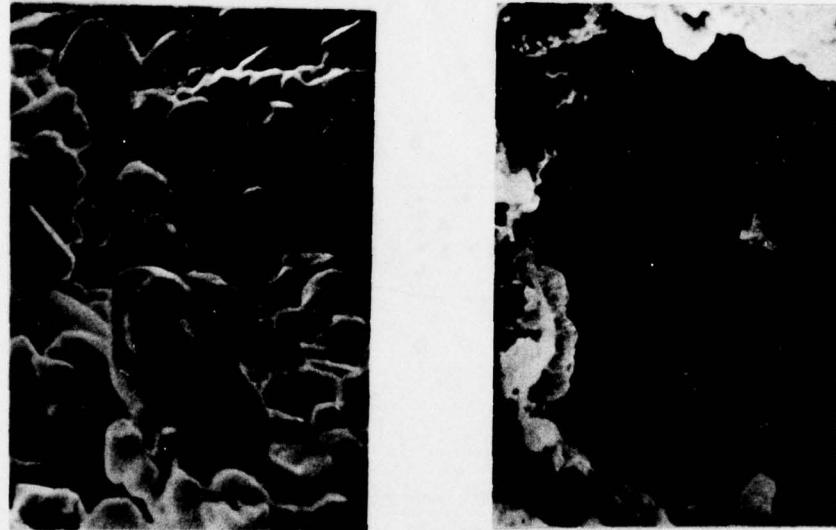
Figs. 4 & 5. Calcium aluminate-phosphate implant before and
during resorbtion (by G. Graves).

Returning again to Fig. 1, bioceramics in the middle of the reactivity spectrum, curves B and C, are based upon the concept of controlled surface reactivity of the material. In this class of bioceramics the composition is designed such that the surface undergoes a selected chemical reactivity with the physiological system establishing a chemical bond between tissues and the implant surface. The chemical reactions are such that ideally the bonded interface protects the implant material from further deterioration with time. Thus the potential of this approach is to combine the high strength of nearly inert bioceramics with surface chemical reactivity favorable to tissue bonding. Since controlled surface reactive implants are not restricted to being stabilized with the tissues only by mechanical interlocking, more flexibility in device design and fabrication is potentially achieved. Bioglass and bioglass-ceramic compositions developed at the University of Florida[17-19] and the Ceravital materials studied by Drs. BROMER, DEUTSCHER, BLENKE, PFEIL and STRUNZ[20,21] are successful examples of this approach towards bioceramics.

Figure 6 shows the compositional range for bonding of bioglass to bone within 30 days or less in rat.[22] Region A is bonding. Region B is nonbonding due to too little reactivity; region C too much reactivity and therefore the implant dissolves in body fluids, i.e., is totally resorbable; and region D is non-glass forming.
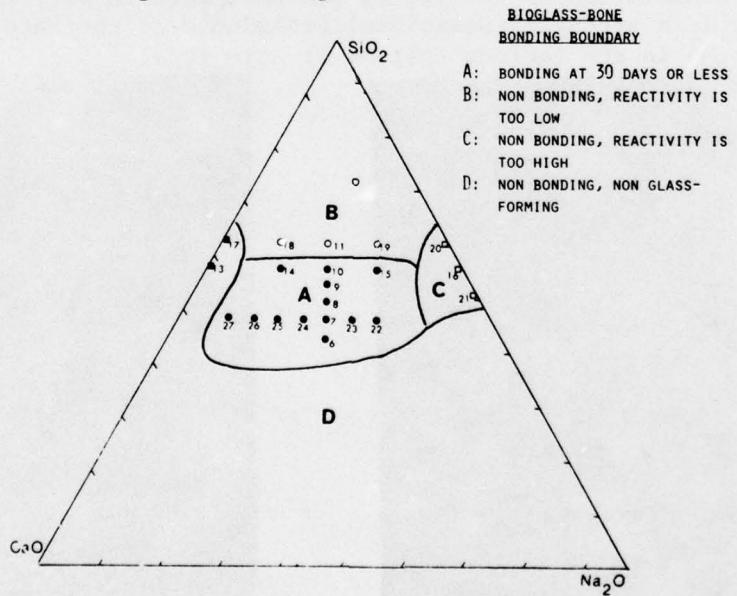
Fig. 6. Compositional range for bonding of rat bone to Bioglass in 30 days.

Several experiments have demonstrated structural contiguity that develops at the interface between a surface reactive bioglass and bone. For example, an implant composition of 45 weight percent SiO_2, 24.5 weight percent CaO, 24.5 weight percent Na_2O, and 6 weight percent P_2O_5 (45S5) is inserted in a hole drilled in the tibia of a rat and allowed to heal for periods as early as 10 days. After 10-30 days a force of 30 newtons is gradually applied with no motion of the implant or fracture of the interface. Subsequently a transverse fracture is made across the interface yielding a contiguous bonded interface suitable for structural analysis.

Evidence of the bonding between bone and bioglass is shown in Figure 7. A microtomed 700 Å thin section of a 45S5 bioglass implant in a rat tibia for 3 weeks is shown in the scanning transmission mode of a Phillips EM 301 microscope. No metal stains were used. The dark areas are structural remanants of the interfacial bridges between bone and bioglass after passage of the microtome, which fractures the section producing the light areas shown in the section.
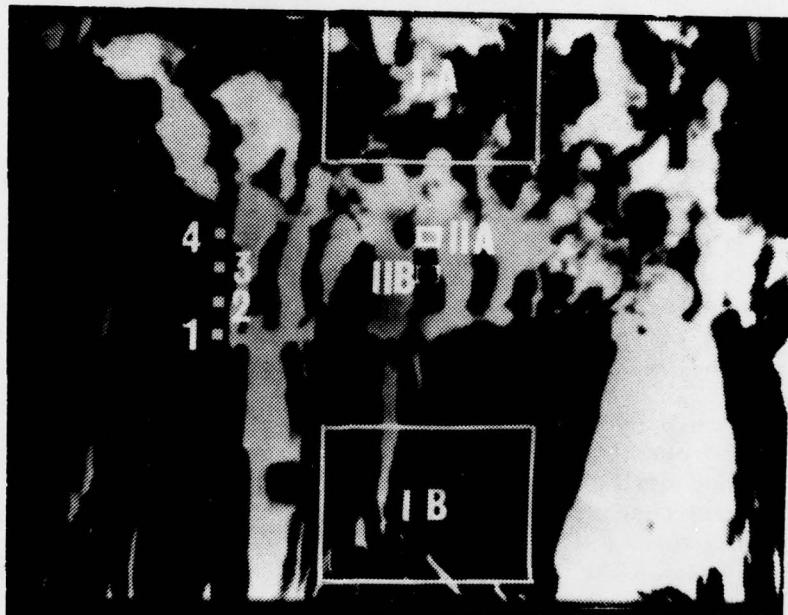
Fig. 7. Electron micrograph of bone-Bioglass bond.

Figure 8 shows the results of compositional point counting at 1.0 μm intervals in the thin section at points 1-4 shown in Fig. 7 using energy dispersive X-ray analysis in the transmission electron microscope. A ∿150 μm beam diameter and
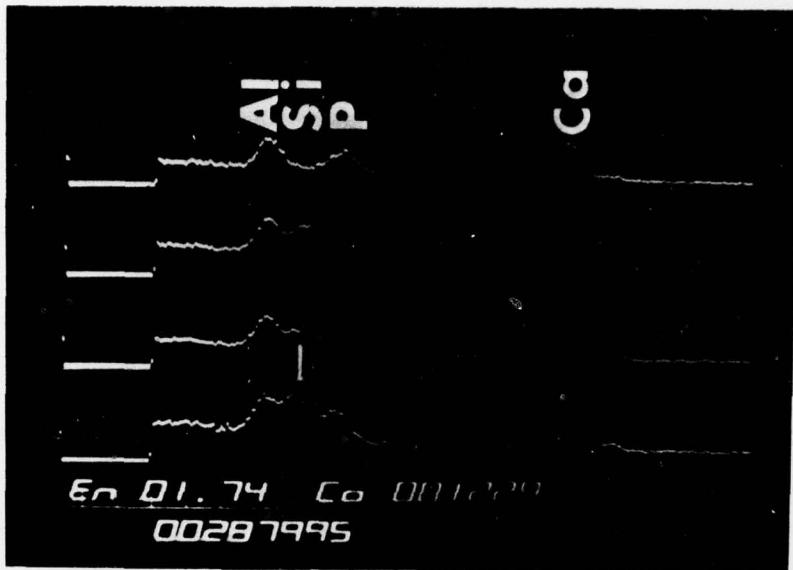
Fig. 8. Energy dispersive X-ray spectra from points 1-4 in
Fig. 7.

40,000-70,000 counts was used. The silicon in the bioglass
implant serves as a tracer to identify the interface. There
is a transition between bioglass and bone between points 3
and 4. The compositional spectrum at point 4 is character-
istic of bone, the spectrum at point 1 is that bioglass and
those in between are characteristic of the interfacial,
chemically bonded bridge between the implant and bone. This
data represents compositional proof of the ability of a bio-
ceramic to form a stable, compatible bond with living tissues.
The bonding interface is very thin, of the order of 0.5 μm.

Dense hydroxyapatite bioceramics developed by JARCHO,
KAY and co-workers also appears to form a bond with bone when
examined with transmission electron microscopy.[23] They have
evidence that epitaxial growth of apatite crystals from re-
pairing bone establish the bond. Work on apatite implants by
AOKI[24] and KATO[25] in Japan also shows evidence of interfacial
bonding.

The high surface activity of plasma sprayed oxide coat-
ings also may produce a chemical bond with bone. Micrographs
of the junction between bone and plasma sprayed gamma-alumina
coatings studied by CINI, PIZZOFERRATO, and SANDROLINI[26] show
regions of contiguity. Plasma sprayed titanium oxide coat-
ings were applied to dental anchors by SCHROEDER, POHLER and
SUTTER.[27] The surface of these implants, when observed in
electron microscopy also show evidence of tissue attachment.

Thus, considerable evidence has been amassed over the
last few years which establishes that bone will bond to bio-
ceramics if the surface chemistry is correct. A recent study
by WALKER and HENCH shows that a critical level of surface
activity is essential.[22] Glasses and glass-ceramics in a
certain compositional range, high surface area plasma sprayed
oxide coatings, and certain apatite ceramics interact at their
surface with body fluids in the first few weeks to form the
tissue bond.

In an effort to understand the mechanism of interfacial
bonding, several series of experiments have been conducted in
our laboratory during the last two years. In one of them,
45S5 bioglass samples were exposed to a very dilute suspension
of collagen fibers at 37°C for 10 days.[28] After this period
control materials such as soda-lime-silica microscope slides
were easily washed clean of any deposit. In contrast, Fig. 9,
a scanning electron micrograph obtained by PANTANO[28] shows
that the collagen has become incorporated within the bioglass
surface. You can see the collagen fibers running in and out
of the surface disappearing within the agglomerates forming on
the surface. Energy dispersive X-ray analysis and electron
diffraction shows that the collagen bonding is within hydroxyl-
apatite agglomerates. Bonding of collagen to the active
apatite layer that forms on bioglass implants has also been
seen in transmission electron microscopy.[17,29,20]

Fig. 9. In-vitro bonding of collagen fibers to Bioglass
        (by C. Pantano).

Also, Auger electron spectroscopy and Argon ion beam milling of 45S5 bioglass samples forming a bond with bone provides direct evidence of the reactive apatite layer incorporating organic species to a depth of hundred of angstroms.[31]

Recently, GRANT and colleagues at the Pfizer and Howmedica research laboratories have succeeded in growing bone cells on bioglass substrates.[32] Transmission electron micrographs show many layers of bone cells after 6 weeks of growth on 52S4.6 bioglass. The cells are healthy and are actively producing collagen. Attachment of the cell layers to the bioglass is clearly evident. Equivalent tissue cultures on control microscope cover slides or plastics show that multiple levels of cells do not develop or generate collagen fibers. Histochemical analysis of the cells growing on bioglass is in progress by Dr. Grant and colleagues.

POTENTIAL CLINICAL APPLICATIONS OF BIOCERAMICS

All three categories of bioceramics (resorbable, nearly inert, and surface reactive) are being studied as tooth implants. Preliminary results show promise for all three types and it is too early to judge which may be successful in the long term. Problems of mechanical fracture of free standing tooth roots indicate that coatings of surface reactive bioceramics on high strength metal[19,33] or alumina substrates[34,35] may be necessary for a successful implant. In a recent study at the University of Washington, SMITH and colleagues showed that bioglass coated alumina can be used as anchors for orthodontic appliances.[36] Loads of up to five pounds were applied over 6 to 8 weeks in monkey with no movement of the anchors or fracture.

For certain types of oral surgery or maxillo-facial reconstruction, the strength of as-cast or ceramed surface reactive bioceramics appears sufficient. Reconstruction of segments of the mandible of baboons has been evaluated by Drs. CLARK, KREUTZIGER, and STANLEY of the University of Florida for over three years. Figure 10 shows an X-radiograph of the 45S5 bioglass segment from their work after more than three years in the animal. The mandibular prostheses is stable, no mechanical or interfacial deterioration is observed, and the gum tissues are healthy. The animal successfully uses the implant in her normal eating function.

The question of long term stability of the interface of surface reactive bioceramics, especially higher alkali bioglasses, has been of increasing interest over the last few years. The baboon mandible sections indicate little problem in this regard. However, a recent effort has been made in our laboratory to quantify the changes that can occur at the
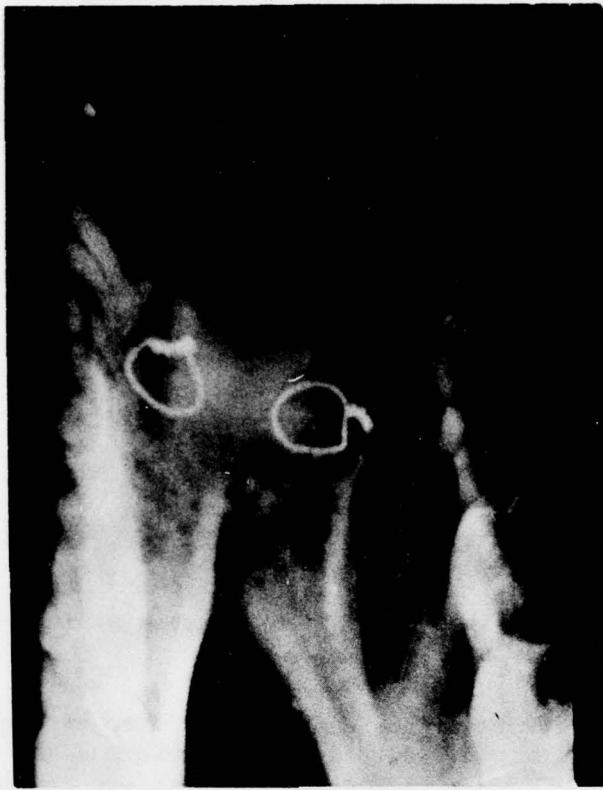
Fig. 10. X-radiograph of Bioglass implant in baboon jaw
after 3 years (by Clark and Kreutziger).

bonding interface. The electron beam microprobe is used for
1 μm point counting across the interface of ground and
polished sections. Figure 11 shows the electron microprobe
results obtained for a 28 month 45S5 bioglass implant in the
rat tibia. The implant was firmly bonded as determined by
the 30 newton minipushout test. Several compositional layers
are present at the bonding interface.

Adjacent to and contiguous with the bone is the active
hydrated calcium phosphate rich layer. Next to it is the
silica-rich layer which was developed as a result of alkali
ion-proton exchange followed by migration of calcium and
phosphate ions. Practically no change in thickness is
observed in the calcium phosphate bonding layer between 3 and
28 months. The silica rich layer does continue to increase
in thickness throughout this time period. Thus, this study
establishes that even the more reactive surface active
implants in the bone-bonding region of Figure 6 remain stable
for the life time of the animal.
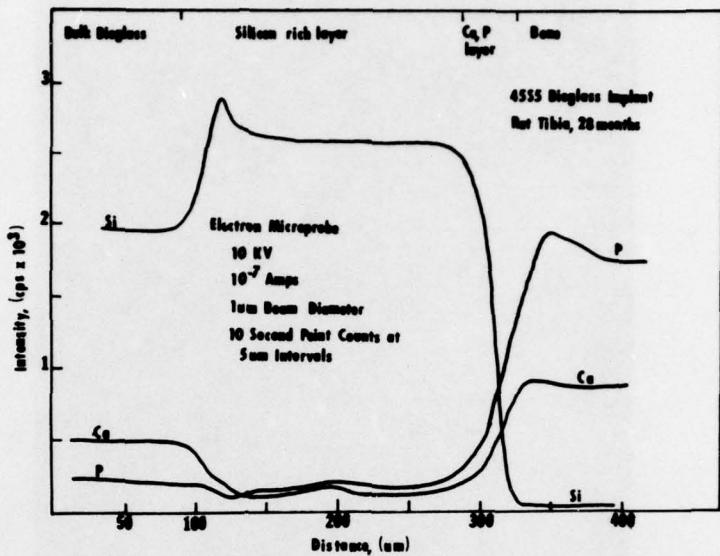
Fig. 11. Compositional gradients across a Bioglass-bone
bond in rat after 28 months.

Bioceramics of the nearly inert category, especially
dense alumina, have already seen widespread use in
patients.[36-38] Excellent success of these implants illus-
trates the safety of using high strength ceramics as pros-
thetic devices when they are correctly designed for the mech-
anical loads encountered.

. Dr. BOUTIN'S implantations in France of more than 700 hip
joints of high density 99% alumina bioceramics have pioneered
the accelerating use of high density alumina in orthopaedic
skeletal repair.[36] The Boutin prosthesis is composed of a
nearly inert high density alumina ball and socket joint. The
ball component of the joint is attached by a mechanical self-
locking joint to a titanium shaft to go into the femur. Both
halves of the joint are cemented into place using polymethyl-
methacrylate (PMMA) bone cement. The purpose of the alumina
joint over the standard prostheses composed of a metal ball
with high density polyethylene or metal cups is to reduce the
wear within the joint and to eliminate metallic or polymeric
wear particles which can be toxic. A five year followup of
590 cases shows no mechanical failure of the alumina
components after implantation.[36]

The efforts of Drs. GRISS and HEIMKE and co-workers have
been directed towards elimination of the use of PMMA bone
cement as well as reduction of wear within the joint.[37,39]

136

They have achieved part of their objective by recently completing the design and implantation of more than 70 high density alumina joints in patients in both Germany and the U.S. The acetabular, or socket component is mechanically screwed into the hip after preparation of a carefully tapped hole in the bone. The femoral component in the Griss-Heimke hip is also a Ti metal shaft and at present is cemented into place with PMMA. Excellent stability has been achieved with this system and it reduces the PMMA required in surgery by approximately 40%.

A further aspect of their study is the collaboration with the author's research team which has resulted in the fabrication of multiple layers of bioglass coatings on high density alumina hip prostheses.[35] Results from bone bonding studies in rats and dogs indicate that the bioglass coated alumina does bond to bone and prevents formation of a fibrous capsule. Total hip prostheses composed of bioglass coated alumina have shown the capability of establishing a direct chemical bond with the bone in sheep. Figure 12 illustrates results from a 3 month implant. Reliability of the bonding has been difficult to achieve, however.

Fig. 12. X-radiograph of Bioglass coated dense alumina hip component in sheep after 3 months (by Griss).

Total hip components made of nearly inert Nucerite[R] glass-ceramic coated steel have been implanted by ENGLEHARDT and co-workers using the PMMA cementing procedures.[40] Preliminary results of this system also look encouraging. There is no indication that elimination of PMMA can be obtained with the use of the Nucerite[R] glass-ceramic coating. However, 45S5 bioglass coatings on stainless steel monkey hip prosthesis have demonstrated high bond strength of the femoral shaft without use of PMMA. Bonding has been shown as early as 3 months. Stability has been demonstrated for over 15 months, the duration of our experiments. Figure 13 shows results from a 6 month experiment. Loading of the implant in tension, Fig. 14, only leads to fracture of the bone.

Figs. 13 & 14. Bioglass coated stainless steel femoral head prostheses in monkey after 6 months. Before (Fig. 13) and after (Fig. 14) Instron testing. The implant-bone interface did not fail (by G. Piotrowski & W. Petty).

Several other investigators are also proceeding to evaluate potential for use of alumina ceramics in hip and knee joints. They include SEMLITSCH, et al.[41] and EYRING.[38]

High density alumina long bone replacements using a non-cementing selflocking conical sleeve device has also undergone extensive tests in humans by a research team of M. SALZER and M. PLENK, et al.[42] Over 20 such prostheses have been utilized to restore the skeletal system for patients that have had to have surgical removal of long bones as a cancer treatment. Mechanical failure of the ceramic has not been

observed for cases that now have been as long as 24 months. Stability of the alumina-bone interface also appears to be reasonable at this stage.

One of the longest histories of the use of ceramic implants is Professor EYRING's seven years of clinical studies in humans using high density alumina as a temporary spacer for osteotomies.[38] The clinical studies were proceded by a series of fibroblast tissue cultures, injection of alumina crystals in rabbit knees and implantation of small blocks of the alumina subcutaneously or intramuscularly in rats. All results showed extremely good biocompatability with only a very small reactive membrane of a few µm thickness being formed. Implantation of a partial replacement of the knee of monkeys also preceded the human studies and recently total hip replacement has been performed successfully in dogs.

High density alumina oxide spacers have been used by Eyring for opening wedge tibial, femoral or phalagenal osteotomies 20 times in 14 patients without any untoward reactions. Use of the material obviates the need for a second operation to remove bone and the spacer saves considerable time and possible morbidity. Use of alumina spacers have also enabled Dr. Eyring and co-workers to perfect a technique for a one stage femoral lengthening up to nearly two inches in seven patients with congenital or growth defects. Repeated osteotomies have gained up to 5 inches in length for one patient.

Bioglass coatings applied to stainless steel shafts have been used by Dr. William Hall in the U.S. to achieve stability of an implanted artificial limb in contact with the bone in a goat model.

Other applications of various types of bioceramics that have been in test throughout the world are: mandibular ridge augmentation with Ceravital and calcium phosphate ceramics; packing of periodontal pockets with Durapatite; endodontic tooth roots with calcium phosphates, tracheal reconstruction with flame sprayed zirconia and porous calcium aluminate ceramics, spinal fusion using bioglass blocks for elimination of chronic pain. X-ray analyses after several months using a modified Cloward procedure with bioglass developed by Cauthen, Fuller and Madden show promise for successful vertebrae fusion.

Nontoxic plasma sprayed zirconia has been tested in contraceptive devices. Ta_2O_5 anodized sintered Ta capacitors

have also shown considerable promise for use in noncorroding, non-toxic neural electrodes for various neurological prostheses.[43] TiO_2 thin films or Ti, TiO, and Sb-doped SnO_2 also show promise as bioceramic electrodes.

Finally, low temperature isotropic carbon ceramics, developed by Jack Bokros, are the most successful ceramic implants used today.[44] Samples of Typical LTI carbon heart valves are shown in Fig. 15. Nearly 150,000 successful implantations of heart valves of this material are a tribute to its high strength and thrombus resistance. The success of this material gives great hope that the many other types of bioceramics in test may provide a new generation of implants. A goal of ceramic scientists is to learn more about the mechanisms of interfacial reactions between bioceramics and body tissues and to learn how to control these reactions through compositional and processing changes. This is a difficult task but the reward is a better life for millions of people.
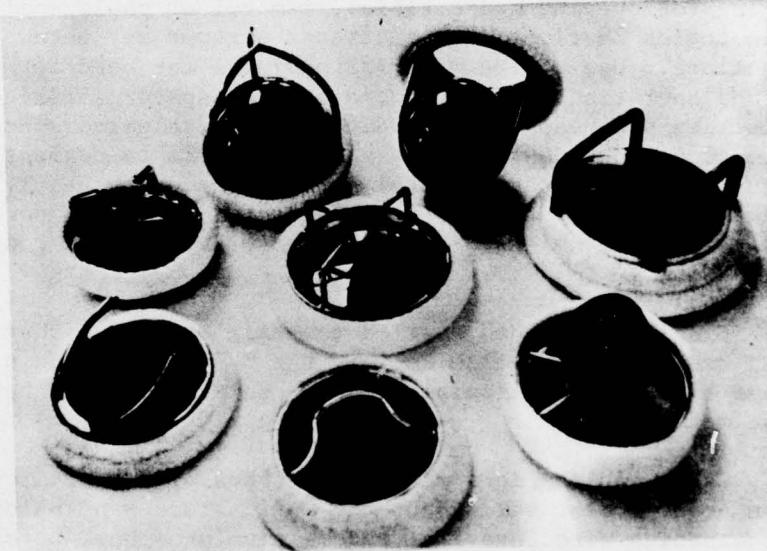
Fig. 15. Heart valve implants of Pyrolite carbon (by J. Bokros).

REFERENCES

1. PHILLIPS, R. W., Skinner's Science of Dental Materials, W. B. Saunders & Co., 7th ed., 1973.
2. PEYTON, F., et al., Restorative Dental Materials, C. B. Mosby Co. 1970.
3. HENCH, L. L and ETHRIDGE, E C., in Advances in Biomedical Engineering, J.H.U. Brown and J. F. Dickson, eds., Academic Press, N.Y., 36-139, 1975.

4. KLAWITTER, J. J. and HULBERT, S. F., J. Biomed. Mater.
    Res. Symp., 2, 231-249, 1971.
5. HULBERT, S. F. and KLAWITTER, J. J., Mater. Res. Bull.,
    7, 1239-1246, 1972.
6. HULBERT, S. F., et al., J. Biomed. Mater. Res. Symp., 4,
    1-23, 1973.
7. HULBERT, S. F., MORRISON, S. J., and KLAWITTER, J. J.,
    J. Biomed. Mater. Res., 6, 347-374, 1972.
8. WHITE, E. W., et al., J. Biomed. Mater. Res. Symp., 6,
    23-27, 1975.
9. WEIDERHORN, S. M., Subcritical Crack Growth in Ceramics,
    in Fracture Mechanics of Ceramics, Vol. 2, R. C. Bradt,
    D.P.H. Hasselman, and F. F. Lange, eds., Plenum Press,
    N.Y., 1974.
10. RITTER, J. E., JR. and LAPORTE, R. P., J. Amer. Ceram.
    Soc., 58, (7-8), 1975.
11. GREENSPAN, D. C., The Chemical, Mechanical, and Implant
    Properties of Glass-Coated Alumina, Ph.D. Thesis,
    University of Florida, 1977.
12. FRAKES, J. T., BROWN, S. D. and KENNER, G. H., Amer.
    Ceram. Soc. Bull., 53, 183-187, 1974.
13. SCHNITTGRUND, G. D., KENNER, G. H. and BROWN, S. D.,
    J. Biomed. Mater. Res. Symp., 4, 435-452, 1973.
14. DRISKELL, T. D., et al., J. Biomed. Mater. Res. Symp.,
    2, 345-361 1971.
15. PEELEN, J., DEGROOT, K., REJDA, B. V., and VERMEIDEN, J.
    M., Sintered Tricalcium Phosphate as Bioceramic,
    Science of Ceramics, 9 (this proceedings).
16. GRAVES, G. A., et al., J. Biomed. Mater. Res. Symp., 2,
    345-361, 1971.
17. HENCH, L. L., et al., J. Biomed. Mater. Res., 2, 117-141,
    1971.
18. HENCH, L. L., Medical Instrumentation, 1, 136-144, 1973.
19. HENCH, L. L., PASCHALL, H. A., ALLEN, W. C. and
    PIOTROWSKI, G., National Bureau of Standards Special
    Publication 415, 19-35, 1975.
20. BROMER, H., DEUTSCHER, K., BLENCKE, B., PFEIL, H. and
    STRUNG, U., Properties of a Bio-Active Implant
    Material, Science of Ceramics, 9 (this proceedings).
21. BLENCKE, B.-A., BROMER, H. and PFEIL, E.,
    Rasterelektronenmikroskopische Untersuchungen der
    Reaktion des Knochens auf glaskeramische Implantate,
    Z. Orthop. 112, 978-980.
22. WALKER, M. M., An Investigation Into the Bonding
    Mechanisms of Bioglass, M.S. Thesis, University of
    Florida, 1977.
23. JARCHO, M., KAY, J. F., GUMAER, K. I., DOREMUS, R. H.
    and DROBECK, H. P., Tissue, Cellular and Subcellular
    Events at a Bone-Ceramic Hydroxylapatite Interface,
    J. Bioengineering, 1, 79-92, 1970.

24. AOKI, H., et al., 1975 Symp. on Biomaters., Kyoto Univ.,
    Kyoto, Japan, August 29-30, 1975.
25. KATO, K., private communication.
26. CINI, L., GASPARINI, F., MITCHIELI, S., PIZZOFERRATO, A.
    and SANDROLINI-CORTESI, S., Impianti dentari metallici
    rivestiti di ceramica, Min. Stom., 24, 75-90, 1975.
27. SCHROEDER, A., POHLER, O. and SUTTER, F., Gewebsreaktion
    auf ein Titan-Hohlzylinderimplantat mit Titan-
    Spritzschichtoberflache, SMfZ/RMSO, 86, 713-727, 1976.
28. PANTANO, C. G. and HENCH, L. L., Surface Reactions
    Mediating the Formation of a Bone-Bioglass Bond, to
    be submitted for publication.
29. HENCH, L. L. and PASCHALL, H. A., J. Biomed. Mater. Res.,
    4, 25-42, 1973.
30. HENCH, L. L. and PASCHALL, H. A., J. Biomed. Mater. Res.,
    5, 49-64, 1974.
31. CLARK, A. E., JR., PANTANO, C. G., JR., and HENCH, L. L.,
    J. Amer. Ceram. Soc., 59, 37-39, 1976.
32. GRANT, R. C., private communication.
33. PIOTROWSKI, HENCH, L. L., ALLEN, W. C. and MILLER, G. J.,
    J. Biomed. Mater. Res. Symp., 9, 47-61, 1975.
34. GREENSPAN, D. C. and HENCH, L. L., Chemical and
    Mechanical Behavior of Bioglass Coated Alumina, J.
    Biomed. Maters. Res., 10, (4), 503-509, 1976.
35. GRISS, P., GREENSPAN, D. C., HEIMKE, G., KREMPIEN, B.,
    BUCHINGER, R., HENCH, L. L. and JENTSCHURA, G.,
    Evaluation of a Bioglass Coated Al$_2$O$_3$ Total Hip
    Prostheses in Sheep., J. Biomed. Mater. Res., 10,
    (4), 511-518, 1976.
36. SMITH, J. R., Bone Dynamics Associated with a Controlled
    Loading of Bioglass Coated Alumina-Oxide Endosteal
    Implants, Master Thesis, University of Washington,
    1977.
37. GRISS, P., HEIMKE, G. and JENTSCHURA, G., Clinical
    Experience with Two Composite Ceramic-Metal Hip
    Prostheses, 2nd Annual Meeting of the Society for
    Biomaterials, April 9-13, 1976, Philadelphia, Pa.
38. EYRING, E. J., High Density Alumina Oxide--Orthopedic
    Uses, 2nd Annual Meeting for the Society for
    Biomaterials, April 9-13, 1976, Philadelphia, Pa.
39. GRISS, P., et al., J. Biomed. Mater. Res., 9, 177-188,
    1975.
40. ENGELHARDT, A., SALZER, M., ZEIBIG, A. and LOCKE, H.,
    J. Biomed. Mater. Res., 6. 227-232, 1975.
41. SEMLITSCH, M., LEHMANN, M., DOERRE, E. and WILLERT, H.
    G., New Prospects for a Longer Service Life of
    Artificial Hip Joints Using a Polyethylene/Al$_2$O$_3$
    Ceramic/Metal Combination, 2nd Annual Meeting of
    the Society for Biomaterials, April 9-13, 1976,

Philadelphia, Pa.

42. PLENK, H., JR., LOCKE, H., PUNZET, G., SALZER, M. and
    SWEYMULLER, K., Attachment of Ceramic Endoprostheses
    to the Exterior of Long Bones without the use of Bone
    Cement, II. Histomorphometrical Analysis of Bone
    Reactions, 2nd Annual Meeting of the Society for
    Biomaterials, April 9-13, 1976, Philadelphia, Pa.

43. JOHNSON, P. F., BERNSTEIN, J. J., HUNTER, G., DAWSON,
    W. W. and HENCH, L. L., An in vitro and in vivo
    Analysis of Anodized Tantalum Capacitive Electrodes:
    Corrosion Response, Physiology, and Histology,
    J. Biomed. Mater. Res., 11, 637-656, 1977.

44. BOKROS, J. C., et al., Carbon in Prosthetic Devices,
    ACS Symp. Series, 21, 237-265, 1975.

DISTRIBUTION LIST

Commanding General   4
U.S. Army Medical Research and Development Command
ATTN: MEDDH-SI
Washington, D. C. 20314

Defense Documentation Center   12
ATTN: DDCIR
Cameron Station
Alexandria, Virginia 22314

Commanding Officer   1
U.S. Army Combat Development Command
Medical Service Agency
Brooke Army Medical Center
Fort Sam Houston, Texas 78231

National Institute of Dental Research   1
Dental Materials Science
Bethesda, Maryland 20014

NASA   1
Materials Science Division
Washington, D. C. 20546

Army Research Office - Durham   1
Metallurgy and Ceramics Division
Durham, North Carolina 27709

National Institutes of Health   1
Division of Orthopaedics
Bethesda, Maryland 20014

Defense Ceramic Information Center   1
Battelle Memorial Institute
505 King Avenue
Columbus, Ohio 43201

National Institutes of Health   1
National Institute of General Medical Sciences
Bethesda, Maryland 20014

Colonel Simon Civjan, DC   1
Chief, Division of Dental Materials
U.S. Army Institute of Dental Research
Washington, D. C. 20012

Air Force Office of Scientific Research   1
Chief, Chemistry Division
Bolling Air Force Base, D. C. 20332

144